THE ASTROPHYSICAL JOURNAL

AN INTERNATIONAL REVIEW OF SPECTROSCOPY AND ASTRONOMICAL PHYSICS

VOLUME 87 MARCH 1938 NUMBER 2

EQUIVALENT WIDTHS AND THE TEMPERATURE OF THE SOLAR REVERSING LAYER

DONALD H. MENZEL, JAMES G. BAKER, AND LEO GOLDBERG

ABSTRACT

Allen's extensive determinations of equivalent widths of Fraunhofer lines provide important observational material for an analysis of the physical state of the solar atmosphere. A comparison of the observed intensities of absorption lines, as read from an empirical curve of growth, with the theoretical strengths of lines in a transition array makes it possible to calculate the effective excitation temperature of the reversing layer. Temperatures of 4350° ± 200° and 4150° ± 50° are computed from the lines of *Ti* I and *Fe* I, respectively.

A qualitative discussion of the errors inherent in the theoretical calculation of multiplet strengths is given, and a method for calculating the reversing-layer temperature by means of the *J*-file sum rule is described. The application of this method to the lines of *Ti* I yields a temperature of 4400° ± 100°. Since the sum rule is independent of the coupling in an atom, and is therefore free of the assumptions involved in the calculation of multiplet strengths, the value 4400° is adopted, for purposes of discussion, as the mean excitation temperature of the solar reversing layer.

If the opacity of the solar atmosphere varies with wave length, we should expect to find the numbers of atoms, as derived from equivalent widths, depending upon wave length as well as upon the temperature and excitation potential. The data for *Fe* indicate an opacity law almost independent of wave length. These results, however, are not definitive. Since the mean lower excitation potentials increase systematically with wave length, opacity and temperature effects are correlated. The data for *Ti*, where no systematic correlation exists, are not inconsistent with an opacity varying as λ^3, whereas theory predicts a law varying approximately as $\lambda^3 e^{-hc/\lambda kT}$. An attempt is made to reconcile the observations and the theoretical values.

The observed intensities of the Fraunhofer lines may be employed in an analysis of the physical state of the solar atmosphere. The functional relationship between the equivalent widths, W, of the solar lines, and the theoretical strengths of the atomic transitions

has been developed by Minnaert and Slob[1] and by Menzel.[2] In this paper we shall combine theory with observational data in an attempt to determine the effective excitation temperature of the solar reversing layer. Baker[3] has derived the following semi-empirical formula that relates W/λ to various atomic and physical parameters:

$$\log \frac{W}{\lambda} = \log X_0 \frac{v}{c}\sqrt{\pi} - \tfrac{1}{2}\log(1 + X_0) - \frac{\tfrac{1}{2}\log 4\sqrt{\pi}\,\dfrac{v}{c}\,\dfrac{\nu}{\Gamma}}{1 + 15e^{-2\log X_0}}, \qquad (1)$$

where[4]

$$\left.\begin{aligned} X_0 &= \frac{N_a}{b(T)}\, e^{-\chi_{J'/kT}}\, \frac{1}{3\sqrt{\pi}R}\, \frac{\pi\epsilon^2}{mc}\, \phi\, \frac{c}{v}\, S\, \frac{s}{\Sigma s} \\ &= \left[3.510 \times 10^{-12}\, \frac{N_a}{b(T)}\, \sqrt{\frac{\mu}{T}}\, \phi\right] S\, \frac{s}{\Sigma s}\, e^{-\chi_{J'/kT}}. \end{aligned}\right\} \qquad (2)$$

Physically, X_0 is equal to the optical depth at the center of the absorption line.

The factor in brackets is constant for all the lines of a transition array. For lines of the same multiplet, the $\chi_{J'}$'s are essentially equal, and X_0 depends only on $s/\Sigma s$. Equation (1) defines the curve of growth as a function of X_0, and hence for a multiplet the curve is a function of $s/\Sigma s$. Furthermore, the curves of growth for different multiplets will all have the same shape, as long as Γ/ν and v are the same. They may be brought into coincidence by a horizontal shift along the X_0 axis. This is the customary procedure for determining the curve of growth. Allen,[5] who utilized his own observational data for the determination, found that W/λ, rather than W, must be employed for the ordinate if lines in different wave-length

[1] *Proc. Amsterdam Acad.*, **34**, Part 1, 542, 1931.

[2] *Ap. J.*, **84**, 462, 1936. A preliminary report of the results of the present investigation appeared in *Pub. A.A.S.*, **8**, 218, 1936.

[3] *Ap. J.*, **84**, 474, 1936. A list of definitions of the various algebraic quantities occurring in the foregoing discussion appears at the end of this paper.

[4] Menzel, *loc. cit.*

[5] *Mem. Comm. Solar Obs.*, **1**, No. 5, 1934.

regions are to be combined on the same diagram. This procedure, by equation (1), is seen to be justified theoretically.[6]

In proceeding to determine the effective excitation temperature of the solar reversing layer, our first act was to rederive the curve of growth from Allen's extensive tabulation of equivalent widths and from the theoretical strengths of multiplet lines. The observational data were tabulated by multiplets, and the quantity log W/λ was computed for each line directly from the tabular values. For each line of a multiplet, log W/λ was plotted against log $s/\Sigma s$. The

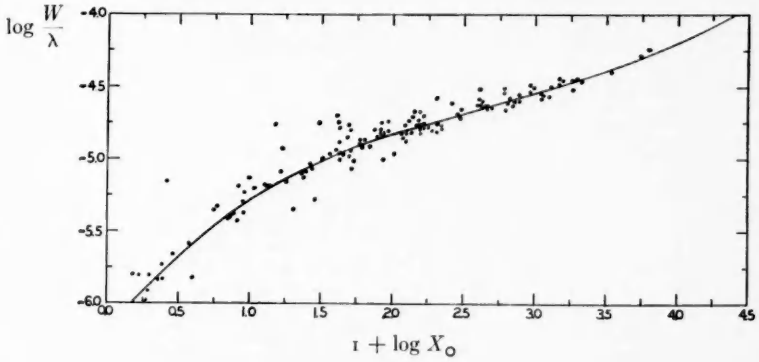

FIG. 1

ten best-determined curves were combined to give a mean curve of growth. The remaining diagrams were then superposed on the master-curve, and the observational points were transferred. The final curve that was drawn through all of these points is reproduced in Figure 1. The observational scatter is small. That the few widely divergent points represent blends is evident, since most of the discrepant points lie *above* the determined curve of growth. The curve agrees substantially with that given by Allen.

The next procedure was to fit the observed curve to the theoretical formula (1). A value of v, corresponding to *Fe* atoms at a temperature of 5740°, was found to fit the observations satisfactorily in the lower part of the curve, and the value of $1.52 \cdot 10^{-6}$ was derived for Γ/ν from the damping portion of the curve.

[6] Menzel, *loc. cit.*

For a given observed value of log W/λ we were able to read off the value of log X_0 from Figure 1. Now, by (2), for each transition array,

$$\log X_0 = L + \log S - \log \frac{\Sigma s}{s} - \frac{5040}{T} \chi_{J'}, \tag{3}$$

where L is equal to

$$\log \left[3.510 \times 10^{-12} \frac{N_a}{b(T)} \sqrt{\frac{\mu}{T}} \phi \right]. \tag{4}$$

If we set

$$\log X_0' = \log S - \log \frac{\Sigma s}{s}, \tag{5}$$

we have

$$Y = \log X_0 - \log X_0' = L - \frac{5040}{T} \chi_{J'}. \tag{6}$$

Y is defined by the foregoing equation.

Log X_0' was computed for each line from equation (5). Values of log $s/\Sigma s$ have been tabulated by Russell.[7] Goldberg[8] has computed values of S, the relative multiplet strengths. The applicability of these theoretical calculations may be questioned on the grounds that complex atoms clearly deviate from LS coupling and are strongly affected by configuration overlapping, but no better values of log X_0' are available. Eventually, when more precise determinations are at hand, either from theoretical calculations or from experiment,[9] the present analysis should be repeated. Further discussion of the effects of configuration interaction and of departures from LS coupling will be found later on in this paper.

For each line of an array we obtain a value of Y. For the present we shall assume that N_a is independent of λ, which is equivalent to ignoring the variation of opacity with wave length. Then (6) is the equation of a straight line of slope $-5040/T$ and intercept L. If, for each transition array, we plot the determined values of Y against the corresponding lower excitation potentials, the slope of the resulting straight line affords a determination of the effective excitation temperature T. A total of fourteen transition arrays, including over four hundred lines, was investigated. Table 1 contains the observa-

[7] *Ap. J.*, **83**, 129, 1936.

[8] *Ibid.*, **82**, 1, 1935.

[9] R. B. King and A. S. King, *ibid.*, p. 377.

TABLE 1

Multiplet	S	$\bar{\lambda}$	$\overline{\log X_0'}$	$\bar{Y}$	$\bar{X}_{f'}$	No. of Lines
	Ca I, 4s4p−4s4d					
$4^3P^o-4^3D$	3	4444	−0.57	3.69	1.883	6
$4^1P^o-4^1D$	1	7326	0.00	1.88	2.920	1
	Ca I, 4s4p−4p²					
$4^3P^o-p^2\,{}^3P$	9	4300	0.10	3.20	1.881	6
$4^1P^o-p^2\,{}^1D$	5	5857	0.70	2.00	2.920	1
$4^1P^o-p^2\,{}^1S$	1	5868	0.00	0.77	2.920	1
	Ca I, 4s4p−4s6s					
$4^1P^o-6^1S$	1	5513	0.00	2.00	2.920	1
	Ca I, 4s4p−4s6d					
$4^1P^o-6^1D$	1	4685	0.00	1.54	2.920	1
	Ca I, 4s4p−4s7s					
$4^1P^o-7^1S$	1	4847	0.00	0.88	2.920	1
	Ca I, 4s3d−4s5p					
$3^1D-5^1P^o$	1	5042	0.00	2.20	2.697	1
$3^3D-5^3P^o$	3	6164	−0.33	2.09	2.512	5
	Ca I, 3d4s−3d4p					
$3^3D-dp^3P^o$	9	5264	−0.09	2.29	2.511	5
$3^1D-dp^1F^o$	7	5349	0.85	1.45	2.697	1
$3^3D-dp^3D^o$	15	5593	0.23	2.36	2.512	6
$3^3D-dp^3F^o$	21	6479	0.07	2.03	2.513	6
$3^1D-dp^1P^o$	3	6718	0.48	1.74	2.697	1
$3^1D-dp^1D^o$	5	7148	0.70	1.64	2.697	1

TABLE 1—*Continued*

Multiplet	S	$\bar{\lambda}$	$\overline{\log X_0'}$	$\bar{\gamma}$	$\bar{X}_{J'}$	No. of Lines
	Ca I, $4s3d-4s6p$					
$3^3D-6^3P^o$	3	4510	0.02	0.72	2.514	2
$3^1D-6^1P^o$	1	4527	0.00	2.20	2.697	1
	Ti I, $3d^24s4p-3d^24s5s$					
$z^5G^o-e^5F$	45	4988	0.59	0.72	1.980	8
$z^5F^o-e^5F$	35	5225	0.36	0.28	2.095	10
$z^5D^o-e^5F$	25	5705	0.44	−0.01	2.290	6
	Ti I, $3d^34s-3d^24s4p$					
$a^1H-x^1H^o$	792	4278	2.90	−0.87	2.567	1
$a^5F-y^5D^o$	2520	5240	2.37	−2.17	0.827	4
$a^3G-v^3F^o$	648	5270	1.78	−1.18	1.875	2
$a^1H-x^1G^o$	1188	5504	3.08	−2.49	2.567	1
$a^3G-z^3H^o$	264	5980	1.93	−1.14	1.872	3
	Ti I, $3d^34s-3d^34p$					
$a^5F-x^5D^o$	25	4290	0.20	2.06	0.821	10
$a^5P-y^5S^o$	5	4285	0.22	1.62	1.732	1
$a^3H-u^3G^o$	27	4322	0.84	0.24	2.227	1
$a^3D-v^3P^o$	9	4354	0.62	0.71	2.165	1
$b^3P-r^3D^o$	15	4420	0.72	0.21	2.235	2
$a^3G-v^3G^o$	27	4450	0.18	0.76	1.872	6
$a^5P-y^5P^o$	15	4480	0.24	1.13	1.733	7
$a^5F-y^5F^o$	35	4535	0.30	1.97	0.824	13
$c^3P-x^3S^o$	3	4558	0.22	0.71	2.335	1
$a^5P-w^5D^o$	25	4640	0.28	0.91	1.734	8
$a^3H-x^3H^o$	33	4752	0.65	0.36	2.234	4
$c^3P-s^3D^o$	15	4803	0.55	0.53	2.33	3
$a^3H-z^3I^o$	39	4874	0.71	0.22	2.235	4
$a^3G-y^3H^o$	33	4908	0.47	0.52	1.873	5
$a^3D-u^3F^o$	21	4932	0.79	0.21	2.153	3
$b^1D-w^1F^o$	7	4975	0.85	−0.37	2.495	1
$a^5F-y^5G^o$	45	5017	0.08	1.73	0.838	12
$a^1H-z^1I^o$	13	5120	1.11	−0.14	2.567	1
$c^3P-w^3P^o$	9	5455	0.57	−0.19	2.335	1
$b^3F-w^3D^o$	15	5500	0.29	0.49	1.435	5
$b^1G-y^1G^o$	9	5644	0.95	−0.11	2.258	1
$b^1G-z^1H^o$	11	6091	1.04	−0.57	2.258	1
$b^3F-y^3G^o$	27	6280	0.63	0.37	1.442	4
$b^3F-x^3F^o$	21	6540	0.84	−0.39	1.445	2

TABLE 1—*Continued*

Multiplet	S	$\bar{\lambda}$	$\overline{\log X'_0}$	$\bar{Y}$	$\bar{X}_{J'}$	No. of Lines
	Ti I, $3d^24s4p-3d^24s4d$					
$z^1G^o-e^1H$	1320	4809	3.12	0.63	3.049	1
	Ti II, $3d^3-3d^24p$					
$a^4P-z^4D^o$	336	4310	1.38	1.28	1.165	7
$a^2G-z^2F^o$	337.5	4471	1.72	0.88	1.116	3
$a^2H-z^2G^o$	660	4550	1.95	0.89	1.569	3
$a^2P-z^2D^o$	9	4563	1.35	1.36	1.227	3
$b^2F-y^2G^o$	112.5	4377	1.68	−0.07	2.582	1
$b^2D-z^2D^o$	156.7	5208	1.50	0.52	1.564	3
	V I, $3d^44s-3d^44p$					
$a^6D-y^6D^o$	15	4115	0.09	2.09	0.278	8
$a^6D-y^6F^o$	21	4405	−0.12	2.07	0.280	11
$a^4H-z^4I^o$	26	4470	0.44	0.60	1.852	4
$a^4D-y^4D^o$	10	5625	0.15	0.36	1.076	2
$a^4D-y^4F^o$	14	5730	0.24	0.45	1.057	5
$a^4D-y^4P^o$	6	6080	−0.06	0.63	1.056	5
	Cr I, $3d^44s4p-3d^44s5s$					
$z^7D^o-f^7D$	35	5220	0.35	0.38	3.398	8
$y^5P^o-e^5D$	15	5240	0.45	−0.28	3.652	1
$z^7F^o-f^7D$	49	4670	0.31	0.82	3.118	14
$y^7P^o-f^7D$	21	5300	−1.14	1.72	3.434	8
$z^5F^o-e^5D$	35	5650	0.74	−0.16	3.831	3
$z^5D^o-e^5D$	25	6630	0.37	0.20	4.157	2
	Cr I, $3d^54s-3d^54p$					
$a^7S-z^7P^o$	7	4270	1.37	3.72	0.000	2
$a^5S-z^5P^o$	5	5206	1.52	3.32	0.937	3
	Mn I, $3d^64s-3d^64p$					
$a^6D-z^6D^o$	15	4050	0.03	2.76	2.152	9
$a^4D-y^4P^o$	6	4250	−0.22	2.05	2.918	7
$a^4D-z^4D^o$	10	4450	−0.10	1.96	2.914	10
$a^4D-z^4F^o$	14	4700	−0.04	1.90	2.904	7

TABLE 1—*Continued*

Multiplet	S	$\bar{\lambda}$	$\overline{\log X_0'}$	$\bar{\Gamma}$	$\bar{\chi}_{J'}$	No. of Lines
	Mn I, $3d^5 4s 4p - 3d^5 4s 5s$					
$z^8P^o - e^8S$	4	4800	0.14	2.91	2.290	3
$z^4P^o - e^4S$	2	5400	−0.22	1.13	3.835	3
$z^6P^o - e^6S$	3	6000	−0.01	1.96	3.060	3
	Mn I, $3d^5 4s 4p - 3d^5 4s 4d$					
$z^6P^o - e^6D$	3	4450	−0.52	2.64	3.060	8
	Fe I, $3d^7 4s - 3d^7 4p$					
$a^3F - y^3F^o$	21	4091	0.37	4.65	1.556	5
$b^3P - z^3S^o$	3	4062	−0.08	3.21	2.833	3
$a^3F - z^3G^o$	27	4251	0.05	4.49	1.523	6
$a^5P - z^5S^o$	5	4317	0.20	3.20	2.189	3
	Fe I, $3d^6 4s 4p - 3d^6 4s 5s$					
$z^7D^o - e^7D$	35	4225	0.40	3.86	2.439	10
$z^7F^o - e^7D$	49	4926	0.20	3.34	2.851	12
$z^3D^o - e^3D$	15	4970	0.22	1.92	3.907	6
$z^3F^o - e^3D$	21	5053	0.43	1.98	3.940	5
$z^7P^o - e^7D$	21	5193	0.31	3.25	2.979	9
$z^5D^o - e^5D$	25	5275	0.20	2.81	3.243	12
$z^3P^o - e^3D$	9	5672	0.14	1.84	4.220	6
$z^5F^o - e^5D$	35	5644	0.14	2.53	3.386	9
$y^5P^o - f^5D$	15	6766	0.15	1.23	4.593	7
	Ni I, $3d^9 4p - 3d^9 4d$					
$z^3P^o - f^3D$	63	4800	0.98	0.72	3.599	5
$z^3F^o - e^3F$	84	4295	1.30	0.59	3.700	2
$z^3F^o - e^3G$	324	4970	2.01	0.71	3.680	3
$z^3D^o - e^3F$	168	5010	1.47	0.42	3.698	4
$z^3D^o - f^3D$	105	5180	1.41	0.53	3.721	3
$z^3P^o - e^3P$	81	4900	1.09	0.67	3.642	4
$z^3P^o - e^3S$	36	5120	1.30	1.15	3.527	1
$z^3F^o - f^3D$	12	5020	0.11	1.53	3.626	2
$z^1F^o - e^1F$	28	5049	1.45	0.44	3.831	1
$z^1F^o - e^1G$	108	5081	2.03	0.53	3.831	1
$z^3D^o - e^3P$	27	5160	0.96	0.79	3.676	2
$z^1D^o - e^1F$	56	5156	1.75	0.41	3.881	1
$z^1D^o - f^1D$	35	5177	1.54	0.14	3.881	1
$z^1P^o - e^1S$	12	5411	1.08	0.16	4.072	1
$z^1P^o - f^1D$	21	5625	1.32	0.00	4.072	1
$z^1P^o - e^1P$	27	5695	1.43	−0.03	4.072	1

TABLE 1—*Continued*

Multiplet	S	$\bar{\lambda}$	$\overline{\log X'_0}$	$\bar{Y}$	$\bar{X}_{J'}$	No. of Lines
	Ni I, $3d^9 4p - 3d^9 6s$					
$z^3P^o - g^3D$	9	4290	0.35	0.51	3.642	1
$z^3F^o - g^3D$	21	4370	0.55	0.63	3.626	3
$z^1D^o - g^3D$	15	4430	0.40	0.60	3.704	4
$z^1F^o - g^1D$	7	4400	0.85	0.40	3.831	1
$z^1D^o - g^1D$	5	4481	0.70	0.75	3.881	1
	Zr I, $4d^3 5s - 4d^3 5p$					
$a^5F - y^5G^o$	45	4688	1.22	−0.93	0.727	1
	Zr II, $4d^3 - 4d^2 5p$					
$b^2F - x^2F^o$	40	4333	1.34	−0.83	2.399	1
$b^4P - z^4D^o$	336	4415	1.52	−0.04	1.208	7
$a^2H - z^2G^o$	660	4420	2.51	−1.53	1.502	2
$a^2G - z^2F^o$	337.5	4640	2.22	−1.06	0.987	2

tional material and reductions for each multiplet of each array. For each transition array the mean value of Y for each multiplet was plotted against the corresponding mean lower excitation potential, $\bar{X}_{J'}$. The value of the excitation temperature T was computed from the slope of the best straight line that could be drawn through the points, and the value of L was determined from the intercept on the Y-axis. Figure 2, *a* and *b*, show the plots for the arrays *Fe* I $3d^6 4s4p - 3d^6 4s5s$ and *Ti* I $3d^3 4s - 3d^3 4p$. Each dot represents a mean value of Y for a multiplet; the size of the dot is indicative of the number of lines in the multiplet. For each of these two arrays it was found desirable to perform a least-squares solution in order to fit the best straight line to the plotted points. The result for *Fe* I turns out to be

$$T = 4150^\circ \pm 50^\circ \text{ (P.E.)},$$

and for *Ti* I

$$T = 4350^\circ \pm 200^\circ \text{ (P.E.)}.$$

The results for each transition array are contained in Table 2. The weights assigned to the temperature determinations are proportional to the product of the number of lines and the range of excitation potential employed for each array. If we include, for the present, all of the material in Table 2, the weighted mean excitation temperature of the reversing layer turns out to be 4200°. If all the errors involved in the temperature calculation were purely observational, it would be correct to adopt the value of 4200° for the

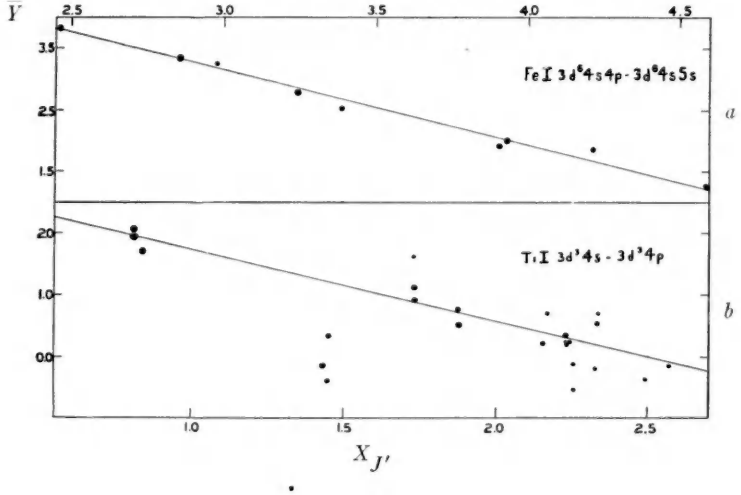

FIG. 2

mean temperature of the reversing layer. The departures of complex atoms from *LS* coupling and the existence of configuration interaction, however, produce errors in the calculation of theoretical multiplet strengths, which may be more serious than the observational errors. In order to facilitate the calculation of multiplet strengths on a large scale, it was necessary to assume that the electrons in an atom obey the rules of *LS* coupling and that individual configurations are isolated. *LS* coupling will occur when the spin-orbit interaction for a single electron is very small compared with the electrostatic interaction between electrons. This condition holds quite well for atoms of small nuclear charge. But as the nuclear charge increases, the spin-orbit interaction increases more rapidly than the

electrostatic interaction, and pronounced deviations from *LS* coupling occur. Certainly, for the atoms in the iron group, with which we have been chiefly concerned in the temperature determination, the assumption of *LS* coupling is no more than a first approximation. The most serious manifestation of departures from *LS* coupling is the overlapping of terms of different multiplicities and the consequent occurrence of intersystem combinations. The presence of

TABLE 2

Element	Transition Array	T	L	Weight
Ca I	$3d4s-3d4p$	1550	4.98	4
	$4s4p-4p^2$	2900	5.14	8
	$4s4p-4s4d$	2900	5.71	7
Ti I	$3d^34s-3d^34p$	4450	2.90	165
	$3d^24s4p-3d^24s5s$	2600	2.71	7
Ti II	$3d^3-3d^24p$	4800	2.51	28
V I	$3d^44s-3d^44p$	3850	2.19	46
Cr I	$3d^44s4p-3d^44s5s$	4150	4.56	20
Mn I	$3d^64s-3d^64p$	4850	5.21	26
	$3d^54s4p-3d^54s5s$	4350	5.43	14
Fe I	$3d^74s-3d^74p$	3650	6.19	17
	$3d^64s4p-3d^64s5s$	4150	6.47	167
Ni I	$3d^94p-3d^94d$	4800	4.78	16
	$3d^94p-3d^96s$	4450	4.74	2

intersystem lines in a spectrum usually implies that the strengths of permitted lines arising from the same lower levels are weaker than the simple theory indicates. The strengths of intersystem lines depend directly on the degree to which the levels of one term perturb the levels of another of differing multiplicity, and hence are a rough measure of the magnitude of departure from extreme *LS* coupling. In intermediate coupling there is no segregation of levels into terms, and all transitions obeying the *J*-selection rule are allowed.

It is significant that, while many intersystem lines are conspicuously strong in the spectra of iron-group atoms, they are considerably weaker, on the whole, than the permitted lines associated

with them. It appears reasonable to conclude, then, that of the two extreme types of coupling, *LS* and *jj*, the former is more nearly approximated by the atoms we are considering. It must be remembered, nevertheless, that *LS* coupling is no more than a first approximation to the true coupling, and that the multiplet strengths calculated on this basis will necessarily exhibit a considerable degree of scatter. In our determination of the solar temperature, however, the scatter will not be too serious a factor, provided a large number of lines varying widely in excitation potential are utilized. If, on the other hand, the calculated multiplet strengths are systematically too large as the excitation potential for the levels of the lower configuration increases, the negative slope of the $5040/T$ line will be too large, and the computed temperature will be too low. Another source of error in the calculation of multiplet strengths arises from the assumption that the configurations of a transition array are well isolated and are unperturbed by neighboring configurations. Actually, such isolation is rare in complex atoms, particularly with regard to the configurations $3d^k4p$ and $3d^{k-1}4s4p$ among atoms of the iron group. Because of the close proximity in the energies of the 3d and 4s electrons, the two configurations overlap and perturb each other to a large extent, with the result that each of the two configurations impresses its radiative characteristics on the other, and in so far as the ordinary selection rules are concerned, the configurations are indistinguishable from each other.

The existence of configuration interaction and of departures from *LS* coupling raises a question as to the reliability of the multiplet strengths utilized in the determination of the reversing-layer temperature. Fortunately, we have a means of checking our temperature calculation through the use of the *J*-file sum rule, which is valid for any coupling and is hence admirably suited to the problem. All the lines of a transition array which originate in (or terminate on) a given level constitute the *J*-file referring to that level—the sum of the strengths of these lines is the strength of the file. The *J*-file sum rule, which was first proved by Shortley, may be stated as follows:[10]

For any coupling, the strengths of the *J*-files referring to the levels

[10] Condon and Shortley, *Theory of Atomic Spectra*, p. 279.

of the initial/final configuration are proportional to $2J + 1$, provided that the jumping electron is not equivalent to any other in the final/initial configuration. In this statement the jumping electron may be equivalent to others in the initial/final configuration. In case it is not equivalent to others in *either* configuration, the sum rule holds for the files referring to *both* configurations. If the quantum numbers of the jumping electron are nl in configuration α and $n'l'$ in configuration β, the actual value of the strength of a file referring to a level of configuration α is

$$k(2J + 1)(l + 1)(2l + 3) \cdot \sigma^2 , \tag{7}$$

if $l' = l + 1$, and

$$k(2J + 1)(2l - 1)l \cdot \sigma^2 , \tag{8}$$

if $l' = l - 1$. Here k is the number of equivalent nl electrons in configuration α.

The determination of the solar temperature by means of the sum rule proceeds in a manner similar to that outlined above, except that the quantity X_0 is replaced by $\sum X_0$, where the summation is taken over the complete set of lines originating from a given lower J-level of the transition array, and the theoretical strength is replaced by the proper J-sum, which we denote by $\sum J$. An excellent feature of the sum-rule method is that it takes account of intersystem and interlimit combinations in the sums from the lower levels. In addition, when a near-by configuration perturbs the upper configuration of a transition array, we include in the sum all the lines from a given lower level to the levels of both upper configurations.[11] The sum-rule method thus takes into account completely both the departures from LS coupling and the influence of near-by configurations. Unfortunately, the application of the method requires the observation of complete sets of lines arising from the lower levels of an atom. For most atoms the material is not available, since many of the lines in a given set occur to the violet of λ 4036, the ultraviolet limit of Allen's measures. The lines of *Ti* I that arise from the configuration $3d^34s$ are nearly all available, however, and we have means of

[11] *Ibid.*, p. 281.

checking our previous temperature determination for *Ti* I. The most important transitions from the configuration $3d^34s$ are those to the configurations $3d^34p$ and $3d^24s4p$. The latter two configurations overlap each other and were therefore regarded as a single extended configuration in the calculation. Then, by (7) and (8), the sum of the strengths of all the lines originating from a level J of the configuration $3d^34s$ is equal to

$$\left.\begin{aligned} &3(2J+1)\phi_{4s-4p} + 18(2J+1)\phi_{3d-4p} \\ &\quad = 3(2J+1)(\phi_{4s-4p} + 6\phi_{3d-4p}) , \end{aligned}\right\} \tag{9}$$

and

$$\sum J = 3(2J+1) .$$

Table 3 lists the levels of $3d^34s$ that were available, the numbers of lines entering into the sum from each level, $\log \sum X_0$ for each set of lines and the corresponding value of $\log \sum J$, $\log \sum X_0/\sum J$, and the excitation potential $X_{J'}$ of each lower level. In Figure 3, $\log \sum X_0/\sum J$ is plotted against $X_{J'}$. The slope of the resulting straight line was computed by least squares and yields a value of $4400° \pm 100°$. The result agrees closely with the value of $4350°$ obtained by the use of individual line strengths. It is interesting to compare Figures 2 and 3 in connection with the qualitative theory of departures from *LS* coupling and of configuration interaction. The small amount of scatter in Figure 3 is conspicuous; what little there is can be ascribed to the presence of blends and to the observational errors. The behavior of the lines arising from the b^3F term provides a striking illustration of the effects of configuration interaction on the calculation of theoretical multiplet strengths. In Figure 2 the points corresponding to these lines fall far below the straight line. A glance at the *Ti* I term spectrum readily provides the explanation. The triad of terms y^3G^o, x^3F^o, and w^3D^o, of the configuration $3d^34p$, which combine with b^3F, are perturbed by neighboring terms of $3d^24s4p$, with the result that the lines of $3d^34s - 3d^34p$ are unduly weakened. When the transitions to the neighboring terms are included by means of the sum rule, the b^3F points are brought into much closer agreement with the others.

In adopting, for purposes of discussion, the best value of the temperature of the solar reversing layer, we need consider only the values derived from the lines of *Fe* I $3d^64s4p - 3d^64s5s$ (4150°),

TABLE 3

Term	J	No. of Lines	$1 + \log \Sigma X_0$	$\log \Sigma J$	$1 + \log \frac{\Sigma X_0}{\Sigma J}$	$X_{J'}$
a^5F.....	5	9	3.37	1.52	1.85	0.85
	4	12	3.30	1.43	1.87	0.83
	3	15	3.23	1.32	1.91	0.82
	2	10	3.22	1.18	2.04	0.82
	1	8	2.95	0.95	2.00	0.81
b^3F.....	4	12	2.51	1.43	1.08	1.45
	3	13	2.43	1.32	1.11	1.44
	2	10	2.30	1.18	1.12	1.42
a^5P.....	3	6	2.38	1.32	1.06	1.74
	2	7	2.16	1.18	0.98	1.73
	1	6	1.92	0.95	0.98	1.73
a^3G.....	5	10	2.28	1.52	0.76	1.88
	4	12	2.22	1.43	0.79	1.87
	3	8	2.05	1.32	0.73	1.87
a^3H.....	6	4	1.96	1.59	0.37	2.25
	5	3	1.83	1.52	0.31	2.24
	4	5	1.60	1.43	0.17	2.23
b^1G.....	4	5	1.68	1.43	0.25	2.26

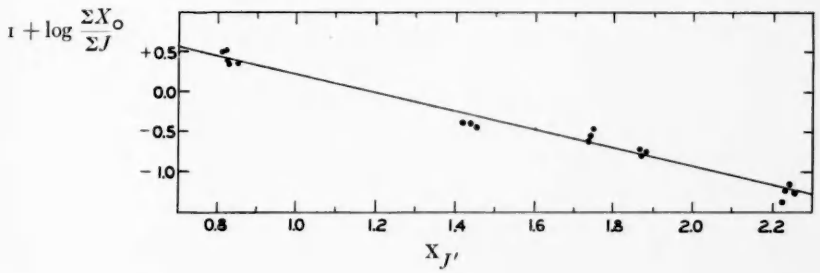

FIG. 3

Ti I $3d^34s - 3d^34p$ (4350°), and the value of 4400° calculated from the *Ti* I lines with the aid of the sum rule. All of the other determinations are of low weight and are of little significance. Since the

sum-rule method allows for all of the errors inherent in the calculation of multiplet strengths, we have chosen 4400° as the value best representing the mean effective excitation temperature of the solar reversing layer. There is still the possibility, however, that the difference between the *Fe* and *Ti* temperatures is real and that it indicates the presence of a temperature gradient in the reversing layer. If a pressure gradient exists in the solar atmosphere, the lines of easily ionized elements should arise from lower levels in the atmosphere than do the lines of elements that are more difficult to ionize. *Fe* I has an ionization potential of 7.8 volts, as compared with 6.8 volts for *Ti* I.

The temperature of 4400° is apparently inconsistent with the value of 5740° adopted in fitting the observations to the theoretical curve of growth. The lower value, however, is an excitation temperature, the higher one a kinetic temperature, and the two need not necessarily be the same. Furthermore, the method of computing the excitation temperature requires only an approximate knowledge of the kinetic temperature. A small error in v will produce an error only in the Doppler portion of the curve of growth, for, in the straight-line portions of the curve, v/c enters as a constant factor.

In the foregoing discussion we have assumed N_a to be constant with wave length. What effect will a variable opacity have on the determination of the reversing-layer temperature? If the general opacity of the solar atmosphere varies with wave length, N_a will exhibit a reciprocal variation. In an attempt to evaluate the opacity law we have assumed various temperatures and have determined the values of L for each multiplet. Since $\log N_a$ differs from L by an additive constant, we may examine the data for an opacity variation by plotting L against λ for each array and by noting the scatter in the observational points. If there is no systematic relation between the lower potential and the wave length, the scatter will obviously be a minimum for the temperature originally determined from the $5040/T$ diagram. Figure 4 shows the relation between excitation potential and wave length for the multiplets of *Ti* I $3d^3 4s - 3d^3 4p$ and for those of *Fe* I $3d^6 4s 4p - 3d^6 4s 5s$. It is quite obvious that the correlation is absent for the *Ti* I multiplets, but the mean lower excitation potentials of the *Fe* I multiplets show a progressive

increase with wave length. We should expect, therefore, that the law of opacity determined by equation (6) from the *Ti* I lines is independent of the temperature chosen. This expectation is verified when we plot the mean value of L for each multiplet against the corresponding mean wave length, with temperatures of 4500°, 5000°, and 5600° (Fig. 5). The three curves are very nearly parallel, but the scatter is slightly less for $T = 4500°$ than for either of the other two curves. Since, for the *Fe* I multiplets the mean lower ex-

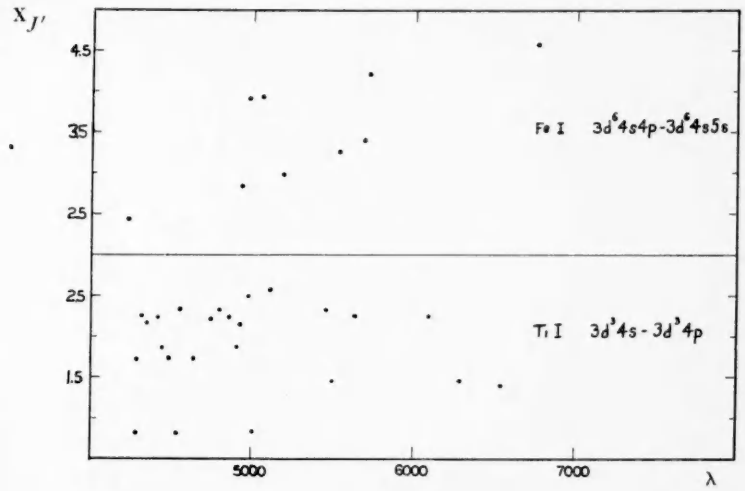

FIG. 4

citation potentials increase systematically with the wave length, the law of opacity determined from these multiplets by (6) should depend on the value of the temperature assumed. In Figure 6*a*, we have plotted the mean L's for the *Fe* multiplets against the mean wave lengths for a number of values of the temperature. The opacity law is seen to change conspicuously with the temperature. It is reasonable to assume, however, that the best value of the temperature to choose is that for which the scatter in the $L - \lambda$ diagram is a minimum. When we compute the sum of the squares of the residuals from the best straight line that can be drawn through each set of points, and plot the sums against the temperature, we find a sharp minimum at $T = 4100°$ (Fig. 6*b*). The resulting opacity

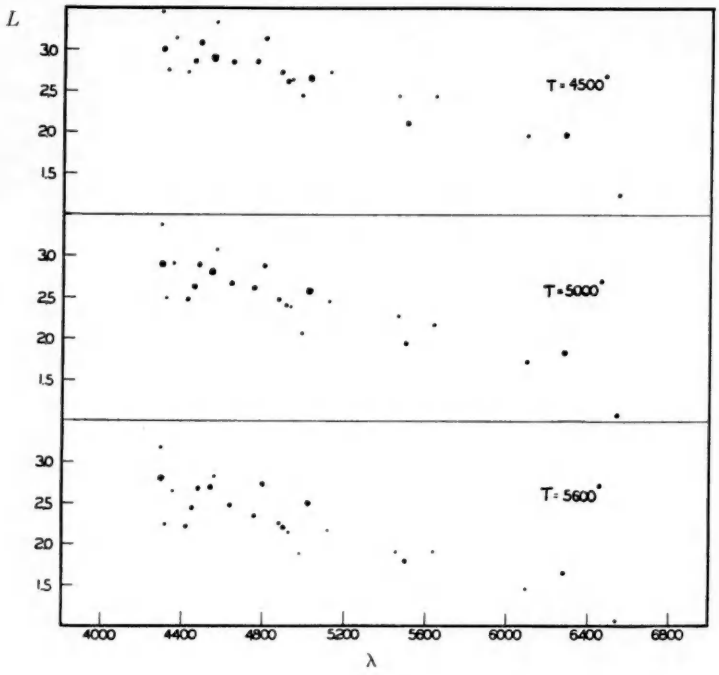
L
30
25
20
1.5
T = 4500°
T = 5000°
T = 5600°
4000
4400
4800
5200
5600
6000
6400
6800
λ

FIG. 5

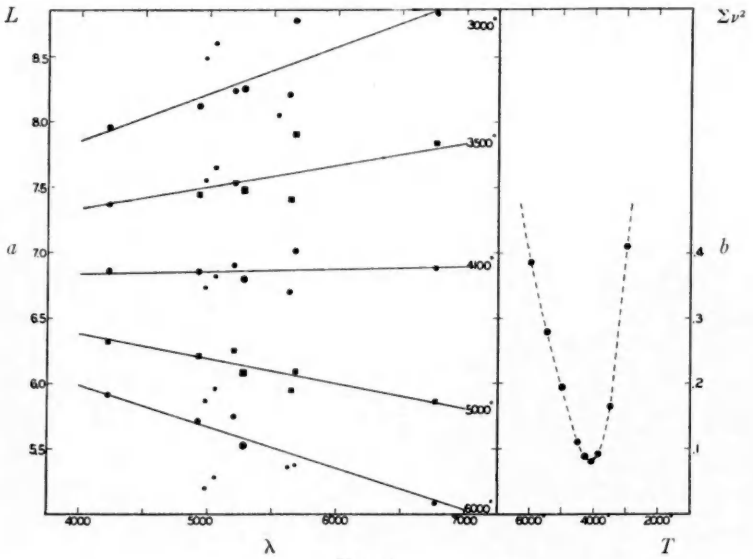
L
Σv²
a
b
8.5
8.0
7.5
7.0
6.5
6.0
5.5
.4
.3
.2
.1
3000°
3500°
4100°
5000°
6000°
4000
5000
6000
7000
6000
4000
2000
λ
T

FIG. 6

law appears to be sensibly constant with λ. The scatter for *Ti* is considerable. The best line that can be drawn to represent the observations is controlled almost completely by the three points arising from the term b^3F. We have already pointed out that the theoretical strengths for these multiplets are probably too large. The points are to be raised by an indeterminable amount. The final opacity law for *Ti* will probably not be inconsistent with the λ^3 relation.

The difference between the opacity laws thus derived for *Ti* and *Fe* remains unexplained. According to Menzel and Pekeris,[12]

$$\left.\begin{aligned} L &= \text{Const.} - 3 \log \lambda - \log (e^{hc/\lambda KT} - 1) \\ &= \text{Const.} - 3 \log \lambda - \frac{1.2 \times 10^{-4}}{\lambda}, \end{aligned}\right\} \qquad (10)$$

for a homogeneous atmosphere (λ in centimeters, and $T = 5000°$). The foregoing expression predicts an increase of L with the increasing wave length, exactly the reverse of the observational results just obtained.

It should be remembered, however, that the theoretical opacity law was obtained on the assumption of a continuously varying quantum defect, to represent the effect of overlapping of successive series limits of the atoms undergoing ionization. The formula probably represents an upper limit for the opacity. The effect of all series limits to the red of a given wave length λ_0 is represented by the formula

$$L = \text{Const.} - 3 \log \lambda - \log (e^{hc/\lambda_0 KT} - 1) . \qquad (11)$$

The relation between L and λ is very sensitive to the distribution of the neglected continua, and perhaps a constant opacity is not seriously in disagreement with theory. The λ^3 opacity law so frequently employed by investigators is seen to have a possible theoretical justification, though it does omit from consideration all continua originating in the visible spectral range.

The quantity L depends only on the product of N_a, the total number of atoms of a given element in a given stage of ionization above 1 square centimeter of the photosphere, and ϕ, the radial quan-

[12] *M.N.*, **96**, 77, 1935; cf. also Menzel, *loc. cit.*

tum integral for a transition array. If the relative ϕ's for different atoms are determined from quantum-mechanical calculations, the relative abundances of the elements may be computed. When the absolute values of the ϕ's are known, it will be possible to determine the absolute abundance of any element in a given stage of ionization. A quantitative study of abundances in the solar reversing layer, based on the foregoing considerations, is now in progress at the Harvard Observatory.

The unexpectedly low temperature here derived is not without precedent. In 1922, R. T. Birge,[13] who analyzed the solar *CN* bands by a method consistent with the one employed here, derived a solar temperature of $4300° \pm 500°$. Later band-spectrum analyses by Richardson[14] gave somewhat higher values but much greater probable errors. The temperature here determined is an effective excitation temperature. Any departures of the partition from thermodynamic equilibrium will be included in the result. The straightness of the line in Figure 3 indicates that such departures are small. The energy most effective for exciting atoms is that close to the center of the already existing Fraunhofer line. Consequently, the excitation temperature deduced might be expected to approach that of a black body emitting, not with photospheric intensity, but with an intensity corresponding to the emission in the line centers.[15] The low excitation temperature may be related to the known deficiency of solar radiation in wave lengths 4000–3000 A. Coblentz and Stair[16] have recorded an effective temperature of 4000°, as deduced from the gradient of intensity in the region 3400–2900 A.

It is a pleasure to record our appreciation to Dr. G. H. Shortley for his useful suggestions and comment on the solar temperature determination.

HARVARD OBSERVATORY
October 1937

DEFINITIONS OF ALGEBRAIC NOTATION

W	Equivalent width in IA
λ	Wave length
ν	Frequency

[13] *Ap. J.*, **55**, 273, 1922.
[14] *Ibid.*, **73**, 216, 1931.
[15] Cf. suggestion by Stewart, *M.N.*, **85**, 732, 1935.
[16] *Nat. Bur. Stand. Research Paper RP 899*, 1936.

v	Root-mean-square kinetic velocity
Γ	Damping factor
f	Oscillator strength
$A(J, J')$	Einstein A
$s/\Sigma s$	Theoretical strength of a line in terms of the summed strength for the multiplet
S	Theoretical strength of a multiplet in a transition array in units of σ^2
σ^2	The square of the first-order radial component of electric moment for the given array
a_0	The radius of the first Bohr orbit
ϵ	Electronic charge
ϕ	$\sigma^2/a_0^2\epsilon^2$, i.e., σ^2 in atomic units
T	Temperature
N_a	The total number of atoms, per square centimeter column, of a given element in a given stage of ionization
$X_{J'}$	Excitation potential
$b(T)$	Partition function
μ	Molecular weight
R	Rydberg constant

NOTE ADDED IN PROOF

Our attention has been directed to a letter in *Nature*, **113**, 338, 1924 (cf. also *M.N.*, **85**, 732, 1925), by J. Q. Stewart, in which he points out that the conventional Schwarzschild value of 0.85 of the photospheric temperature for the temperature of a stellar reversing layer is subject to question, since in view of the small observed central intensities of absorption lines a stellar atmosphere may by no means be considered as a gray body. Stewart shows that the conventional temperature of 5100° for the solar reversing layer leads to a central intensity of 0.50 for the sodium D lines, and that a temperature of about 4000° is required by the Planck formula to reduce the central intensity to the observed value of 0.10. He suggests that an average temperature of about 0.7, that of the photospheric temperature, should be adopted for stellar reversing-layer temperatures.

ULTRAVIOLET ABSORPTION SPECTRA OF SOME EARLY-TYPE STARS*

WALTER S. ADAMS AND THEODORE DUNHAM, JR.

ABSTRACT

Measures of wave length, estimates of intensity, and identifications are given for absorption lines in the ultraviolet spectra of two O-type stars and six stars of types B0 to B2. The region investigated is between λ 3050 and λ 3400, results in some cases being added as far as λ 3650. Especially prominent elements are *O* II, *O* III, *Si* III, *Si* IV, *S* III, *S* IV, *Ne* II, *He* I, *He* II, and *N* II. A list of the interstellar lines observed in the spectrum of 55 Cygni is also given.

The spectra of stars in the region λλ 3100–3500 have, in the past, been studied in detail comparatively little, partly because of the necessity for the use of a quartz spectrograph or concave grating but chiefly because of the low reflecting-power of silver-on-glass telescopes in this region. The use of aluminium coats on glass mirrors has now obviated the greatest difficulty, and the development of the Schmidt spectrographic camera and of plane gratings with great concentration of light in the first or second order has facilitated the use of slit spectrographs of relatively high dispersion.

The results given in this brief communication were obtained largely as a by-product in the course of a search for new interstellar lines in the ultraviolet region; and the spectrograms measured are, in several cases, those upon which the *Ti* II and a few unidentified interstellar lines appear. The stars were selected for observation either on the basis of the intensity of the interstellar H and K lines or for the characteristics of their spectra in the usual photographic region. The narrowness and, in some cases, the extreme faintness of the newly observed interstellar lines have made it necessary at times to use contrasty fine-grained plates (such, for example, as the Eastman III-O emulsion); and such spectrograms have been most useful in the detection and measurement of faint stellar lines as well.

Two spectrographs have been used in the course of the investigation, both at the coudé focus of the 100-inch telescope. In one instrument a 30° quartz prism aluminized on the rear surface forms the

* *Contributions from the Mount Wilson Observatory, Carnegie Institution of Washington*, No. 583.

spectrum, the light passing through the slit to an aluminized parabolic collimating mirror (figured for use off the axis), thence to the prism, which returns it to the mirror, which in turn focuses the spectrum on a plate immediately below the slit. The focal length of the mirror, which serves as both collimator and camera, is 9 feet. The spectrograph gives a linear scale of about 8 A/mm at λ 3200 and good definition over a range of a few hundred angstroms. This limitation of field is unavoidable, owing to the use of a mirror as the camera. A further drawback with this instrument is the short extent of spectrum which is suitably exposed, plate sensitivity and reduced dispersion both tending to make the spectrograms overexposed at λ 3400 when at λ 3100 the density is barely adequate.

The second spectrograph consists of a Schmidt camera[1] with a focal length of 32 inches used in the bright second order of a plane Wood grating. The thin correcting plate is of Vitaglass and transmits light to below λ 3100, although at this wave length the quartz spectrograph is slightly superior. With the Schmidt camera the full length of spectrum on the suitably curved plate is in excellent focus, and the density is such that individual spectrograms have been measured from λ 3100 to λ 3700 and from λ 3300 to λ 4400. The linear scale of the spectra is 10.3 A/mm.

Tables 1 and 2 contain the results of the measures of stellar lines and the laboratory wave lengths of the lines with which identifications have been made. These have been taken almost wholly from the *Multiplet Table of Astrophysical Interest* by Charlotte E. Moore. The stellar wave lengths are followed by figures in parentheses, giving visual estimates of intensity on a scale of 1 to 10. These are to be considered merely as approximate. The wave lengths are given to the nearest tenth of an angstrom, the quality of the stellar lines in most cases not admitting of higher precision. A colon placed after the element in the column of identifications indicates uncertainty.

The spectrograms of the stars listed in Table 1 were taken with the 9-foot quartz spectrograph and have been measured over but a limited region from below λ 3100 to about λ 3350. Several of the stars in Table 2, however, have been observed with the Schmidt spectrograph; and the measures have been extended to longer wave

[1] Dunham, *Phys. Rev.*, **46**, 326, 1934.

TABLE 1

STELLAR LINES

λ_1 Orionis O8	ι Orionis O8	ϵ Orionis Bo	τ Scorpii B1	Identification
3023.4 (2)				3023.4 *O* III
3024.5 (2)				3024.6 *O* III
3035.3 (1)				3035.4 *O* III
3037.7 (1)				
3043.2 (2)		3043.1 (2)		3043.0 *O* III
3047.1 (5)		3047.2 (3)		3047.1 *O* III
3059.2 (3)		3059.4 (2)		3059.3 *O* III
3063.4 (1)		3063.4 (1)		
3067.5 (1)				
		3086.3 (2)		3086.3 *Si* III
		3093.5 (2)		3093.5 *Si* III
3097.3 (4)		3097.4 (4)	3097.4 (2)	3097.5 *Si* IV
3117.8 (3)		3117.7 (3)		3117.8 *S* IV
3121.7 (1)		3121.8 (1)		3121.7 *O* III
3133.1 (2)				3132.9 *O* III
		3134.7 (2)	3134.9 (2)	3134.8 *O* II
			3136.4 (1)	
3149.6 (1)		3149.8 (2)	3149.7 (3)	3149.6 *Si* IV
		3165.6 (2)	3165.9 (3)	3165.7 *Si* IV 3165.7 *Ne* II
3187.7 (2)	3187.2 (3)	3187.9 (3)	3187.9 (5)	3187.7 *He* I
3194.0 (1)	3193.8 (2)			3194.4 *O* III
3203.1 (4)	3203.4 (4)	3203.4 (2)	3203.2 (3)	3203.2 *He* II
3218.3 (1)				
	3219.5 (2)			
	3225.2 (2)			
			3232.6 (1)	3232.4 *Ne* II
			3244.2 (1)	
	3247.5 (3)			
3260.8 (2)	3261.0 (2)	3260.9 (2)		3261.0 *O* III
3265.4 (2)	3265.6 (2)	3265.4 (1)		3265.5 *O* III
3267.3 (1)				3267.3 *O* III
	3278.0 (2)			
	3309.1 (2)			
	3312.3 (2)			3312.3 *O* III
	3334.9 (3)	3335.0 (3)		3334.9 *Ne* II
	3341.2 (4)	3341.5 (2)		3340.7 *O* III
	3354.9 (2)	3354.9 (2)		3354.5 *He* I 3355.0 *Ne* II

TABLE 2

STELLAR LINES

β Can. Maj. cB1	ε Can. Maj. B1	χ^2 Orionis cB1	γ Pegasi B2	Identification
3086.5 (5)	3086.3 (5)	3086.4 (8)	3086.3 (6)	3086.3 *Si* III
3093.5 (4)	3093.4 (5)	3093.6 (7)	3093.6 (4)	3093.5 *Si* III
3096.8 (3)	3096.9 (2)	3096.9 (3)	3096.8 (2)	3096.8 *Si* III
.....	3104.8 (1)	3104.4 (1)	3104.8 (2)	3104.7 *Mg* II
.....	.....	3106.9 (1)	.....	.....
3115.8 (1)	.....	.....	.....	3115.7 *O* III:
3117.4 (1)	.....	.....	.....	.....
3122.6 (1)	.....	.....	.....	3122.6 *O* II
3129.3 (2)	3129.3 (1)	.....	.....	3129.4 *O* II
3134.1 (1)	.....	.....	.....	3134.3 *O* II
3134.7 (3)	3134.6 (2)	3134.7 (2)	.....	3134.8 *O* II
3136.4 (1)	3136.6 (2)	.....	.....	.....
3138.4 (2)	3138.3 (1)	.....	.....	3138.4 *O* II
3139.7 (1)	3139.7 (1)	.....	.....	3139.8 *O* II
3149.6 (1)	.....	.....	.....	3149.6 *Si* IV
3159.1 (1)	.....	.....	.....	.....
3165.7 (2)	.....	.....	.....	3165.7 *Si* IV 3165.7 *Ne* II
3174.1 (1)	3174.1 (2)	.....	.....	.....
3175.9 (2)	3175.9 (1)	3176.2 (2)	.....	.....
3178.1 (1)	3178.0 (1)	.....	.....	.....
3179.3 (1)	3179.1 (1)	.....	.....	.....
3185.2 (1)	3185.1 (1)	.....	.....	.....
3186.0 (1)	.....	.....	.....	.....
3187.7 (10)	3187.7 (6)	3187.8 (6)	3187.8 (6)	3187.7 *He* I
3196.5 (1)	3196.5 (1)	.....	.....	3196.7 *He* I
3198.7 (1)	.....	3199.1 (1)	.....	3198.6 *Ne* II
3210.6 (1)	.....	.....	.....	.....
3218.2 (1)	.....	.....	.....	3218.2 *Ne* II
3219.4 (1)	.....	.....	.....	3219.3 *P* III:
3230.4 (1)	.....	.....	.....	3230.2 *Ne* II
3234.0 (2)	.....	.....	.....	3234.0 *Si* III
3241.7 (2)	3241.8 (2)	3242.0 (1)	.....	3241.7 *Si* III
3244.1 (1)	.....	.....	.....	.....
.....	3258.3 (1)	.....	.....	.....

TABLE 2—*Continued*

β Can. Maj. cB1	ε Can. Maj. B1	χ^2 Orionis cB1	55 Cygni cB2	Identification
3266.9 (3)	3266.9 (2)	3267.0 (4)	3267.0 (3)	
3270.8 (1)				3270.8 *Ne* II 3271.0 *O* II
				3273.5 *O* II
3273.5 (1)	3273.5 (1)	3276.3 (2)	3276.2 (2)	
3276.1 (3)	3276.4 (2)			
3277.5 (1)				3277.7 *O* II
		3280.5 (1)		
3285.9 (1)				
3287.5 (2)				3287.6 *O* II
3288.9 (2)		3288.9 (2)		
3290.0 (1)				3290.1 *O* II
3296.7 (1)		3296.9 (2)		3296.8 *He* I
3305.2 (2)	3305.2 (2)	3305.3 (2)		3305.2 *O* II
3306.4 (1)				3306.6 *O* II
		3318.1 (1)		3318.1 *N* II
3323.8 (1)				3323.8 *Ne* II 3324.0 *S* III
3324.9 (3)	3324.9 (2)	3324.9 (2)		3324.8 *S* III
3327.2 (1)				3327.2 *Ne* II
3328.8 (1)		3328.8 (2)		3328.8 *N* II
3334.9 (2)		3334.9 (1)		3334.9 *Ne* II
3339.4 (1)		3339.4 (1)		
3344.5 (1)				3344.4 *Ne* II
3354.7 (3)	3354.6 (2)	3354.7 (3)	3354.6 (2)	3354.5 *He* I 3355.0 *Ne* II
3360.6 (1)				3360.7 *Ne* II
3367.2 (2)		3367.2 (1)		3367.2 *S* III
3369.4 (1)		3369.7 (1)		3369.5 *S* III
3370.4 (1)				3370.4 *S* III
3377.2 (2)				3377.2 *O* II
3387.2 (1)				3387.1 *S* III
3390.3 (3)	3390.5 (2)			3390.3 *O* II
3407.3 (1)				3407.4 *O* II
3437.2 (2)	3437.1 (2)	3437.2 (4)	3437.0 (3)	3437.2 *N* II
3447.6 (4)	3447.7 (2)	3447.7 (3)	3447.6 (2)	3447.6 *He* I 3448.0 *O* II
3470.6 (3)				3470.6 *O* II
			3479.1 (2)	
		3487.7 (2)	3487.7 (1)	
3497.3 (3)	3497.5 (2)	3497.4 (1)		
		3498.9 (1)	3498.7 (2)	
			3508.9 (1)	

TABLE 2—*Continued*

β Can. Maj. cB1	ε Can. Maj. B1	χ^2 Orionis cB1	55 Cygni cB2	Identification
.....	3512.6 (2)	3512.5 (3)	3512.7 (2)	.....
3530.5 (2)	.....	3530.5 (3)	3530.5 (3)	3530.8 *K* II:
3554.4 (4)	3554.5 (4)	3554.5 (4)	3554.6 (3)	3554.5 *He* I
3586.0 (1)	.....	.....	3586.1 (1)	.....
3587.3 (5)	3587.4 (4)	3587.5 (5)	3587.3 (4)	3587.3 *He* I
3590.5 (3)	3590.6 (2)	.....	.....	3590.5 *Si* III
3595.0 (1)	.....	.....	.....	.....
3599.4 (1)	.....	3599.3 (1)	.....	3599.4 *He* I
3600.9 (1)	.....	.....	.....	.....
3601.7 (2)	3601.6 (2)	3601.5 (2)	3601.8 (2)	3601.3 *Al* III
3604.0 (2)	.....	3603.9 (1)	.....	.....
3612.4 (2)	.....	.....	3612.3 (1)	3612.4 *Al* III
3613.6 (5)	3613.7 (3)	3613.7 (3)	3613.6 (3)	3613.6 *He* I
3626.6 (1)	.....	.....	.....	.....
3632.0 (2)	.....	3632.1 (1)	.....	3632.0 *S* III
3634.2 (6)	3634.3 (4)	3634.3 (5)	3634.3 (4)	3634.3 *He* I
3649.8 (1)	.....	.....	.....	.....
3652.1 (3)	.....	.....	.....	3652.1 *He* I
3656.6 (1)	.....	.....	.....	3656.6 *S* III
3661.8 (1)	.....	.....	.....	3662.0 *S* III
3664.0 (1)	.....	.....	.....	.....

lengths. Lines of the Balmer series of hydrogen have not been included.

An examination of the results shows satisfactory identifications for a large proportion of the stronger lines. Of the unidentified lines in Table 1, the greater part appear in the spectrum of ι Orionis and are vague and difficult of measurement. Some may, perhaps, be portions of the atmospheric ozone bands which occur in this region of the spectrum. In Table 2 two fairly prominent unidentified lines at λ 3267 and λ 3276 have been observed in the spectra of all four stars. It seems probable that these lines and perhaps λ 3289 are due to the same element.

A comparison of the identified lines shows clearly the change in degree of ionization even within the relatively small spectral range of the stars observed. The *O* III and *S* IV lines of Table 1 have been replaced by lines of *O* II and *S* III in the stars of Table 2. As would be expected, the *He* II line at λ 3203 has disappeared in the later stars, while lines of *He* I have become more prominent. *Ne* II lines are especially well marked in the stars of Table 2, and 7 lines due

wholly to this element have been recognized in the spectrum of β Canis Majoris between λ 3166 and λ 3407. The *Mg* II line at λ 3105, which is the analogue of λ 4481, is well seen in the spectrum of γ Pegasi of type B2. Of other elements, the identification of λ 3219 with a line due to *P* III seems possible, the other line of the doublet at λ 3233.6 being masked by *Si* III; the identification of λ 3530.5 with *K* II is doubtful, while that of the *Al* III pair at λ 3602 and λ 3612 seems quite certain.

A spectrogram of 55 Cygni taken with the 32-inch Schmidt camera on a plate of the III-O emulsion is well exposed over the range $\lambda\lambda$3300–4400 and has been measured throughout. To the red of λ 3800 the spectra of early B-type stars have been thoroughly studied

TABLE 3

INTERSTELLAR LINES

55 Cygni cB2	Identification	55 Cygni cB2	Identification
3302.37 (3)	3302.38 *Na* I	3968.48 (7)	3968.49 *Ca* II
3303.00 (1)	3302.98 *Na* I	4226.73 (1)	4226.74 *Ca* I
3383.77 (2)	3383.77 *Ti* II	4232.59 (2)	.....
3933.69 (12)	3933.68 *Ca* II	4300.32 (1)	.....
3957.75 (1)	.....	.....	.....

by Struve,[2] and for this reason the stellar lines are not repeated here. The spectrum of this star, however, shows the interstellar lines exceptionally clearly; and for the sake of completeness their wave lengths are listed in Table 3, including those which have not yet been identified.[3]

A few spectrograms of β Orionis cB8 taken in the extreme ultraviolet show a remarkable amount of detail between λ 3040 and λ 3300. Lines of *Fe* II, *Cr* II, and *Ti* II are numerous and prominent; λ 3104.7 of *Mg* II is strong; and the principal lines of the *Si* III multiplet beginning at λ 3086 are well measurable. The *Ca* II triplet $\lambda\lambda$ 3159, 3179, and 3181, which is prominent in the spectrum of α Cygni, is present but much fainter in the spectrum of β Orionis.

CARNEGIE INSTITUTION OF WASHINGTON
MOUNT WILSON OBSERVATORY
October 1937

[2] *Ap. J.*, **74**, 225, 1931. [3] Dunham, *Pub. A.S.P.*, **49**, 26, 1937.

THE SPARK SPECTRUM OF IRON, λλ 5016–7712 WITH IDENTIFICATIONS OF *Fe* II LINES IN THE SOLAR SPECTRUM*

ARTHUR S. KING

ABSTRACT

The spectrum of iron from a strong spark discharge was examined in the region of wave length above λ 5000. Wave lengths of 127 lines due to ionized iron were obtained, in the main belonging to *Fe* II, although the structure of a few lines suggests *Fe* III as a possible origin.

A comparison with the solar spectrum resulted in the identification of 78 lines in this region as due at least in part to *Fe* II. Of these, 37 were identified as *Fe* II in the *Revised Rowland*. Other solar lines were found to agree with *Fe* II lines previously predicted from term values and now measured in the spark spectrum. In addition to the solar lines clearly identified, 13 *Fe* II lines are masked by foreign lines, and their identifications are uncertain. Since a large proportion (31) of the lines identified as *Fe* II have the faintest solar intensities (−2 and −3), the identification of solar *Fe* II lines in this region is probably essentially complete.

The lines measured in the spark spectrum include lines, some of them predicted, which are prominent in the spectra of novae.

The spectrum of the iron spark produced by a discharge with high capacity has been examined in an endeavor to find additional lines of *Fe* II in the region of wave length greater than λ 5000. For shorter wave lengths, the vapor close to the pole of an iron arc is very effective in giving *Fe* II lines; and as these "polar" lines can be measured with high precision, it has been a preferred source. In the region beyond λ 5000, however, comparatively few lines of ionized iron have been recorded, although hundreds may be predicted from known term values. Most of these predicted lines are doubtless very faint, but the fact that a considerable number correspond to lines in the solar spectrum[1] (conforming to the criterion for enhanced lines by being weaker or absent in the sunspot spectrum) suggests that a strong source of *Fe* II radiation might bring out lines not previously observed in the laboratory.

A study of the spectrum of high-power spark discharges was therefore undertaken, two distinct sets of apparatus being available. In

* *Contributions from the Mount Wilson Observatory, Carnegie Institution of Washington*, No. 584.

[1] C. E. Moore, *A Multiplet Table of Astrophysical Interest*, Princeton, 1933.

one, a large condenser connected, by leads with minimum inductance, with a pair of bluntly pointed iron electrodes 5–6 mm apart. The condenser, made up of vertical glass plates coated with copper foil, in air, had its sections connected to give approximately 2 microfarads. The voltage of the transformer was adjusted to give a condenser discharge across the gap about sixty times per minute. These highly disruptive sparks produced little heating or wear of the spark terminals. The spectrum was photographed in the first order of the 15-foot concave grating, an exposure of one hour giving a strong spectrum on the Eastman I-F plate as far as λ 6600.

The second apparatus was that regularly used in the production of spark spectra. An oil-immersed condenser of approximately 0.05 microfarad capacity was charged without rectification by a 40,000-volt Wappler transformer. A spark gap between brass spheres was connected in series with the iron spark gap. This series gap was lengthened to a maximum which permitted the passage of a very noisy stream of sparks at the iron gap without fusion of the terminals. Eastman III-F plates were used, with exposures of 5–20 minutes for the panchromatic region.

When spectra produced by the two discharge arrangements were brought to the same general intensity, gauged by the approximate equality of *Fe* I lines, the air spectrum, and the continuous background, no appreciable difference in the strength of the *Fe* II spectrum was to be seen. Evidently the proportion of ionized atoms was about the same in each spark, and the high luminosity of the spark passing once per second was compensated by the greater frequency of the discharge with smaller capacity. The radiation of the latter was probably intermittent to a small degree only, owing to the persistence of ionized vapor between successive discharges.

To facilitate the selection of *Fe* II lines, a strong spectrum of the iron arc was photographed adjacent to the spark spectrum on one side, and on the other to the spectrum of the spark in air between aluminium electrodes. The latter gave very strong air lines and at once identified those occurring in the iron spark spectrum. As standards for measuring the *Fe* II lines, low-temperature *Fe* I lines of moderate strength were used, these being sharp in the spark spec-

trum. The very slight displacement of such lines to be expected from the high excitation appeared to be within the errors of micrometer settings, as no systematic differences from either the predicted wave lengths or those of the corresponding solar lines were observed. The *Fe* II lines, although never really sharp, even with the moderate dispersion used, were in nearly all cases symmetrical. For the stronger ones, good agreement, sometimes justifying three decimal places, was found in the wave lengths from seven spectrograms for the range λλ 5000–6700, and from four plates in the near infrared. The spectrograms reached to λ 9000, but no *Fe* II lines beyond λ 7712 were detected.

Close coincidences with *Fe* I lines are sometimes found, in which the spark wave length is affected by the blend. Noteworthy among these are λλ 7307.9, 7320.7, and 7376.4, blending with *Fe* I lines which, in the arc, in each case measured within 0.03 A of the spark wave length. The blends are shown by distinct enhancement in the spark spectrum, and two of the lines are predicted members of the *Fe* II multiplet $b^4D - z^4D^o$, the other members of which did not appear in the arc spectrum.

A group of lines which are wide and diffuse in the iron spark spectrum deserve special mention. These resemble air lines but are absent in the air spectrum. Their structure is denoted by "N" and "n" after the intensity number, and in some cases only very rough wave-length measures could be made. Some of these lines may be found to come from doubly ionized iron. Two of them, λ 5785 and λ 6061, were, however, predicted by Charlotte E. Moore, and their high E.P. (7.7 volts) indicates that all lines of the group may be from high levels of *Fe* II. One of these hazy lines, λ 5833.65, shows fair agreement with a solar line, also of nebulous structure, and apparently masks a predicted *Fe* II line, λ 5833.66.

The wave lengths in Table 1 were measured by the writer, with the exception of two for which the arc wave lengths were preferable, on account of their great strength in the spark, and three very faint ones for which the predicted values were used. The intensities were estimated from the spark spectrum. For much of the other material in the table, and especially for assistance in the identification of solar

TABLE 1

THE SPECTRUM OF IONIZED IRON, λλ 5018–7712

λ	Int.	Multiplet	Lower E.P.	Solar λ	Solar Int.		Solar Ident.
					Disk	Spot	
5018.437[1]	800	$a^6S_{2\frac{1}{2}}-z^6P^\circ_{2\frac{1}{2}}$	2.879	.452	4	3	Fe^+
5036.4	3N	.....	.....	.....	.....	.....	.....
5036.92[2]	2	$b^4F_{3\frac{1}{2}}-z^6P^\circ_{3\frac{1}{2}}$	2.816	.931	−1	od	Fe, Fe^+
5074.07	2	.....	.....	.071	−3N	.....	Fe^+?
5086.8[3]	1	.....	.....	.....	.....	.....	.....
5087.25[4]	3	.....	.....	.....	.....	.....	.....
5093.53	4	.....	.....	.....	.....	.....	.....
5100.95[5]	15	.....	.....	.939	−2	.....	Fe^+
5101.48	2N	.....	.....	.....	.....	.....	.....
5127.859	8	$c^2F_{2\frac{1}{2}}-z^2F^\circ_{2\frac{1}{2}}$	5.547	.884	−3	.....	Fe^+, C_2
5147.09	2	.....	.....	.106	−2	ob	Fe^+?
5149.7	5N	.....	.....	.....	.....	.....	.....
5156.10	6	.....	.....	.072	−2	.....	Fe^+
5159.93	4	.....	.....	.....	.....	.....	.....
5160.84	5	$c^2F_{3\frac{1}{2}}-z^2F^\circ_{3\frac{1}{2}}$	5.545	.838	−3N	.....	Fe^+
5169.029[6]	1000?	$a^6S_{2\frac{1}{2}}-z^6P^\circ_{3\frac{1}{2}}$	2.879	.052	4	2	Fe^+
5197.590	100	$a^4G_{2\frac{1}{2}}-z^4F^\circ_{1\frac{1}{2}}$	3.217	.578	2	o	Fe^+
5216.5	10N	.....	.....	.....	.....	.....	.....
5227.0	15N	.....	.....	.....	.....	.....	.....
5234.630	150	$a^4G_{3\frac{1}{2}}-z^4F^\circ_{2\frac{1}{2}}$	3.207	.632	2	1	Fe^+
5256.93[7]	1	$a^6S_{2\frac{1}{2}}-z^6F^\circ_{2\frac{1}{2}}$	2.879	.934	−1	−3	Fe^+
5261.0	15N	.....	.....	.....	.....	.....	.....
5264.796	15	$a^4G_{2\frac{1}{2}}-z^4D^\circ_{1\frac{1}{2}}$	3.217	.810	1	o	Fe^+
5272.476[8]	15	$d^2D_{2\frac{1}{2}}-y^2_4D^\circ_{2\frac{1}{2}}$	5.930	.406	−2	ob	Fe^+
5276.00	100	$a^4G_{4\frac{1}{2}}-z^4F^\circ_{3\frac{1}{2}}$	3.186	.001	3	1	Fe^+
5278.99	4	$d^2D_{1\frac{1}{2}}-x^4F^\circ_{1\frac{1}{2}}$	5.885	.962	−2	ob	Fe^+-S?
5284.09	8	$a^6S_{2\frac{1}{2}}-z^6F^\circ_{3\frac{1}{2}}$	2.879	.114	2	o	Fe^+
5316.654[9]	400	$a^4G_{5\frac{1}{2}}-z^4F^\circ_{4\frac{1}{2}}$	3.139	.622	4	2	Fe^+
		$a^4G_{3\frac{1}{2}}-z^4D^\circ_{2\frac{1}{2}}$	3.207	.783	3	2	Fe^+
5325.563	10	$a^4G_{3\frac{1}{2}}-z^4F^\circ_{3\frac{1}{2}}$	3.207	.562	2	1	Fe^+
5337.74	4	$a^4G_{2\frac{1}{2}}-z^4D^\circ_{2\frac{1}{2}}$	3.217	.729	o	−1bl	Fe^+
5346.55[10]	1	$a^4G_{2\frac{1}{2}}-z^4F^\circ_{3\frac{1}{2}}$	3.217	.549	od	o	Fe^+-
5362.87	60	$a^4G_{4\frac{1}{2}}-z^4D^\circ_{3\frac{1}{2}}$	3.186	.871	3	2	Fe^+
5387.8	2N	.....	.....	.....	.....	.....	.....
5408.86[11]	5	.....	.....	.....	.....	.....	.....
5414.09	5	$a^4G_{3\frac{1}{2}}-z^4D^\circ_{3\frac{1}{2}}$	3.207	.077	o	−1	Fe^+
5425.262	8	$a^4G_{4\frac{1}{2}}-z^4F^\circ_{4\frac{1}{2}}$	3.186	.261	1	oN	Fe^+
5427.832	30	.....	.....	.815	−2	ob	Fe^+
5466.94[12]	20	.....	.....	.995	1	2	Fe
5485.51	2n	.....	.....	.....	.....	.....	.....

TABLE 1—*Continued*

λ	Int.	Multiplet	Lower E.P.	Solar λ	Solar Int.		Solar Ident.
					Disk	Spot	
5507.2	10N	.....	.....	.....	.....	.....	.....
5534.85	40	$b^2H_{5\frac{1}{2}} - z^4F^\circ_{4\frac{1}{2}}$	3.231	.849	2	1	Fe^+
5567.815[13]	10	.....	.....	.....	.....	.....	.....
5781.2	5N	.....	.....	.....	.....	.....	.....
5785.0	5N	$y^4F^\circ_{4\frac{1}{2}} - e^4D_{3\frac{1}{2}}$	7.673	.....	.....	.....	.....
5795.87[14]	4n	.....	.....	.....	.....	.....	.....
5813.67	3	$c^2F_{2\frac{1}{2}} - z^2D^\circ_{1\frac{1}{2}}$	5.547	.672	−2	ob	Fe^+
5823.17	3	$c^2F_{3\frac{1}{2}} - z^2G^\circ_{4\frac{1}{2}}$	5.545	.176	−2	.....	Fe^+?
5833.65	10N	.....	.....	.675	−3N	.....	Fe^+
5835.61	3n	.....	.....	.589	−1	−2	Fe^+?
5885.73[15]	6N	.....	.....	.....	.....	.....	.....
5891.36	8	.....	.....	.369	−3	.....	Fe^+?
5891.5[16]	10N	.....	.....	.....	.....	.....	.....
5891.9[17]	3	.....	.....	.....	.....	.....	.....
5898.18[18]	4n	.....	.....	.....	.....	.....	.....
5903.6[19]	8N	.....	.....	.....	.....	.....	.....
5920.0	4N	.....	.....	.....	.....	.....	.....
5953.65	3n	.....	.....	.....	.....	.....	.....
5956.5	4N	.....	.....	.....	.....	.....	.....
5962.4	30N	.....	.....	.....	.....	.....	.....
5978.90	2n	.....	.....	.....	.....	.....	.....
5991.383	10	$a^4G_{5\frac{1}{2}} - z^6F^\circ_{4\frac{1}{2}}$	3.139	.383	2	1	Fe^+
5999.30	4n	.....	.....	.....	.....	.....	.....
6032.30	8n	.....	.....	.....	.....	.....	.....
6036.40	2n	.....	.....	.....	.....	.....	.....
6045.497	6	.....	.....	.497	−2	.....	Fe^+
6048.18	5N	.....	.....	.....	.....	.....	.....
6061.04	3n	$x^4D^\circ_{3\frac{1}{2}} - e^4D_{3\frac{1}{2}}$	7.771	.....	.....	.....	.....
6084.11	5	$a^4G_{4\frac{1}{2}} - z^6F^\circ_{3\frac{1}{2}}$	3.186	.118	0	−2	Fe^+
6103.54[20]	8	.....	.....	.484 .591	−2 −3	.....	.....
6113.33	2	$a^4G_{3\frac{1}{2}} - z^6F^\circ_{2\frac{1}{2}}$	3.207	.334	0	−1?	Fe^+
6147.79[21]	30?	$b^4D_{1\frac{1}{2}} - z^4P^\circ_{\frac{1}{2}}$	3.871	.749	2	ob	Fe^+
6149.265	20	$b^4D_{\frac{1}{2}} - z^4P^\circ_{\frac{1}{2}}$	3.872	.255	2	−2	Fe^+
6175.158	15	.....	.....	.165	−3	.....	Fe^+
6179.41	5	$c^2F_{3\frac{1}{2}} - z^2D^\circ_{2\frac{1}{2}}$	5.545	.404	−2	.....	Fe^+
6199.16[22]	2	$c^2F_{3\frac{1}{2}} - z^4G^\circ_{2\frac{1}{2}}$	5.545	.....	.....	.....	.....
6233.52[23]	3	.....	.....	.....	.....	.....	.....
6238.411	20	$b^4D_{1\frac{1}{2}} - z^4P^\circ_{1\frac{1}{2}}$	3.871	.396	2	ob	Fe^+
6239.95[24]	2n	$b^4D_{\frac{1}{2}} - z^4P^\circ_{1\frac{1}{2}}$	3.872	.962	−1	ob	Fe^+
6247.560	80	$b^4D_{2\frac{1}{2}} - z^4P^\circ_{1\frac{1}{2}}$	3.875	.569	2	−1	Fe^+

TABLE 1—*Continued*

λ	Int.	Multiplet	Lower E.P.	Solar λ	Solar Int.		Solar Ident.
					Disk	Spot	
6248.916	4	.....	.....	.919	−2	.....	Fe^+?
6293.0	6N	.....	.....	.....	.....	.....	.....
6305.318	15	.....	.....	.321	−2N	.....	Fe^+
6317.401	3	.....	.....	.....	.....	.....	.....
6331.969	12	.....	.....	.971	oN	ob	Fe^+
6369.45	4	$a^6S_{2\frac{1}{2}}-z^6D^\circ_{1\frac{1}{2}}$	2.879	.479	o	ob	Fe^+
6375.96	4n	.....	.....	.....	.....	.....	.....
6383.753	15	.....	.....	.726	oN	ob	Fe^+
6385.473	5	.....	.....	.474	−2N	.....	Fe^+?
6386.75	2	.....	.....	.....	.....	.....	.....
6407.30[25]	1	$b^4D_{1\frac{1}{2}}-z^4P^\circ_{2\frac{1}{2}}$	3.871	.310	oN	ob	Fe^+−
6416.942	20	$b^4D_{2\frac{1}{2}}-z^4P^\circ_{2\frac{1}{2}}$	3.875	.935	1	−1	Fe^+
6432.654	8	$a^6S_{2\frac{1}{2}}-z^6D^\circ_{2\frac{1}{2}}$	2.879	.690	1	−2	Fe^+
6433.85	3	.....	.....	.....	.....	.....	.....
6442.97	6	.....	.....	.976	−2	.....	Fe^+?
6446.43	20	.....	.....	.415	−3	.....	Fe^+
6456.41	200	$b^4D_{3\frac{1}{2}}-z^4P^\circ_{2\frac{1}{2}}$	3.887	.396	3	−1	Fe^+
6487.43	4	.....	.....	.....	.....	.....	.....
6491.28	4	.....	.....	.254	−3N	.....	Fe^+?
6493.05	8	.....	.....	.....	.....	.....	.....
6506.33[26]	5	.....	.....	.....	.....	.....	.....
6516.053	20	$a^6S_{2\frac{1}{2}}-z^6D^\circ_{3\frac{1}{2}}$	2.879	.094	2	o	Fe^+
6517.01	5	.....	.....	.....	.....	.....	.....
6586.69[27]	5	.....	.....	.....	.....	.....	.....
6627.28[28]	5	.....	.....	.32?	−3	.....	Fe^+?
6651.03	1	.....	.....	.....	.....	.....	.....
6677.33	3	.....	.....	.31	−3	.....	Fe^+
6966.9	2	.....	.....	.....	.....	.....	.....
7067.44[29]	20	.....	.....	.460	o (n to v)	.....	Fe^+−Fe
7134.99	5	.....	.....	5.03	−3	.....	Fe^+?
7193.23	8	.....	.....	.183	oN	.....	−Fe^+
7222.39	8	$b^4D_{1\frac{1}{2}}-z^4D^\circ_{\frac{1}{2}}$	3.871	.397	2	.....	Fe^+
7224.51	12	$b^4D_{\frac{1}{2}}-z^4D^\circ_{\frac{1}{2}}$	3.872	.404	1	.....	Fe^+
7264.99	10	.....	.....	.....	.....	.....	.....
7287.36[30]	6	.....	.....	.....	.....	.....	.....
7301.54[31]	2	$b^4D_{2\frac{1}{2}}-z^4F^\circ_{2\frac{1}{2}}$	3.875	.577	−1	.....	Fe^+
7307.97[32]	50	$b^4D_{1\frac{1}{2}}-z^4D^\circ_{1\frac{1}{2}}$	3.871	8.08	1	.....	Fe, Fe^+
7310.24	6	$b^4D_{\frac{1}{2}}-z^4D^\circ_{1\frac{1}{2}}$	3.872	.201	2	.....	Atm, Fe^+
7320.70[33]	40	$b^4D_{2\frac{1}{2}}-z^4D^\circ_{1\frac{1}{2}}$	3.875	.689	4	.....	Fe, Fe^+
7334.66	8	.....	.....	.62	−3	.....	Fe^+?

TABLE 1—*Continued*

λ	Int.	Multiplet	Lower E.P.	Solar λ	Solar Int.		Solar Ident.
					Disk	Spot	
7376.46[34]	20	.....	.....	.494	5	.....	*Fe? Fe*$^+$
7449.34	6	$b^4D_{1\frac{1}{2}} - z^4D^\circ_{2\frac{1}{2}}$	3.871	.338	2	.....	*Fe*$^+$
7462.38	20	$b^4D_{2\frac{1}{2}} - z^4D^\circ_{2\frac{1}{2}}$	3.875	.40	9 bl	.....	*Fe*$^+$
7515.88[35]	6	$b^4D_{3\frac{1}{2}} - z^4D^\circ_{2\frac{1}{2}}$	3.887	.837	1	.....	*Fe*$^+$
7533.42	2	$b^4D_{3\frac{1}{2}} - z^4F^\circ_{3\frac{1}{2}}$?	3.887	.373	3	.....	*Fe*$^+$—
7655.47	1	$b^4D_{2\frac{1}{2}} - z^4D^\circ_{3\frac{1}{2}}$	3.875	.48	−1	.....	*Fe*$^+$
7711.71	15	$b^4D_{3\frac{1}{2}} - z^4D^\circ_{3\frac{1}{2}}$	3.887	.731	4	.....	*Fe*$^+$

NOTES TO TABLE 1

1. λ is Burns's arc value. Too strong in spark for close measurement.
2. Blends with faint *Fe* I line measured in very strong arc spectrum as λ 5036.93.
3. Solar line at 5086.776, *Mn?* −2.
4. Solar line at 0.261 (−3) due to C_2.
5. Forms violet edge of wide structure reaching beyond λ 5101.48.
6. λ is Burns's arc value. Blends in spark with *Fe* I 5168.904.
7. Predicted λ. Spark line too faint to measure.
8. Probably double, with violet side stronger, which may account for difference from solar λ.
9. Spark line is an unresolved *Fe* II doublet.
10. Predicted λ. Just visible in spark.
11. Spark λ affected by *Fe* I λ 5409.125.
12. Close blend with *Fe* I which was measured in arc spectrum as λ 5466.990 (Burns, 0.993). Solar line is probably due chiefly to *Fe* I.
13. A line is present in the solar spectrum at 0.773 (−2d?) which is probably due to *Mn*.
14. A line is present in the solar spectrum at 0.891 (−2) which is probably due to *Ce* II.
15. Possibly masked in sun by atmospheric line, λ 5885.761 (−3).
16. Shading extends beyond adjacent lines.
17. Partly obscured by λ 5891.5. Unidentified solar line at λ 5891.896 (−2).
18. Blend in arc with band structure and may be *Fe* I. Masked by strong atmospheric line in sun.
19. Hazy patch in spark, about 1 A wide.
20. Spark λ is mean of two faint solar lines. Identification uncertain.
21. Blend in spark with *Fe* I line, measured in arc by writer as λ 6147.832. Probable intensity of *Fe* I subtracted.
22. Masked in sun by *V*.
23. An unidentified solar line at λ 6233.518 (−3d?) is strengthened and probably double in the sunspot spectrum.

[Notes to Table 1 continued on following page]

24. Predicted λ. Spark line too faint to measure.
25. Solar line may be blend.
26. An atmospheric line at λ 6506.340 (−3N) is present in the solar spectrum.
27. An atmospheric line at λ 6586.703 (−3) is present in the solar spectrum.
28. Measurement of spark line difficult on account of adjacent line *Fe* I λ 6627.56. Solar line also uncertain.
29. Blend in spark with *Fe* I λ 7067.41 (measured in arc) (10).
30. Masked in sun by atmospheric line λ 7287.378.
31. Predicted λ. Spark line too faint to measure.
32. Blend in spark with *Fe* I λ 7307.970 (measured in arc).
33. Blend in spark with *Fe* I λ 7320.710 (measured in arc).
34. Blend in spark with *Fe* I λ 7376.434 (measured in arc).
35. Close to air line in spark. Measurement difficult.

lines according to the criteria used in compiling the *Revised Rowland*, I am greatly indebted to Charlotte E. Moore, who kindly supplied data collected for a revised edition of her "Multiplet Table." These data include predicted wave lengths, multiplet designations, and lower excitation potentials, obtained from the term values published by Dobbie.[2] The solar wave lengths, with the intensities in disk and sunspot spectra, are from the *Revised Rowland*, supplemented by a few recent solar measures. Numbers adjacent to the wave lengths refer to explanatory notes at the end of the table.

A comparison of the spark lines in Table 1 with the lines of the solar spectrum has resulted in the identification of 78 as probably due, at least in part, to *Fe* II. Thirteen others are masked by foreign lines to such an extent that the part taken by *Fe* II in their formation is highly uncertain. These blends are mentioned in the notes at the end of the table. Of the 78 lines now identified, 37 were assigned to *Fe* II in the *Revised Rowland*. This number included the lines placed in multiplets by Russell,[3] of which some had been observed by Merrill and Anderson[4] as polar lines in the arc spectrum, and 16 were predicted from term values. All the lines listed by Russell above λ 5000 have been found in my spark spectra, as a rule being lines of considerable strength.

The columns giving intensities of lines in the solar disk and in sunspots show that the usual condition for enhanced lines prevails,

[2] *Proc. R. Soc. Lon.*, A, **151**, 703, 1935.

[3] *Mt. W. Contr.*, No. 318; *Ap. J.*, **64**, 194, 1926.

[4] Unpublished.

namely, a decided weakening or absence of the line in the spot spectrum except when disturbed by a foreign line.

Thirty-one of the solar lines identified as *Fe* II are of intensities −2 (17) and −3 (14) and therefore among the faintest to be detected in the sun. On that account it seems unlikely that the future detection in the laboratory of *Fe* II lines weaker than those recorded here will give any considerable addition to the number of solar *Fe* II lines in this region.

The spectra of novae, at certain stages, show *Fe* II lines of notable strength. Their variations in the spectrum of Nova Herculis are described by Merrill[5] and by McLaughlin.[6] The latter identifies, in the emission stage of the nova, 21 lines above λ 5000 as *Fe* II, 7 being predicted lines. All are now found in the spark spectrum, including λ 5991 and λ 6084, only recently assigned to *Fe* II, which the nova at times emitted with high intensity.

CARNEGIE INSTITUTION OF WASHINGTON
MOUNT WILSON OBSERVATORY
October 1937

[5] *Mt. W. Contr.*, No. 530; *Ap. J.*, **82**, 413, 1935.

[6] *Pub. Obs. of the U. of Michigan*, **6**, No. 12, 1930.

STUDIES BASED ON THE INTENSITIES AND DISPLACEMENTS OF INTERSTELLAR LINES*

PAUL W. MERRILL AND ROSCOE F. SANFORD

ABSTRACT

I. *Relative intensities of lines of calcium and of sodium.*—The ratio of intensity D2:K derived by direct comparison from spectra in which both lines were measured is, in equivalent angstroms, 1.59. A determination based on the distance-intensity curves of the two lines gives 1.65. There is little evidence of a change of ratio with intensity. The value provisionally adopted is 1.6, which probably indicates about three times as many atoms of singly ionized calcium as of neutral sodium.

II. *Absolute magnitudes of early-type stars.*—A readjustment of the relative luminosities of the various spectral subdivisions has been obtained from the distance-intensity relationships previously found. The results show (*a*) that differences between stars with diffuse lines and those whose lines are better defined are smaller than the original values; (*b*) that there is a smaller decrease from O9 to B8; (*c*) that c stars of classes B3 to B9 are fainter than the assumed mean value, −5.0, while those of classes A0 to A2 are brighter; and (*d*) that the mean magnitude of a few Wolf-Rayet stars is −2.9.

III. *Galactic rotation.*—All available measurements of interstellar lines were utilized to form curves of residual radial velocity against longitude for the four distances, 300, 600, 1200, and 2400 parsecs. These curves approximate fairly closely the double sine curves characteristic of galactic rotation of the "planetary" type, although in longitudes 125°–164° curves for the nearer interstellar material are distorted by a local stream motion which may possibly have some connection with that of the Taurus group. A least-squares solution yields for the constants of galactic rotation

$$l_0 = 329^\circ$$

$$A = 14.8 \text{ km/sec per } 1000 \text{ parsecs}.$$

The nearer gases give a somewhat larger value of the constant A than those at a greater distance. Obscuration seems inadequate to account for this result, which may possibly be due in part to an average decrease in the density of interstellar gas beyond about 1000 parsecs from the sun.

I. RELATIVE INTENSITIES OF LINES OF CALCIUM AND OF SODIUM

Photometric measurements of interstellar lines, recently completed at Mount Wilson,[1] together with previous investigations by E. G. Williams[2] and C. S. Beals,[3] permit a fairly extensive comparison of the intensity of the D2 line of sodium with that of K of ionized

* *Contributions from the Mount Wilson Observatory, Carnegie Institution of Washington*, No. 585.

[1] *Mt. W. Contr.*, No. 576; *Ap. J.*, **86**, 274, 1937.

[2] *Mt. W. Contr.*, No. 487; *Ap. J.*, **79**, 280, 1934.

[3] *M.N.*, **96**, 661, 1936.

calcium. An investigation already published[4] has shown that the displacements of the D lines, in general, agree closely with those of H and K.

For direct determinations of the relative intensity of K and D2 in the same spectra, we have utilized all stars of class B3 or earlier in whose spectra both lines have been measured, except those, chiefly

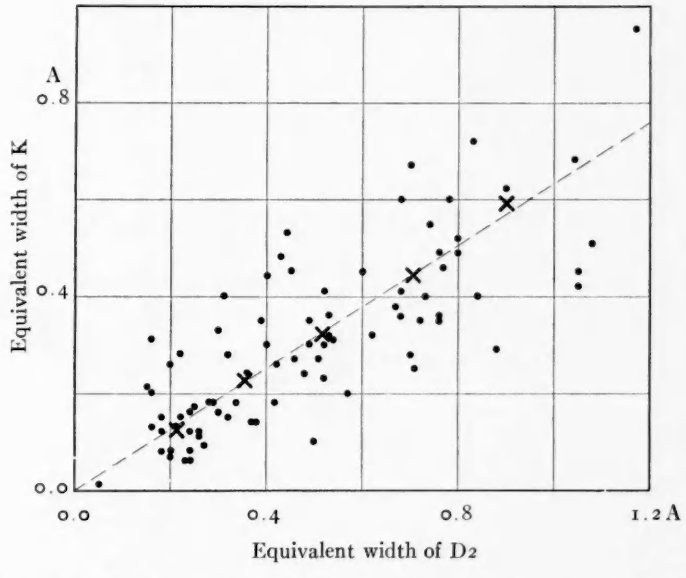

FIG. 1.—Comparison of intensities of the interstellar lines K and D2 in individual stars.

of class cB3, in which it appeared that the effect of a superposed stellar K line might be appreciable and a few others in which it was feared that stellar lines of *C* II might be blended with D2. Results for 83 stars are plotted in Figure 1. Five normal places (Table 1), formed from a series of means of overlapping groups, appear to be represented within errors of observation by the equation, D2/K = 1.59.

Beals's mean value,[3] based on 22 stars, is 2.08.[5]

[4] *Mt. W. Contr.*, No. 564; *Ap. J.*, **85**, 73, 1937.

[5] Converted from Beals's published value of 1.39 for which the unit was a displacement corresponding to 1 km/sec.

Meager data for the ratio D1:H yield the value 2.1, but the weight is low. A special investigation of the ratio K:H is being made by Sanford and Wilson.

Another determination of the relative intensity of K and D2 may be made by comparing the distance-intensity curves of the two lines. The ratio D2:K yielded by the most reliable portions of the published curves,[6] corresponding to intensities of D2 from 0.4 A to 1.0 A, is 1.5. A new determination of the distance-intensity curve for K, which utilizes a larger number of stars, yields the value 1.65. The portions of the curves, near the origin, corresponding to weak lines

TABLE 1

RELATIVE INTENSITIES OF K AND D2

(Mean values in equivalent angstroms)

K	D2	D2:K
0.125	0.215	1.72
.228	.355	1.56
.321	.518	1.61
.442	.707	1.60
0.592	0.900	1.52

indicate ratios about 2.0, but these values are decidedly uncertain. On the whole, the data afford little reliable evidence of a change of ratio with intensity.

The ratio of intensity provisionally adopted is, in equivalent angstroms,

$$\frac{D2}{K} = 1.6 .$$

The equivalent width in angstroms of an intrinsically narrow absorption line whose observed shape is determined by Doppler effect is given approximately by the equation

$$W = \frac{\pi e^2 \lambda^2}{mc^2} \times 10^8 Nf , \qquad (1)$$

[6] *Mt. W. Contr.*, Nos. 569 and 573; *Ap. J.*, **86**, 28, 1937; *ibid.*, p. 136. The curve derived from the sodium lines is for 0.5 (D2+D1).

where N represents the number of atoms in the lower quantum level and the other symbols have their usual significance. For the relative number of calcium and sodium atoms we have, since

$$f_K = f_{D_2} = 2/3 ,$$

$$\frac{N_K}{N_{D_2}} = \frac{W_K}{W_{D_2}} \times \left(\frac{5890}{3934}\right)^2 = 1.40 .$$

The equation for W is faulty for deep lines, since no account is taken of saturation. To allow for this effect, introduce a new quantity N' defined by the relationship,

$$N = 2^{N'} . \tag{2}$$

Then

$$\frac{N_K}{N_{D_2}} = 2^{(N'_K - N'_{D_2})} ;$$

or

$$\log \frac{N_K}{N_{D_2}} = 0.301 \, (N'_K - N'_{D_2}) \tag{3}$$

To evaluate $N'_K - N'_{D_2}$, let R be the ratio of intensity when one line is formed by twice as many atoms as the other. Then the intensity, W, of a line will, in general, no longer be proportional to the number of atoms, N, as in equation (1), but, instead,

$$W = \text{constant} \times \lambda^2 \times R^{N'} . \tag{4}$$

Hence for the ratio K to D2,

$$\frac{W_K}{W_{D_2}} = \left(\frac{3934}{5890}\right)^2 \times R^{(N'_K - N'_{D_2})} ;$$

from which

$$R^{(N'_K - N'_{D_2})} = 2.24 \div \frac{W_{D_2}}{W_K} ;$$

$$N'_K - N'_{D_2} = \frac{0.350 - \log \dfrac{W_{D_2}}{W_K}}{\log R} . \tag{5}$$

Doubling the number of absorbing atoms cannot decrease the intensity of a line, nor can it more than double the intensity. Hence R must lie between 1 and 2. For the sodium lines D2 and D1, its value is 1.2 except for weak lines.[7] For K and H we should expect nearly the same ratio, but the meager data indicate a somewhat larger value. Table 2 shows the relative number of atoms, N_K/N_{D_2}, for various values of W_{D_2}/W_K and of R, computed from equations (3) and (5). We consider the most probable value of N_K/N_{D_2} to be about 3.0, which, since all the atoms are in the ground state, means that there are three times as many atoms of singly ionized calcium as of neutral sodium. This result, which is in line with the conclusion by Wilson and Merrill[7] that the numbers of the two kinds of atoms

TABLE 2

VALUES OF THE RATIO $N_K : N_{D_2}$

W_{D_2}/W_K	R		
	1.2	1.6	2.0
1.4	6.0	2.0	1.6
1.6	3.6	1.6	1.4
1.8	2.3	1.4	1.2
2.0	1.5	1.2	1.1

are of the same order, appears difficult to explain if the relative abundance of calcium and sodium is the same as on the earth or in stellar atmospheres.[8]

II. ABSOLUTE MAGNITUDES OF EARLY-TYPE STARS

Using the observed apparent magnitude, m, and an adopted absolute magnitude, M, depending on the spectral type, the distance, D, of a star may be computed from the well-known equation,

$$\log D = 0.2(m - M) + 1 ,$$

based on the photometric inverse-square law. Distances computed in this way have been used in determining the distance-intensity relationship of interstellar lines of *Ca* and of *Na*.[6] It is now possible

[7] *Mt. W. Contr.*, No. 570; *Ap. J.*, **86**, 44, 1937.

[8] A. S. Eddington, *M.N.*, **95**, 2, 1934.

to invert the problem and to find from the distance-intensity curve the absolute magnitude of a star in whose spectrum the intensities of the interstellar lines have been measured. Taking the group of stars as a whole, it is obvious that no improvement in the adopted system of magnitudes will result from this procedure, but a valuable readjustment of the relative luminosities of individual stars and of mean values for the various spectral subdivisions may nevertheless be obtained.

In computing the absolute magnitude from the equation,

$$M = m - 0.00035D - 5(\log D - 1),$$

the distance, D, in parsecs, was obtained from the published distance-intensity curves for calcium and for sodium.[6] The term $-0.00035D$ is the correction for space absorption.

TABLE 3

COMPARISON OF ASSUMED AND READJUSTED ABSOLUTE MAGNITUDES

Type	Lines Diffuse or Winged		Others	
	Assumed	Readjusted	Assumed	Readjusted
O5–O9	−3.4	−3.2	−3.4	−3.2
B0	−3.1	3.1	3.3	3.3
B1	−2.7	2.8	3.0	2.8
B2	−2.2	2.3	2.7	2.5
B3	−1.5	2.3	2.2	2.0
B5	−0.4	(2.2)	1.2	(1.8)
B8	+0.1	(−1.3)	0.4	(2.2)
B9	+0.4	.....	0.2	.....
cB0–cB2	.....	.....	5.0	4.9
cB3–cB9	.....	.....	5.0	4.3
cA0–cA2	.....	.....	−5.0	−5.5

The final results, listed in Table 3, show differences between stars with diffuse lines (symbol *n*) and those whose lines are better defined, which are smaller than the original values. Also the decrease in luminosity from O9 to B8 appears somewhat less than that assumed. Unfortunately the results for B5 and B8 are of low weight. The data indicate that c stars of classes B3 to B9 are fainter than the assumed mean value, −5.0, while those of classes A0 to A2 are brighter. Tables 4, 5, and 6 give the data in more detail.

TABLE 4

ABSOLUTE MAGNITUDES OF O STARS

(Numbers of stars are in parentheses)

Type	K	D	Mean	
Oa	−2.8 (3)	−3.5 (3)	−3.2	−2.9 (Wolf-Rayet)
Ob	2.6 (2)	2.6 (3)	2.6	
O5	3.4 (1)	2.9 (2)	3.1	−3.2 (O5–O9)
O6	3.4 (6)	3.5 (5)	3.4	
O7	3.1 (6)	2.7 (6)	2.9	
O8	3.4 (11)	3.4 (10)	3.4	
O9	−3.2 (9)	−3.0 (10)	−3.1	

TABLE 5

ABSOLUTE MAGNITUDES OF B STARS

(Numbers of stars are in parentheses)

Type	Lines Diffuse or Winged			Others			Mean of All
	K	D	Mean	K	D	Mean	
B0	−2.7 (7)	−3.5 (6)	−3.1	−3.3 (25)	−3.4 (19)	−3.3	−3.3
B1	2.0 (3)	3.2 (4)	2.8	2.6 (6)	3.1 (5)	2.8	2.8
B2	2.2 (9)	3.4 (1)	2.3	2.4 (8)	2.6 (16)	2.5	2.4
B3	−2.0 (13)	2.6 (14)	−2.3	−2.1 (10)	1.9 (5)	−2.0	2.2
B5	.....	2.2 (4)	.....	.....	1.8 (5)	.....	(2.0)
B8	.....	−1.3 (3)	.....	.....	−2.2 (4)	.....	(−1.8)

TABLE 6

ABSOLUTE MAGNITUDES OF c STARS

(Numbers of stars are in parentheses)

Type	K	D	Mean	
cB0	−4.9 (3)	−4.6 (6)	−4.7	−4.9 (cB0–cB2)
cB1	4.6 (8)	5.1 (8)	4.8^5	
cB2	5.3 (4)	4.8 (4)	5.0^5	
cB3	−4.7 (4)	4.3 (6)	−4.5	−4.3 (cB3–cB9)
cB5	.....	4.0 (2)	.....	
cB8	.....	4.1 (5)	.....	
cB9	.....	4.5 (7)	.....	
cA0	.....	5.3 (9)	.....	−5.5 (cA0–cA2)
cA2	.....	5.7 (8)	.....	
cA3, 4, 5	.....	−5.1 (3)	.....	.....

The value, -2.9, for a few Wolf-Rayet stars, indicates that the luminosity of these objects is nearly as great as that of types O5–O9.

III. GALACTIC ROTATION

The following computations are based on all available measures of the displacements of the detached D lines of sodium and the H and K lines of ionized calcium.[9] For stars in whose spectra both pairs of lines have been measured, the weighted mean was adopted. The distances employed were those derived from the absolute magnitudes listed in Table 2, *Mt. W. Contr.*, No. 569.[10] Use of the revised magnitudes in Table 3 of the present *Contribution* would yield slightly improved distances, but changes in the final results would be inconsequential.

The stars were first divided according to longitude into fourteen groups, Table 7, which were subdivided according to distance in general accordance with the following limits:

0–400 parsecs	801–1400 parsecs
401–800	> 1400

The average values of longitude, distance, and residual radial velocity were then computed for each group as indicated in Table 7. The next step, taken for the sake of homogeneity, was to reduce the average residual velocity of each group to that corresponding to one of the rounded values 300, 600, 1200, and 2400 parsecs, on the assumption that the residual velocity is proportional to distance. These values also are given in Table 7 and are plotted in Figure 2. It will be noticed that the plotted points for each of the four distance groups form an approximate double sine curve, whose amplitude increases with distance. Since each of these groups is quite independent of the others, the ensemble constitutes strong evidence for motions of interstellar material characteristic of the standard "planetary" type of galactic rotation. Some disagreement is shown in longitudes 125°–164°, where the nearer material appears to ex-

[9] *Mt. W. Contr.*, No. 576; *Ap. J.*, **86**, 274, 1937. Plaskett and Pearce, *Pub. Dom. Ap. Obs.*, **5**, 222, 1933.

[10] *Ap. J.*, **86**, 28, 1937.

TABLE 7

MEAN RESIDUAL VELOCITIES

Longitude Interval	No. Stars	Average Long. l	Distance (Parsecs)	Residual Velocity Km/Sec	Reduced		
					Distance (Parsecs)	Velocity Km/Sec	Velocity Km/Sec for 1000 Parsecs
300°–320°	11	315°	504	− 0.6	600	− 0.7	− 1.2
321 –340	8	324	222	− 0.7	300	− 0.9	− 3.0
	8	332	662	− 0.5	600	− 0.5	− 0.8
	6	340	1030	+ 1.0	1200	+ 1.2	+ 1.0
	4	340	1852	+ 9.0	2400	+11.7	+ 4.9
341 –360	5	350	277	+ 0.9	300	+ 1.0	+ 3.3
	4	358	520	+ 5.8	600	+ 6.7	+11.2
1 – 33	9	22	290	+ 5.0	300	+ 5.2	+17.3
	11	21	630	+ 5.2	600	+ 5.0	+ 8.3
	7	23	976	+ 8.0	1200	+ 9.8	+ 8.2
	2	24	2245	+14.4	2400	+15.4	+ 6.4
34 – 45	8	40	266	+ 0.6	300	+ 0.7	+ 2.3
	7	40	591	+ 6.0	600	+ 6.1	+10.2
	17	41	1188	+ 7.2	1200	+ 7.3	+ 6.1
	18	40	2459	+ 7.6	2400	+ 7.4	+ 3.1
46 – 53	5	49	167	+ 0.4	300	+ 0.7	+ 2.3
	13	50	641	+ 5.0	600	+ 4.7	+ 7.8
	5	49	1472	+ 1.9	1200	+ 1.5	+ 1.2
54 – 67	8	60	250	− 2.2	300	− 2.6	− 8.7
	18	63	597	− 0.9	600	− 0.9	− 1.5
	7	64	1098	− 0.4	1200	− 0.4	− 0.3
	5	61	1900	− 3.9	2400	− 4.9	− 2.0
68 – 79	6	71	312	− 2.6	300	− 2.5	− 8.3
	22	73	613	− 2.2	600	− 2.2	− 3.7
	20	72	1069	− 2.8	1200	− 3.1	− 2.6
	4	70	2407	− 7.9	2400	− 7.9	− 3.3
80 –107	12	88	258	− 3.8	300	− 4.4	−14.7
	11	87	679	− 6.8	600	− 6.0	−10.0
	17	93	1115	− 8.4	1200	− 9.0	− 7.5
	45	95	2452	−14.9	2400	−14.6	− 6.1
108 –124	7	115	393	− 2.0	300	− 1.5	− 5.0
	7	115	989	− 4.3	600	− 2.6	− 4.3
	7	112	1776	−11.0	2400	−14.8	− 6.2
125 –144	5	128	278	+ 4.4	300	+ 4.8	+16.0
	10	135	671	+ 1.6	600	+ 1.4	+ 2.3
	7	138	1112	+ 1.0	1200	+ 1.1	+ 0.9

TABLE 7—*Continued*

Longitude Interval	No. Stars	Average Long. l	Distance (Parsecs)	Residual Velocity Km/Sec	Reduced		
					Distance (Parsecs)	Velocity Km/Sec	Velocity Km/Sec for 1000 Parsecs
145°–164°	13	156°	291	+ 2.5	300	+ 2.6	+ 8.7
	10	159	529	2.3	600	2.6	4.3
	6	155	1375	0.5	1200	0.4	0.3
165 –180.....	14	173	239	3.6	300	4.5	15.0
	18	175	618	3.6	600	3.5	5.8
	7	174	1070	4.5	1200	5.0	4.2
	4	174	1700	4.5	2400	6.2	2.6
181 –220.....	11	196	305	0.9	300	0.9	3.0
	11	195	681	+ 7.6	600	+ 6.7	+11.2

hibit a *backward* rotation. This is probably to be interpreted as a stream motion in this region, which may possibly be related to a group motion in the local system such as Kapteyn's first star stream or the motion of the Taurus group.

Finally the velocities for all groups were reduced to the standard distance, 1000 parsecs (see the last column of Table 7, and Fig. 3).

To facilitate a least-squares solution, the normal places in Table 8 were formed from the last column in Table 7, measures of stars in longitudes 125°–164° being omitted. The weight of each is the number of stars times the mean distance in parsecs divided by 1000. The solution for the constants of the equation,

$$\rho = A \sin 2(l - l_0) ,$$

yielded the values,

$$A = 7.4 \text{ km/sec} ,$$
$$l_0 = 329° .$$

The distances used in the solution (and in all the tables and plots) are those of the stars in whose spectra the interstellar lines were measured. The effective center of absorption appears on the average to be at half these distances. Accordingly, the value of A is really

for 500 parsecs. For 1000 parsecs, therefore, A = 14.8 km/sec, a result not differing radically from Plaskett and Pearce's value of 16.6 for interstellar matter, or 15.5 for O- and B-type stars. For reasons stated in the next paragraph it appears probable that our value is slightly small. The double sine curve in Figure 3 has an amplitude of 8.0 km/sec.

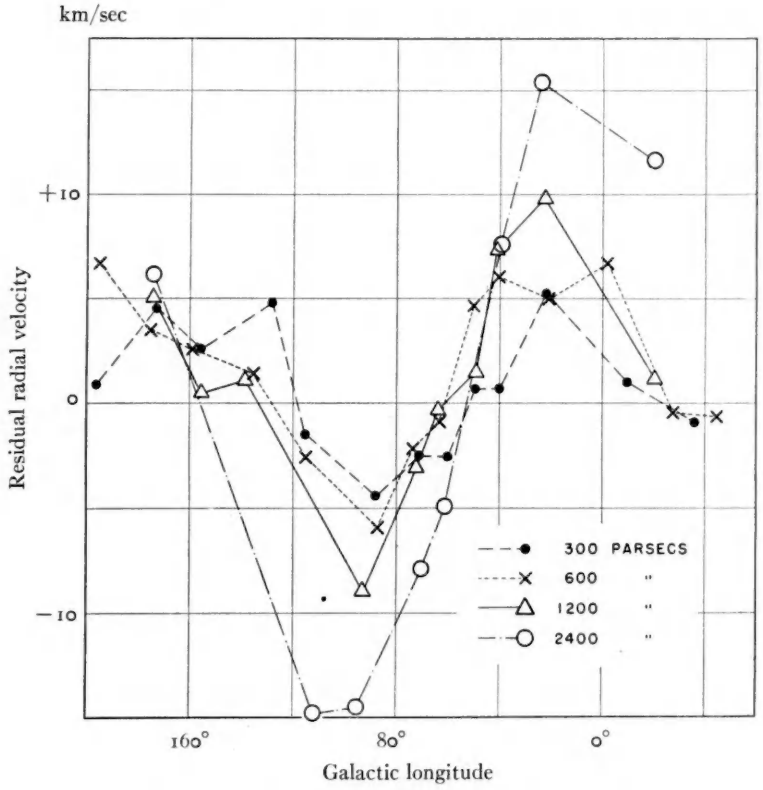

FIG. 2.—Residual radial velocity and galactic longitude

If no motions except those of galactic rotation affect the data, then all points in Figure 3 should differ from a double sine curve only by errors of measurement. We note, however, that points corresponding to the nearer material seem systematically to give larger amplitudes than the points corresponding to material at a greater distance. The same effect may be seen by comparing groups of stars

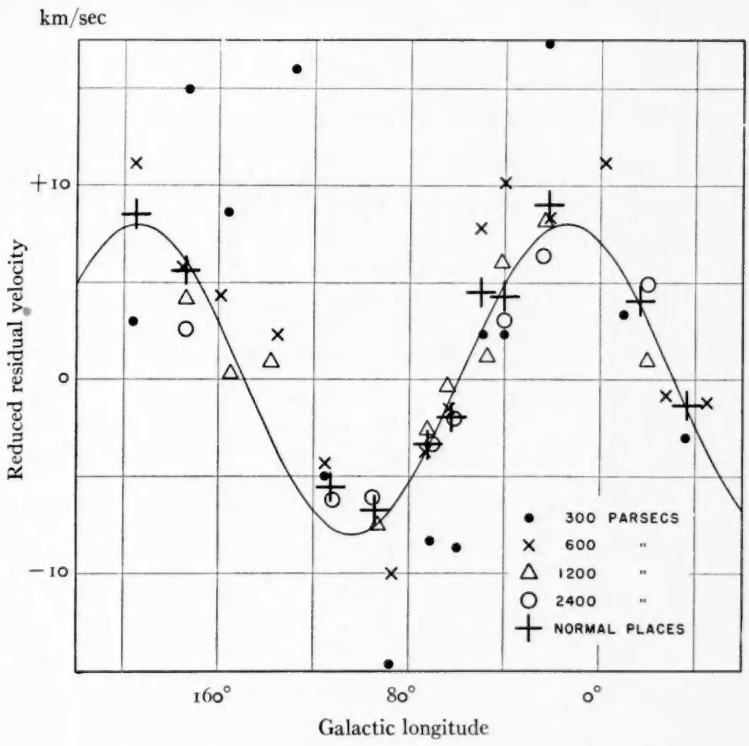

FIG. 3.—Residual radial velocity reduced to a distance of 1000 parsecs

TABLE 8

NORMAL PLACES FOR GALACTIC ROTATION

(Velocities reduced to a distance of 1000 parsecs)

Longitude	Residual Radial Velocity	Weight
	km/sec	
323°	−1.3	12.6
343	+4.1	17.1
22	+9.0	20.8
40	+4.3	70.7
50	+4.6	16.5
62	−1.9	29.9
72	−3.3	46.4
94	−6.7	139.9
113	−5.5	22.1
174	+5.7	28.7
195	+8.6	10.9

TABLE 9

AMPLITUDES OF GALACTIC ROTATION

Longitude l	Distance (Parsecs)	Residual Velocity	No.	$\sin 2(l-329°)$	Amp.	Weight
		km/sec			km/sec	
323°	467	− 0.6	27	−0.208	+ 2.9	6
340	1030	+ 1.0	6	+ .375	2.7	2
340	1852	+ 9.0	4	+ .375	24.0	2
350	277	+ 0.9	5	+ .669	1.3	3
358	520	+ 5.8	4	+ .848	6.8	4
21	472	+ 5.1	20	+ .970	5.3	19
23	976	+ 8.0	7	+ .951	8.4	7
24	2245	+14.4	2	+ .940	15.3	2
40	591	+ 6.0	7	+ .616	9.7	4
40	2459	+ 7.6	18	+ .616	12.3	11
41	1188	+ 7.2	17	+ .588	12.2	10
44	228	+ 0.5	13	+ .500	1.0	6
49	1472	+ 1.9	5	+ .342	5.6	2
50	641	+ 5.0	13	+ .309	16.2	4
65	276	− 2.4	14	− .208	11.5	9
65	2125	− 5.7	9	− .208	27.4	2
68	606	− 1.6	40	− .309	5.2	12
70	1076	− 2.2	27	− .375	5.9	10
88	258	− 3.8	12	− .848	4.5	10
91	944	− 7.8	28	− .899	8.7	25
95	2452	−14.9	45	− .951	15.7	43
112	1776	−11.0	7	− .961	11.4	7
115	393	− 2.0	7	− .927	2.2	6
115	989	− 4.3	7	− .927	4.6	6
174	452	+ 3.6	32	+ .766	4.7	24
174	1070	+ 4.5	7	+ .766	5.9	5
174	1741	+ 4.5	4	+ .766	5.9	3
195	681	+ 7.6	11	+ .999	7.6	11
196	305	+ 0.9	11	+0.998	+ 0.9	11
	Final Normal Places					
	366	.....	.....	.....	+ 3.2	66
	608	.....	.....	.....	6.2	60
	1048	.....	.....	.....	8.8	66
	2349	.....	.....	.....	+15.3	67

having nearly the same longitude but at different distances (see the last column of Table 7). In most instances the velocities, reduced to 1000 parsecs, are larger for the smaller distances. It appears, therefore, that in proceeding outward from the solar system the velocity components attributable to rotation increase less rapidly than in proportion to the distance.

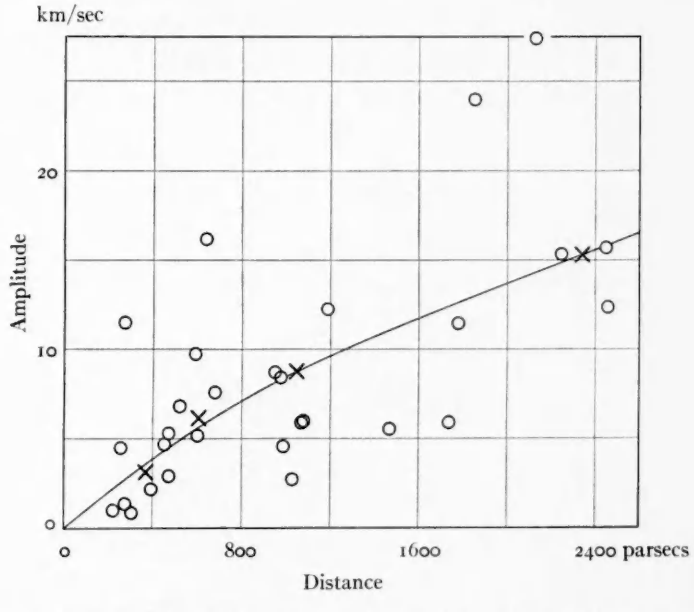

FIG. 4.—Amplitude of galactic rotation plotted against distance. The crosses represent normal places. For weights of the various points see Table 9.

To exhibit the effect in another way, we have computed the hypothetical amplitude, i.e., the residual radial velocity divided by sin $2\,(l - 329^\circ)$, for the groups shown in Table 9, which are combinations of those in Table 7. In Figure 4 the results are plotted against distance without regard to longitude. The four final normal places do not lie on a straight line through the origin but indicate a relatively small amplitude for the larger distances. This result may occur because the larger distances have been taken relatively too great. Obscuration would have just this effect, but the usual value of 0.35 mag. per kiloparsec (visual absorption) is insufficient to rectify the

curve. To do this would require approximately 0.9 mag. per kiloparsec, which seems an inadmissably large value.[11] Obscuration, therefore, may be supplemented by some other effect which acts in the same general manner. One possibility is that the density of interstellar calcium and sodium tends to decrease beyond (say) 1000 parsecs from the sun. For a more distant star the effective position of absorption in interstellar space, corresponding to the measured displacement of detached lines, would then be less than halfway to the star. To test this hypothesis, we need additional observations of interstellar lines in the spectra of stars more than 1000 parsecs and especially those more than 2000 parsecs distant.

CARNEGIE INSTITUTION OF WASHINGTON
MOUNT WILSON OBSERVATORY
November 1937

[11] See, e.g., F. H. Seares, *Mt. W. Contr.*, No. 428; *Ap. J.*, **74**, 91, 1931.

THE SECONDARY VARIATION OF δ SCUTI

T. E. STERNE

ABSTRACT

It is found by harmonic analysis of Fath's photoelectric measures of δ Scuti that its magnitude contains a periodic component, superimposed upon the fundamental variation, and whose period differs from that ($0^d.19377$) of the fundamental variation and all its submultiples. Since all the photoelectric measures have been made at nearly the same part of the Julian day, there is a major indeterminacy in the value of the secondary periodicity. Two of the possible values are $0^d.157388$ and $0^d.186876$, each of which is, in turn, uncertain by a small amount because of the seasonal distribution of the observations. Corresponding to the former value, the (semi-)amplitude of the secondary variation is found by least squares to be $0^m.0177 \pm 0.0013$; corresponding to the latter value, the amplitude is $0^m.0187 \pm 0.0013$. The secondary period does not have the value, $0^d.20120$, suggested by Fath. Further observations, made from different longitudes, are needed to remove the major indeterminacy.

The radial velocity is found, from a preliminary examination, to contain, in all probability, a periodic secondary variation having the same period—at present indeterminate—as that of the secondary variation in magnitude. The latter variation cannot be attributed, therefore, to a variation of the comparison star employed by Fath.

The periodic variation in the range, reported by Fath, can be explained by a secondary variation in the magnitude, having a period $0^d.157388$ or $0^d.186876$.

A periodic term in the ephemeris of the dates of median increasing magnitude is predicted on the basis of the secondary variation in magnitude; and such a term is found, with almost exactly the predicted amplitude and phase. It is suggested (*a*) that all (or nearly all) real "sine terms" in ephemerides of short-period Cepheids may arise from secondary variations having periods different from the fundamental periods and their submultiples, and (*b*) that such periodic secondary variations may be fairly common among short-period Cepheids.

From the absolute magnitude and spectral type a value is obtained for the mean density. The fundamental period could be explained as the lowest mode of radial oscillation of an Eddington model having this mean density and a value of γ equal to about 1.54. Such a model could not, however, have the period $0^d.186876$ for any other of its possible radial modes. Even if the preceding value of the mean density is rejected, the pair of periods $0^d.19377$ and $0^d.186876$ cannot be reconciled with the pulsations of any of the stellar models (which include Eddington's and cover a wide range of degrees of central condensation) considered by the author (*M.N.*, **97**, 582, 1937); and they appear to be inconsistent with the pulsation theory. The period $0^d.157388$ and the fundamental period are probably not inconsistent with the pulsation theory, provided that a suitable choice can be made of the stellar model.

1. INTRODUCTION

The star δ Scuti has been found by Fath,[1] from photoelectric measures made during July, 1935, and July and August, 1936, to be variable with a range of the order of $0^m.2$ and a period $0^d.19377$. The radial velocity had previously been found by Colacevich[2] to be variable with that period. Neither the light curve nor the radial-

[1] *Lick Obs. Bull.*, **17**, 175, 1935; **18**, 77, 1937.

[2] *Ibid.*, **17**, 171, 1935.

velocity curve, however, is regularly periodic. The light curves measured on different nights disagree among themselves by amounts altogether too large to be entirely attributable to errors of observation. The radial-velocity curves obtained from spectroscopic observations on different nights also disagree significantly among themselves; both light and radial-velocity curves appear to be in a state of continual change. It has, furthermore, been found, from the several nights during which simultaneous light and radial-velocity measures were made, that the changes in the light curve are correlated with changes in the radial-velocity curve. The existence of this correlation renders it unlikely that the irregularity of the light curve can be attributed to changes in the light of the comparison star, α Scuti, that was employed in the photoelectric measures.

The photoelectric observations made by Fath were extensive and thorough. He has published the differences in photoelectric magnitude, $\delta - \alpha$, observed on twelve nights between JD 2427991 and JD 2428010, 1935, and on twenty-four nights between JD 2428353 and JD 2428387, 1936. There are, in all, 544 published observations. On each of the nights in 1935 he made, on the average, about fourteen observations, and on each of the nights in 1936 about sixteen observations, each consisting of five measures of the variable, ten of the comparison star, and five more of the variable. The observations made on any night extended from about 0.7 to about 0.9 of the Julian day, and on most of the nights they covered more than a whole period. The 1935 series includes sequences of three and four consecutive nights; and the 1936 series, sequences of seven, four, and eleven consecutive nights. Fath found that, when the range of the light curve was plotted against the phases of a period of $5^{d}.24774$, a significant periodicity[3] was shown. He has suggested that the period $5^{d}.24774$ may be due to interference between the fundamental period $0^{d}.19377$ and a period slightly larger, $0^{d}.20120$, since two sine curves with those periods and with (semi-) amplitudes $0^{m}.091$ and $0^{m}.023$, respectively, interfere in such a way that the resultant ranges follow closely the smooth curve drawn through the observed range-phase points in his Figure 3. Fath has stated that a secondary period slightly shorter than $0^{d}.19377$ was

[3] Fath, *ibid.*, **18**, 77, 1937, Fig. 3.

tried, instead of the period $0^d.20120$, but that it did not fit the range curve as well as the first and was therefore discarded. This discarded period must have been $0^d.18687$.

Since the observed relation of the radial velocity of δ Scuti to its light is essentially the same as the relation observed among Cepheid variables generally, of both the short-period and the classical types, it is natural to try to interpret the behavior of δ Scuti in terms of the pulsation theory. When one tries to do this, however, a difficulty immediately arises, from the near equality of the two periods that were suggested by Fath as being capable of producing the interference. An inspection of the tables in section 5 of the author's paper[4] on modes of radial oscillation reveals no tabular entries, for any one of the four models considered or for any possible value of γ, that stand to each other in a ratio as close to unity as the ratio of $0^d.20120$, or of $0^d.18687$, to $0^d.19377$. Since a wide range of different degrees of central condensation is covered by the four different stellar models considered in the tables, it does not appear possible for any model to have so near an equality between the periods of different modes of low order. It might be supposed that a way out of the difficulty could be found by assuming that modes of high order were concerned. Referring to page 592 of the paper cited, one sees that for each of the three models for whose radial oscillations analytical solutions were found, the dominant term in A is j^2, where j is the order of the mode. Thus, for large j the period

$$T \sim \frac{\text{Const.}}{j}$$

for each of the three analytical models considered. To obtain a ratio 1.037 between the periods of the modes, it would be necessary for the order of the modes concerned to be twenty-seven or higher. It is likely that for any reasonable distribution of density the modes would have to be assumed to be of very high order, indeed, before the ratio 1.037 could become dynamically possible. Aside from the inherent implausibility of an assumption that the two most strongly active modes in δ Scuti were of very high order, the periods of modes of such high order—on the most reasonable assumptions concerning

[4] Sterne, *M.N.*, **97**, 582, 1937.

the value of the mean density of δ Scuti—would be considerably smaller[5] than the periods found by Fath. One is therefore practically forced to the conclusion that the existence of the pair of periods[6] suggested by Fath would be inconsistent with the pulsation theory. It then becomes important to determine, if possible, from the observations themselves, whether the period $0^d.20120$ (or $0^d.18687$) may not be a spurious one, and whether there may not be present, instead, a true secondary period that differs, more than this does, from the fundamental period $0^d.19377$.

2. THE HARMONIC ANALYSIS

A mean magnitude curve of δ Scuti was formed from Fath's observations, plotted against the phases of the period $0^d.193770$. It was found that a better agreement was obtained between the 1935 and 1936 observations when the slightly different period $0^d.193775$ was used for this purpose; this revised value of the fundamental period was thereafter consistently used. The corresponding heliocentric elements of the fundamental variation are

$$\text{Max.} = \text{JD } 2427991.777 + 0^d.193775E\,,$$
$$\text{Min.} = \text{JD } 2427991.883 + 0^d.193775E\,.$$

On the basis of the revised fundamental period, a final mean magnitude curve was obtained from all the observations; and the residual[7] from it of each observation was plotted against the time of the observation. These residuals were thus free[8] from all effects that

[5] For a more complete discussion of this point, the reader is referred to a subsequent section.

[6] Either the pair $0^d.19377$, $0^d.20120$, or the pair $0^d.19377$, $0^d.18687$.

[7] The residuals were taken in such a sense that a positive residual corresponded to the star's being brighter than the mean magnitude at the phase.

[8] The residuals are not entirely free, perhaps. The mean magnitude curve was drawn free hand through a set of normal points, and would thus contain small errors which would reappear in the residuals, with a period $0^d.193775$. They would not influence the subsequent harmonic analysis for different periods. They were found actually to be very small, probably of the order of thousandths of a magnitude; when the residuals were plotted against the phases of the fundamental period, the plot showed no evidence of periodicity. It will be noticed that the residuals were taken in magnitude, not in light. Since the range of δ Scuti is but $0^m.2$, it is a matter of no practical consequence whether they are taken in magnitude or in light.

were periodic in an interval[9] $0^d.193775$, and contained (besides aperiodic variations and errors of observation) all periodic secondary variations whose periods differed from the fundamental period and its submultiples, and such periodic variations only.

The residuals were plotted against the phases of the period, $0^d.201120$, suggested by Fath. The plot showed no evidence of periodicity; there is therefore no evidence for the real existence of such a period in δ Scuti.

The observations, and therefore the residuals, occur in groups of about $0^d.2$ duration; and the groups occur at intervals of an integral number of mean solar days. It was impossible to be sure, by mere inspection, of the value of the period present in the residuals. They showed upon examination, however, fairly well-defined maxima and minima on a considerable number of the nights; and when these well-defined maxima and minima occurred on consecutive nights, they were seen to occur earlier by about $0^d.05$ on the later night than on the earlier. The interval $0^d.95$ thus contained an integral number of cycles of the secondary variation. It was thought best to make a least-squares solution for a more accurate value of this interval and at the same time for the interval between the maxima and minima that occurred on the same night. For this purpose the 1936 residuals were used; and the times of the well-defined maxima and minima were determined by a method which involved the superposition, on the plotted residuals, of idealized maxima and minima, smoothly drawn on tracing paper and adjusted in the time co-ordinate. Maxima and minima which were not well defined were ignored; those used involved five or more consecutive individual residuals. The observational equations were written in the form

$$Aa + Bb + Cc + Dd + Rr = F\,,$$

[9] A variation whose period is a submultiple of the fundamental period must here be regarded as periodic in the latter period (as technically it always is), since the mean magnitude curve from which the residuals were measured was drawn free hand, was not a simple sine curve, and must have contained all the submultiple periodicities that were present.

where d is the amount, of the order of 0^d05, by which a maximum or minimum occurs earlier on any night than on the preceding night; r is one-half the period sought; and a, b, and c are the epochs (fractions of a day) from which the three independent counts start. There are thus five unknowns. The maxima and minima that could be used occurred in three groups of consecutive nights; and since it

Minima	Maxima	Observational Equations					
		A	B	C	$-D$	R	F
JD 2428000+	JD 2428000+						
362.838	.....	1	0	0	0	0	0.838
363.770	.....	1	0	0	1	0	.770
.....	363.853	1	0	0	1	1	.853
.....	364.789	1	0	0	2	1	.789
364.890	.....	1	0	0	2	2	.890
365.840	.....	1	0	0	3	2	.840
366.761	.....	1	0	0	4	2	.761
.....	366.843	1	0	0	4	3	.843
371.770	.....	0	1	0	0	0	.770
.....	372.848	0	1	0	1	1	.848
.....	373.800	0	1	0	2	1	.800
373.863	.....	0	1	0	2	2	.863
374.786	.....	0	1	0	3	2	.786
.....	374.858	0	1	0	3	3	.858
377.797	.....	0	0	1	0	0	.797
.....	378.797	0	0	1	1	1	.797
.....	379.733	0	0	1	2	1	.733
379.800	.....	0	0	1	2	2	0.800

was not possible to be sure, at the outset, of the number of maxima and minima between the groups, independent epochs, a, b, and c had to be included as unknowns. The adopted times of the maxima and minima that were employed are listed in the accompanying table. The observational equations are also listed, and a comparison of them with the listed maxima and minima should make clear the meaning of the equations. The assumption was made that the interval from minimum to maximum was equal to the interval from maximum to minimum, so that both could be set equal to the single unknown r; separate unknowns could have been used if the accu-

racy of the adopted dates had warranted it. The solution yielded the values

$$\begin{aligned} a &= 0^d8356 \\ b &= .8071 \\ c &= .7741 \\ d &= .0568 \pm 0.0080 \text{ (m.e.)} \\ r &= 0.0786 \pm 0.0101 \text{ (m.e.)} \end{aligned}$$

so that the period, $2r$, was $0^d1572 \pm 0.0203$. Now the interval $1 - d = 0^d9432 \pm 0.0080$ must contain an integral number, n say, of cycles; no use had previously been made of this fact. Corresponding to several values of n, the following values of the period were found:

n	P
5.....	$0^d1886 \pm 0.0016$
6.....	.1572 .0013
7.....	0.1347 ± 0.0011

It is seen that the second of these, 0^d1572, is in exact agreement with the less accurate value $2r$ found directly in the least-squares solution, but that the value 0^d1347 is possible and that the value 0^d1886 is possible but less likely. Periods corresponding to still other n's are inconsistent with the value of $2r$, if full reliance can be placed[10] upon the mean errors. We have described the least-squares procedure in detail partly because it may be of general use in similar problems, and also to show the nature of the major indeterminacy involved in the period of the residuals. The major indeterminacy arises from the circumstance that the observations were made between about 0.7 and 0.9 of the Julian day and could be resolved if observations, made from different longitudes and thus at different parts of the Julian day, were available. There is also a minor indeterminacy arising from the seasonal distribution of the observational series.

The period 0^d1572 was improved by least squares to fit as well as possible all the well-determined 1936 maxima and minima; the revised value was 0^d15737. All the 544 residuals were next plotted against the phases of that period, and it was found that a further small change was necessary to fit the 1935 residuals. The final

[10] This may not be advisable, however.

adopted value was $0^d.1573883$, the final digits of which are uncertain[11] because of the uncertainty in the number of epochs between the 1935 and 1936 series. A plot of the residuals against the phases of this period, reckoned from the arbitrarily chosen epoch JD 2428357.790, appears in Figure 1. A sine curve passed through this plot by least squares is also shown; its (semi-)amplitude is $0^m.0177 \pm 0.0013$, and its phases are such as to yield, for the date of maximum of the secondary variation:

$$\text{Sec. max.} = \text{JD } 2427991.786 + 0^d.1573883E .$$

Because of the major indeterminacy previously mentioned, we are not sure of the value of the period; but the amplitude found is of

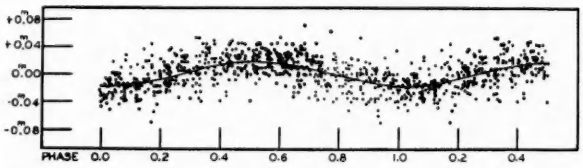

FIG. 1.—The residuals of the magnitude of δ Scuti from its mean magnitude curve plotted against the phases of a period $0^d.1573883$.

great statistical significance and forces us to conclude that a real periodic variation, with a period different from the fundamental period and all its submultiples, is present in the magnitude of δ Scuti.

In a similar manner, the period $0^d.1886$ was revised to $0^d.186876$, uncertain, as before, in its final digits; and a least-squares solution yielded the amplitude $0^m.0187 \pm 0.0013$, slightly, although not significantly, larger than before. The maximum of the least-squares curve yields for the date of maximum of the secondary variation:

$$\text{Sec. max.} = \text{JD } 2427991.786 + 0^d.186876E .$$

The period $0^d.1347$ was revised to $0^d.1360325$; a least-squares solution yielded the amplitude $0^m.0131 \pm 0.0013$, significantly smaller than the amplitudes previously found; and the corresponding formula was

$$\text{Sec. max.} = \text{JD } 2427991.792 + 0^d.1360325E .$$

[11] A period $0^d.157455$ would be indistinguishable in the present series of observations. This is an instance of the minor indeterminacy previously referred to.

The small amplitude indicates, probably, that this period is not the real one and that the choice lies between the other two that have been tested.

The standard deviation of the residuals is $0^m.024$. After the secondary variation is removed from them, their standard deviation is $0^m.020$ for either of the periods, $0^d.1573883$ or $0^d.186876$. The accuracy of the observations themselves may be determined from a list of thirty differences[12] of magnitude, 12 Aquilae *minus* α Scuti, which has kindly been supplied to the author by Dr. Fath. The standard deviation of these differences about their mean is $0^m.013$; this value contains, besides the effects of observational error, the effects of any possible variation in 12 Aquilae and α Scuti, and it should therefore be an upper limit to the standard deviation of the residuals of δ Scuti from its mean magnitude curve after all superimposed variations have been removed. The standard deviation $0^m.020$ is thus probably too large to be explicable entirely in terms of observational error and the possible variation of the comparison star α Scuti, and may contain the effects of still other periodicities. If it were certain which of the periods we have studied is correct, it would be possible to analyze the residuals, after that period had been removed from them, for remaining periodicities; but it does not seem advisable to attempt so refined an analysis before the outstanding ambiguity has been removed.

One should expect, on the basis of the pulsation theory, that if there is a real secondary periodicity in the magnitude of δ Scuti, there should also be one, with the same period, in the radial velocity. A list of radial velocities, corrected for exposure time, has been published by Colacevich;[2] and since the fraction of the Julian day that is covered by the radial-velocity measures is not much greater than the fraction covered by the photoelectric measures, the ambiguity associated with the latter should be associated with the former as well, and the residuals of the radial velocity from the mean radial-velocity curve should yield a significant periodicity when plotted

[12] The averages of the first fifteen of these, in groups of three, appear in the small table on page 175 of Fath's first-mentioned article (*Lick Obs. Bull.*, **17**, 1935); the averages of the last fifteen, in groups of three, appear in the small table on page 77 of Fath's second article (*ibid.*, **18**, 1937).

against the phases of either of the periods, $0^d.1573883$ or $0^d.186876$. A refined study of the radial velocity of δ Scuti does not appear to be desirable before the publication by the Lick Observatory of the new series of measures promised in a footnote to Fath's second paper. The author has, however, made a provisional study based on the last forty-nine measures, made between June 26 and September 10, 1935, and published by Colacevich. A mean radial-velocity curve was formed from these measures on the basis of the period $0^d.193775$; the residuals from the mean curve were plotted against the phases of the period $0^d.186876$; and a least-squares solution yielded the (semi-)amplitude 0.98 ± 0.37 km/sec. This amplitude is large enough, in relation to its mean error, for its significance to be suggested; and thus in all probability a real periodic secondary variation, with the same period as that in the magnitude, must exist[13] in the radial velocity. From the least-squares solution the epoch of algebraic *minimum* of the secondary radial-velocity curve is JD 2427991.792 ± 0.011 for the period tested, and is thus the same, within the accuracy of its determination, as the epoch JD 2427991.786 that has been found for the *maximum* of the secondary variation in magnitude corresponding to the same period. It is not considered worth while to test the period $0^d.1573883$ against the radial velocities, at present.

The existence of a secondary periodicity in the magnitude has two immediate consequences that may be observationally verified. There should be a periodic variation in the range of δ Scuti, and there should be a periodic variation in the residuals between the observed dates of median increasing magnitude and the dates computed from a uniform ephemeris. In the first phenomenon, those of the original residuals are involved which occur near the fundamental maxima and minima of the star; in the second phenomenon, those which occur near the mid-time of the rise to maximum light. Unless we are greatly mistaken, both phenomena should show periodicities

[13] This preliminary result renders it even less likely than before that the secondary variation in the magnitude, which we have shown to exist, can be attributed to a periodic variation in the magnitude of the comparison star that was employed by Fath.

with respect to $0^d.1573883$ and $0^d.186876$, for, since all the residuals do not suffice for removing the ambiguity, those involved in the two phenomena to be considered cannot do so.

3. THE PERIODIC VARIATION OF THE RANGE

Fath has found that the range of the light curve is periodic, with an apparent period of $5^d.24774$. Let us see whether the periods $0^d.1573883$ and $0^d.186876$ are consistent with the observed range. Consider the differences between the magnitude at the time of a maximum of the fundamental variation and the magnitude at the time of an adjacent minimum of the fundamental variation. This difference should depend[14] upon the phase of the superimposed secondary variation at the time of the fundamental maximum, or minimum, involved. We list in column I of Table 1 the number of Fath's plot from which the amplitude was measured; in column II, the range (in hundredths of a magnitude) measured between consecutive maxima and minima of Fath's curve at times of fundamental maximum and minimum.[15] Column III gives the epoch number, E, of the fundamental minimum involved in the measured range. Column IV gives the phase, with respect to the period $0^d.186876$, of the time of the fundamental minimum, the phase being expressed in thousandths of that period and reckoned from the date JD 2427991.883. A plot of the range against the phases appears in Figure 2, showing a very close correlation between range,

[14] If the time interval from fundamental maximum to fundamental minimum equals the interval from fundamental minimum to fundamental maximum, the difference should depend merely upon the phase of the secondary variation at fundamental maximum (or minimum); but if the two time intervals differ, then the difference between the magnitudes at fundamental maximum and at minimum will be a two-valued function of the secondary phase at primary maximum (or minimum), taking one set of values when the measured maximum precedes, and the other when it follows, the measured minimum. Although the two time intervals actually differ somewhat in δ Scuti, we shall ignore this small refinement.

[15] The reason for measuring the range in this somewhat artificial fashion is to avoid the considerable complication that would result if the actual maxima and minima of Fath's curves were used. Owing to the secondary variation, the actual maxima and minima of the light curve are being continually displaced, to and fro, with respect to the computed times of fundamental maximum and minimum. We have already given the formulae by which those times are computed.

as here defined, and phase. The smooth curve represents a sine curve fitted by least squares. Its amplitude is $0^m.045 \pm 0.004$, and

TABLE 1

I	II	III	IV	V	VI	VII
				2420000+		
1.....	22	0	000	.....	.....	.....
2.....	17	5	185	7992.892	− 5	944
3.....	.....	.....	.....	7993.872	+ 6	128
4.....	21	20	738	7995.813	+10	497
5.....	.....	.....	.....	7999.882	+ 9	273
6.....	20	51	883	8001.823	+13	642
7.....	16	62	289	8003.738	−10	011
8.....	17	72	658	8005.890	+10	417
9.....	19	82	027	8007.815	− 2	786
10.....	15	87	212	8008.776	−10	971
11.....	14	92	396	8009.760	+ 5	155
12.....	16	98	618	8010.728	+ 4	340
13.....	22	1868	962	8353.890	− 9	721
14.....	20	1889	737	8357.786	+11	459
15.....	14	1914	660	8362.818	+ 5	419
16.....	21	1919	845	8363.790	+ 8	604
17.....	23	1925	066	8364.755	+ 4	788
18.....	18	1930	251	8365.715	− 5	973
18.....	.....	.....	.....	8365.910	− 4	010
19.....	12	1935	435	8366.873	− 9	194
20.....	16	1940	620	8367.851	0	379
21.....	16	1945	805	8368.820	0	563
22.....	13	1961	395	8371.723	− 4	117
23.....	14	1966	580	8372.893	+ 4	339
24.....	17	1971	764	8373.871	+13	523
25.....	24	1976	949	8374.826	− 1	708
26.....	13	1992	540	8377.731	− 3	262
27.....	16	1997	724	8378.711	+ 8	446
28.....	22	2002	909	8379.868	+ 3	668
29.....	20	2007	093	8380.845	+11	852
30.....	15	2012	278	8381.797	− 6	037
31.....	13	2017	463	8382.777	+ 5	222
32.....	15	2023	684	8383.750	+ 9	406
33.....	18	2028	869	8384.720	+10	591
34.....	24	2033	053	8385.859	−13	812
35.....	15	2038	238	8386.833	− 8	997
36.....	12	2043	422	8387.818	+ 8	181

the standard deviation of the points from it is but $0^m.017$, somewhat smaller than that of the points about the curve in Fath's Figure 3.

The phase of the sine curve, furthermore, is in substantial agreement with what one would expect from the formula for secondary maximum, JD 2427991.786 + $0^d.186876E$. Theoretically, the amplitude of the secondary variation should be one-half of $0^m.045 \pm 0.004$, or $0^m.022 \pm 0.002$, to be compared with the observed $0^m.0187 \pm 0.0013$. The discrepancy is not serious when account is taken of the mean errors.

The period $0^d.1573883$ was tried, and the resulting points showed a somewhat greater dispersion about a smooth curve having a somewhat smaller amplitude. The period $5^d.24774$ found by Fath was also tried, and the fit was essentially the same as with the period

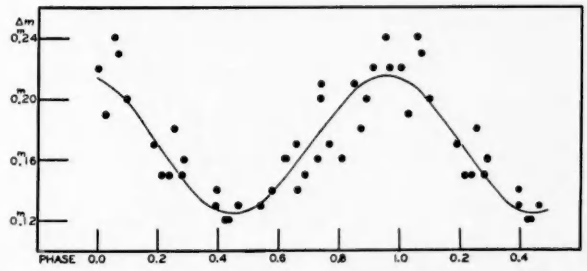

FIG. 2.—The range of δ Scuti plotted against the phase of a period $0^d.186876$

$0^d.186876$. The reason is easy to see: a period of $0^d.186876$ interferes with the fundamental period in a period of $5^d.2489$, which is indistinguishable, over a time interval of one year, from Fath's period. It is also easy to see why the period $0^d.1573883$ must fit the observed range if Fath's does. The period $0^d.1573883$ interferes with the fundamental period in a period of $0^d.8381611$, and the latter interferes with the mean solar day (according to which the observations are spaced) in a period of $5^d.179$. The latter period remains nearly indistinguishable from Fath's over an interval of a month or two, and is again in step a year later, so that it must fit both the 1935 and 1936 observations; accordingly, the period $0^d.1573883$ must fit also. The alternative value $0^d.157455$ previously given in a footnote leads to a period of $5^d.2522$ that is indistinguishable from Fath's over an interval of one year. If the real period of the secondary variation in the magnitude is $0^d.1573883$, then Fath's period is not the true

period of the range but is a spurious period[16] related to the real period ($0^d.8381611$) of the range through the mean solar day.

4. THE SINE TERM IN THE EPHEMERIS OF THE DATES OF MEDIAN INCREASING MAGNITUDE

No sine term has been reported in the dates of median increasing magnitude of δ Scuti, although the existence of a secondary variation would lead us to expect one. Since the slope of the mean light curve at the phase in question is about $2^m.5$ per day, the periodic term may be predicted to have an amplitude of about (0.0187/2.5) days, or about $0^d.0075$, for the period $0^d.186876$. The median magnitude was found, from the mean light curve, to be about $0^m.036$ on Fath's scale; and the times at which Fath's curves pass upward through this ordinate are listed in column V of Table 1. Column VI contains the residuals O−C in thousandths of a day, where O is taken from column V and the provisional formula for the date of median increasing magnitude has been taken to be

$$C = JD\ 2427991.734 + 0^d.193775E .$$

Column VII contains the phase (in thousandths) of the dates C, computed with respect to the period $0^d.186876$ and reckoned from any maximum of the secondary variation. This phase is obviously the fractional part of the product of the reciprocal of the secondary period, here 5.3511419 $days^{-1}$, and the difference C − JD 2427991.786, and hence is equal to the fractional part of $0.772 + 1.0369175E$ or, since E is an integer, of $0.722 + 0.0369175E$, where E is the same number that appears in the formula for C. Before looking into the observed relation between O − C and this phase, let us predict the sine term that should appear in the final formula for the time, C′, of median increasing magnitude. This should be a term which reaches a minimum when the phase, as above defined, is zero, for then the secondary variation is at a maximum and the observed date should be displaced a maximum amount toward earlier times. The term should be, therefore, $-0^d.0075 \cos (360° \times \text{phase})$, which reduces to

[16] The period $5^d.24774$ found by Fath, like all of ours, is subject to a major indeterminacy arising from the daily, and a minor indeterminacy arising from the seasonal, distribution of the observations.

$+0^d.0075 \sin (13^\circ.290E + 170^\circ)$. To compare this prediction with observation, we merely plot the time intervals in column VI against the phases in column VII. The plot appears in Figure 3, in which the smooth curve is a sine curve[17] fitted by least squares. The amplitude of this curve is $0^d.0072 \pm 0.0014$, significantly large in relation to its mean error, and in excellent agreement with the expected $0^d.0075$. The phase of minimum is found to be 0.00 ± 0.03, in agreement with the expected value zero. The least-squares solution also yields a

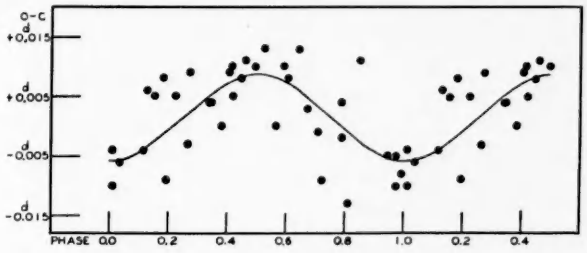

FIG. 3.—The residuals, O − C, of the dates of median increasing magnitude of δ Scuti, plotted against the phases of a period $0^d.186876$.

small correction to the constant Julian-day epoch, and thus we obtain the formula for median increasing magnitude:

$$C' = \text{JD } 2427991.736 + 0^d.193775E + 0^d.0072 \sin (13^\circ.290E + 169^\circ).$$

Corresponding to the secondary period $0^d.1573883$, the expected formula is

$$C' = \text{JD } 2427991.736 + 0^d.193775E + 0^d.0071 \sin (83^\circ.229E + 151^\circ).$$

The amplitude obtained by a least-squares solution is $0^d.0060 \pm 0.0014$, in agreement with that predicted, and smaller, as was to be expected, than the amplitude previously found; the phase of minimum O − C is found to be -0.01 ± 0.04, in agreement with the expected value zero.

[17] We use sine curves in this paper to represent the secondary variation and the associated phenomena, not because they are necessarily sinusoidal (although there are reasons for believing that a small oscillation should be sinusoidal), but because the use of more complicated curves, involving higher Fourier terms, would not be warranted by the available observational data.

One should bear in mind that the possibility of explaining the behavior of the range, and of the residuals of the dates of median increasing magnitude, follows naturally from the existence of a periodic secondary variation—superimposed upon the fundamental —in the magnitude. We have discussed the range, and the dates of median increasing magnitude, not to obtain further evidence of the reality of the secondary variation, but merely to show beyond all doubt that the two phenomena first referred to can be understood in terms of the third phenomenon. All three phenomena are related; and the real proof that a secondary variation is present lies in the harmonic analysis, which has already shown the actual magnitudes to contain a periodicity different from the fundamental period and its submultiples. The last two sections contain no further evidence of the reality of the secondary variation, nor can they be considered to have resolved the old ambiguity concerning the value of the secondary period.

Ephemerides containing sine terms have been found for many other short-period Cepheids, but probably this is the first time that such terms have been predicted. It is possible, and perhaps even likely, that all (or nearly all) such real terms in the ephemerides of short-period Cepheids are of the same nature; and one is strongly tempted to conclude that the existence of secondary variations having periods different from the fundamental periods and their submultiples may be fairly common among short-period Cepheids. The author[18] has been studying in detail the light curve of RR Lyrae, in whose ephemeris there is a sine term, and has obtained strong evidence for the existence of a secondary variation similar to that in δ Scuti; but the period of the secondary variation in RR Lyrae is even less determinate[19] than that in δ Scuti.

[18] The author was assisted in the analysis of RR Lyrae by Mr. D. Norman, Miss C. Nottage, Mr. J. A. O'Keefe, and Mr. R. R. Procter.

[19] The observational problem of finding these secondary periods in short-period Cepheids is difficult; and as the studies of δ Scuti and RR Lyrae have shown, the usual observational procedures must be expected to be often, if not usually, inadequate to yield the periods of the secondary variations. One needs many homogeneous observations of great accuracy, distributed throughout the Julian day and preferably over a short interval of time. The essential requirement as to distribution throughout the Julian day can be met only by the use of different observing stations widely distributed in longitude. The observational difficulties do not appear to be of an insuperable nature.

5. PHYSICAL CONSIDERATIONS

According to the *Draper Catalogue*, the visual magnitude of δ Scuti is 4.74 and its spectral class is Fo. Its revised spectral class is given as F5 by the Lick observers and as F4s by Mount Wilson. Its absolute visual magnitude is given by Mount Wilson as +1.4, in good agreement with the trigonometric parallax, 0".021. From these values the star's radius is found[20] to be about 3.6 times the sun's, and its mass[21] about 2.5 times the sun's. Its mean density, $\bar{\rho}$, to the extent that it can be thus determined, is therefore about 0.076 gm/cm.^{3} Using the value of the fundamental period $0^d.193775$ in seconds and the value 6.66×10^{-8} CGS units for the constant of gravitation, G, we find that

$$T\sqrt{\frac{G\bar{\rho}}{6\pi}} = 0.274 .$$

This value may be compared directly with the tabular entries on pages 592 and 593 of the author's paper on radial oscillations (*loc. cit.*). It is seen that with a reasonable choice (about 0.4) of α, and thus (about 1.54) of γ, the fundamental variation may be explained as the lowest radial mode of an Eddington model having the adopted mean density. However, it is seen from the tables that for that model it is then possible for another mode to exist with a period $0^d.186876$, or, for that matter, $0^d.1573883$. For none of the models considered in that paper, which cover a wide range of degrees of central condensation, and for no possible values of γ, can anything like an agreement be obtained between the value 0.274 and the ratio between $0^d.186876$ and $0^d.193775$. Even if the adopted mean density were considered to be considerably in error, then (as has already been pointed out) the ratio of periods will still demand for its explanation that modes of very high order were involved, and this is in itself physically implausible.

[20] Russell, Dugan, and Stewart, *Astronomy*, p. 783, eq. (11). Corresponding to values of T equal to 7400° and 6500°, this equation yields values of 3.2 and 4.1, respectively, whose average is 3.65.

[21] The curve in Russell, Dugan, and Stewart's *Astronomy* (p. 690) leads to the value 2.5, corresponding to the absolute visual magnitude +1.4. The same value is obtained from Table 14, after a reduction to bolometric magnitude has been made according to Table 15, in Eddington's *The Internal Constitution of the Stars* (pp. 137, 138).

If the value $0^d.186876$ is correct, the pulsation theory is seriously jeopardized; if the period $0^d.1573883$ is correct, the pulsation theory is perhaps not seriously jeopardized, although the Eddington model may[22] be. Until matters shall have been decided by further observations of δ Scuti that may make it possible to fix definitively the value of its secondary period, these various possibilities must remain open, along with the additional possibility that the value of the secondary period may yet be found to be different from any of those that have been considered.

It is a pleasure for the author to acknowledge the opportunities, kindly offered him, for discussions with Dr. Fath and Dr. Shapley.

HARVARD COLLEGE OBSERVATORY
October 3, 1937

[22] How seriously, it is not possible at present to say. As was pointed out in the author's paper on radial oscillations (*loc. cit.*), the periods, computed by J. A. Edgar (*M.N.*, **93**, 422, 1933) for the first mode of the Eddington model and included with reservations in the author's tables, had been challenged by Miss H. A. Kluyver (*B.A.N.*, **7**, 313, 1936). A correction to the values found by Edgar might render the period $0^d.1573883$ consistent (although this is not certain) with the Eddington model; but not the period $0^d.186876$.

A DETERMINATION OF SELECTIVE ABSORPTION BASED ON THE SPECTROPHOTOMETRY OF REDDENED B STARS

JESSE L. GREENSTEIN

ABSTRACT

An observational program has been carried out for the determination of the gradients of reddened B stars relative to normal B stars. Short-dispersion spectra, taken in series, were standardized on the tube photometer. The spectra were analyzed in the Moll self-recording microphotometer. The magnitude differences between reddened and normal stars along the spectrum were used to determine the gradients and the change of gradient with wave length.

The stars observed were taken from the Stebbins and Huffer catalogue of photoelectric color indices, which permits a discussion of the relation between the color indices, the present system of gradients, and the Greenwich system. The relative gradients were found to be substantially linear over a wide range of wave length. The photoelectric color index is found to be a representative measure of the reddening of the B stars. The curvature of the gradients is such that the selective absorption in interstellar space must vary nearly as $1/\lambda$.

Measures of the total photographic absorption in front of the reddened stars were obtained from star counts, and an independent estimate was made of the ratio of the color excess to the photographic absorption. The variation of selective absorption with wave length is again found to be nearly as $1/\lambda$. The total photographic absorption is between four and six times the color excess on the International Scale.

An interpretation on the basis of my theoretical discussion of the selective absorption confirms the hypothesis there advanced, that the interstellar absorption is caused by small dust particles, with a frequency distribution close to that of hyperbolic meteors.

INTRODUCTION

A direct determination of the variation of the interstellar absorption coefficient with wave length may be obtained from the spectrophotometry of the continuous energy background of reddened stars. Measures of the relative intensity differences along the spectra of two stars of the same spectral type and absolute magnitude are measures of the variation of interstellar extinction with wave length. If we know the actual absorption at one wave length, we can obtain the dependence of extinction on wave length and, of course, a measure of the ratio of the interstellar selective absorption coefficient to the photographic absorption coefficient. A list of reddened stars scattered along the Milky Way in galactic longitudes 40° to 200°, with widely varying degrees of reddening, have been selected from among the B stars for which Stebbins and Huffer[1] give photoelectric color

[1] *Pub. Washburn Obs.*, **15**, No. 5, 1934.

indices. The program involved a comparison of the energy distribution in the continuous spectra of 38 reddened stars over the wavelength range from 6500 A to 3500 A with that in the spectra of normal B stars of the same spectral subdivisions.

Let us assume that all B stars radiate essentially like black bodies with effective temperatures equal to the excitation temperatures T given by the spectral lines. Then the relative spectrophotometric gradient, $\Delta\varphi$, between two stars of temperatures T_1 and T_2 is defined as

$$\Delta\varphi = \varphi_1 - \varphi_2 = 0.921 \frac{d(\Delta m_\lambda)}{d(1/\lambda)}, \tag{1}$$

where Δm_λ is the difference in magnitudes between the energy in the two spectra at a given wave length, λ, in microns, and where the gradient φ is defined by

$$\varphi = \frac{C_2}{T}(1 - e^{-C_2/\lambda T})^{-1}. \tag{2}$$

The quantity φ approaches C_2/T at low temperatures and is very nearly independent of wave length. A plot of relative energy differences, Δm_λ, against $1/\lambda$, is a straight line.

If there is any selective extinction of radiation in space the relative gradient will be changed. Let us approximate the law of dependence of the extinction coefficient, k_λ, on wave length by a relation of the form

$$k_\lambda = \frac{k}{\lambda^n}. \tag{3}$$

If one of the two stars has suffered a total absorption of $k_\lambda\ r$, where r is the distance, then equation (1) takes the form

$$\frac{d(\Delta m_\lambda)}{d\frac{1}{\lambda}} = 1.086\left(\varphi_1 - \varphi_2 + \frac{nkr}{\lambda^{n-1}}\right). \tag{4}$$

The relative gradient varies with wave length unless $n = 1$ or $n = 0$. The curvature of the relation between Δm_λ and $1/\lambda$ depends on n and on the distance traversed. In Table 1 the percentage change of

gradient, C, between two wave-length regions employed in this investigation is given as a function of the index, n. The table also gives the value of ϵ, the ratio of the interstellar selective absorption coefficient, E, to the photographic absorption coefficient A_{pg}:

$$\epsilon = \frac{E}{A_{pg}} = \frac{A_{pg} - A_{pv}}{A_{pg}} = 1 - \frac{A_{pv}}{A_{pg}} = 1 - \frac{k_{5500}}{k_{4400}}, \qquad (5)$$

where A_{pv} is the absorption coefficient at the photovisual wave length. The table shows that a large variation of the relative gradient might be observed in the spectrum of a reddened star if the interstellar

TABLE 1

MEASURES OF THE SELECTIVITY OF VARIOUS LAWS OF ABSORPTION

n	$C = \frac{\varphi_{4350} - \varphi_{5500}}{\varphi_{\text{Mean}}}$	ϵ
0.0	0.00	0.00
0.5	− .12	.10
1.0	.00	.20
1.5	+ .12	.28
2.0	+ .22	.36
3.0	+ .47	.49
4.0	+0.70	0.59

extinction should follow the law of Rayleigh scattering, with $n = 4$. The value of ϵ, of importance in the interpretation of observed color excesses of distant stars, also varies strongly with n; Rayleigh scattering corresponds to a photographic absorption coefficient only 1.7 times as large as the selective absorption coefficient. Both C and ϵ are, of course, independent of the distance or the total absorption suffered by the star.

OBSERVATION AND REDUCTION

The Stebbins and Huffer catalogue gives the color excesses of 733 B stars brighter than 7.5 mag. If we assume that the color excess of a B star is produced by interstellar absorption, the catalogue is a useful observing list for the present investigation, giving pairs of stars of similar spectral type and known difference in color. The spectrophotometry of the reddened stars also becomes of interest as

a means of relating the photoelectric color indices, which are measured over a small range of wave length, to the color indices over the normal base line.

The 24-inch reflector at the Oak Ridge station of the Harvard College Observatory is provided with a 24-inch objective prism having an angle of 3°. It yields excellent spectra of low dispersion (500 A/mm at $H\beta$) in good focus from 3500 A to 6500 A, with very short exposures. Approximately three hundred and fifty series plates have been obtained on twenty-four observing nights. A series normally consisted of eight plates cut from a single 8×10-inch plate and exposed in succession on three normal B stars, three reddened stars, and a star from the Greenwich[2] list of standard stars. Two exposures were obtained for each star, with different densities, to permit measurement over a wide range of intensities. A plate was reserved for standardization in a tube photometer. In order to avoid the effects of humidity as far as possible,[3] plates were kept at the observing platform for about thirty minutes before exposure, to permit adjustment to the conditions of temperature and humidity in the telescope. The average total duration of a series of seven plates, involving fourteen spectra, was about one hundred and fifty minutes.

The range in apparent magnitude of the stars photographed was 3.1 to 7.5 mag., the Greenwich standard stars being particularly bright. A variation of three magnitudes in the intensity of the image could be obtained by a set of diaphragms in front of the objective prism. A further adjustment of intensity was obtained by loading the driving pendulum of the Gerrish drive, which alters the rate of trailing of the spectral image. This rate was never varied by more than a factor of 2, in order to avoid changes of characteristic curve with effective exposure time. Experimentally, the effect of change of rate of trailing[2] was found to be smaller than the error of its determination. The system of apertures involves the use of slightly different mean optical thicknesses of glass in the prism; but this effect was also found to be negligible, at least as far as $\lambda = 3900$ A. The use of two exposures of a star on one plate introduces the possi-

[2] Dyson, Greaves, Davidson, and Martin, *Pub. Greenwich*, 1932.

[3] Cuffey, *Harvard Bull.*, No. 905, 12, 1937.

bility of pre-exposure effects. These are probably eliminated by the shortness of the exposures (one to four minutes). No sky fog was measurable on any of the plates.

The standardization plate was exposed in the Cambridge tube photometer for forty-five seconds at a temperature close to that of the stellar exposures. Since the standardization exposure time is about ten times as long as the effective stellar exposures, small differences may exist between the characteristic curves for the stellar and calibration exposures.[2] The tube photometer impresses simultaneously four series of spots, with intervals of 0.75 mag. between spots, for the plate calibration curves. Four Eastman filters of known spectral transmission give calibration curves with effective wave

TABLE 2

STANDARD WAVE LENGTHS MEASURED

Point	λ in μ	$1/\lambda$ in μ^{-1}	Point	λ in μ	$1/\lambda$ in μ^{-1}
1	0.625	1.60	6	0.424	2.36
2	.575	1.74	7	.394	2.54
3	.532	1.88	8	.370	2.70
4	.495	2.02	9	0.351	2.85
5	0.463	2.16			

lengths of 3650 A, 4700 A, 5600 A, and 6300 A. The plates used were Eastman 1F and Ilford Astra III panchromatic plates. The plates of a night's series were developed together in a tank, with constant agitation, for five minutes in Eastman developer formula D-11, at 65° F.

The spectra were analyzed in the Moll self-recording microphotometer. The projected slit-width was equivalent to about 15 A. The projected height of the slit was 0.4 mm; the plate was driven at 1.5 mm/minute, and the recording drum at a rate such as to yield a linear magnification of the spectrum of 27. The tracings show hydrogen lines as far as $H\epsilon$; beyond $H\epsilon$ the lines become confluent. Standard wave lengths can be identified on the tracings with uncertainties of 10 A to 30 A. Nine wave lengths listed in Table 2 were chosen for measurement on all the tracings. Point 7 is slightly affected by the hydrogen lines, and points 8 and 9 lie within the region of continuous hydrogen absorption.

The characteristic curves, as determined from the tube photometer, were such that the red and the green curves could be combined in a mean curve for the range of points 1–4 (6250 A to 4950 A). In some cases a mean curve could be used for points 4–9 (4950 A to 3510 A), while in others the violet curve had a "toe" sufficiently extended to make it necessary to reduce points 4–7 separately from points 7–9. The magnitude scale of the tube photometer is fundamental to the present investigation, but it should be noted that most of the spectra were of comparable density and that small scale errors in the tube photometer will therefore not produce serious systematic errors. On the other hand, effects of pre-exposure in the underexposed ultraviolet part of the spectra remain the most probable source of photometric errors in this investigation, since the tube-photometer curves in this region are poor.

The extinction correction adopted was based on that used by the observers of the Smithsonian Institution[4] at Washington, D.C. By comparison with the Cambridge and Oak Ridge values of extinction for various effective wave lengths,[5,6,7] it was found that the Washington coefficients were too large by 1.28. The Washington extinction coefficients at the zenith were reduced by this factor. The extinction corrections were usually less than 0.2 mag. and do not introduce errors of a systematic character. After the observed magnitudes along the spectra had all been reduced to the zenith, there were available for each star nine measures of spectral intensity, in stellar magnitudes of arbitrary zero point.

It was found that the steadiness of sky transparency and plate sensitivity were such that whole series of plates could be combined, even if taken during an interval as long as four hours. In general, the blue stars of similar photoelectric color index, taken in a given series, gave accordant results. It was therefore convenient to combine several blue stars of similar spectral type and color to obtain the magnitudes along the spectrum of a mean blue star, correspond-

[4] *Smithsonian Physical Tables*, pp. 608, 611, 1933.

[5] Leavitt, *Harvard Ann.*, **71**, Part 4, 1917; also private communication from Dr. W. A. Calder.

[6] Payne, *Harvard Ann.*, **89**, Part 1, 1931.

[7] Gaposchkin, *Harvard Bull.*, No. 904, 22, 1936.

ing to the mean spectral type and color index of the individual stars. The greater accuracy of the normal spectral magnitudes so obtained far outweighed the disadvantages. If obvious discordances existed within a series, it was thought proper to reduce each reddened star by comparison with those normal B stars which were taken in the interval closest to the exposure of the reddened star. The normal B stars used were of early type (O9 to B6) and of small range in photoelectric color index (-0.25 to -0.15 mag.).

The relative magnitude at each point, Δm_λ, obtained by subtracting the magnitude of the mean blue star from that of the reddened star, was plotted against $1/\lambda$ in microns^{-1}. There were 169 plotted sets of points, many of which contained two complete determinations

TABLE 3

MEASURED GRADIENTS

Relative Gradient	Mean λ in μ	$1/\bar{\lambda}$ in μ^{-1}
$\Delta\varphi_{1\text{-}4}$	0.55	1.82
$\Delta\varphi_{4\text{-}9}$	.44	2.30
$\Delta\varphi_{1\text{-}9}$	0.51	2.00

of the relative gradient from the two exposures of a star on a plate, yielding 239 determinations of relative gradients. The energy distributions in the mean blue stars were determined from 117 spectra of normal B stars with 190 individual spectra. Thirty determinations of gradient were made of 21 stars not in the Stebbins and Huffer catalogue and of later spectral types (B8 to Mo), as a check on the scale of relative gradients. Of the total of 38 reddened B stars, there were 33 well-determined gradients that are based on at least three plates. The gradients were determined by stretching a string through the plotted points; the slope was determined for three sets of points, namely, 1–4 in the red, 4–9 in the violet, and finally 1–9 for the complete spectrum. The determination of the relative gradient in the violet is particularly weak, since the absorption of the hydrogen lines and the continuum cause points 7–9 to deviate at times from the normal relationships.

The gradients so obtained were relative to those of the mean blue

star for each series, the mean color indices of which, $\bar{I}$, lay between -0.21 and -0.15 mag. All relative gradients were then reduced to gradients relative to a star of photoelectric color index, I, equal to -0.20 mag., by a small correction:

$$+3.08(\bar{I} + 0^m.20) . \tag{6.1}$$

This formula is derived from the relation between the photoelectric color indices and the revised Greenwich gradients,[8] φ_{Gw}, shown in

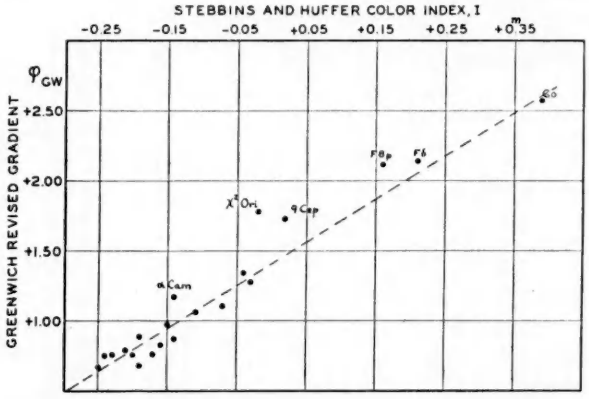

FIG. 1.—Relation between Greenwich gradient and photoelectric color index

Figure 1 for 18 stars earlier than Fo common to both lists. The linear relation is good and is found to be

$$\varphi_{Gw} = 1.40 + 3.08I . \tag{6.2}$$

The Greenwich standard stars chosen for this investigation were α Cam (HD 30614), χ^2 Ori (HD 41117), and 9 Cep (HD 206165). They were reduced as reddened stars and were to be used to adjust the zero point of the present series of gradients to the zero point of the revised Greenwich system. These stars are the reddest B stars in the Greenwich list and are also the most discordant points in Figure 1. They seem, therefore, to be unsuitable for the determination of the zero point of the present set of gradients. The three stars agree well with the relation found between the Harvard gradients

[8] Greaves, Davidson, and Martin, *M.N.*, **94**, 488, 1934.

TABLE 4

THE GRADIENTS OF REDDENED B STARS

HD	Spectral Type	Color Index (I)	$\Delta\varphi_{1-4}$	w	$\Delta\varphi_{4-9}$	w	$\Delta\varphi_{1-9}$	w	Curvature (C)	Gradient (φ)
2083.....	Bo	−0.12	0.44	2	0.30	2	0.26	3	−0.53:†	1.04
9105.....	B6s	.16	1.29	4	1.28	4	1.25	5	.00	2.03
14010.....	B8s	.10	1.66:	1	1.09	1	1.42	4	.....	2.20
15690.....	(B3)	.18	1.05	1	1.24	1	1.12	1	.....	1.90
17088.....	(B2)	.25	1.72	3	1.51	3	1.67	4	− .08	2.45
19243.....	B2ne	.06	0.91	2	0.66	2	0.82	3	− .30:	1.60
21483.....	B3	.11	0.88	2	0.81	2	0.87	3	− .06:	1.65
21803.....	B2s	− .08	0.56	1	0.49	1	0.43	1	.....	1.21
23800.....	B2n	.01	1.35	2	0.96	1	1.11	3	.....	1.89
25090.....	B1s	.04	1.04	2	0.91	2	0.94	4	− .17:	1.72
27795.....	B3s	.02	0.73	3	0.82	3	0.79	4	.10	1.57
30614.....	O9se	− .14	0.39	6	0.37	6	0.39	11	− .05†	1.17
31327.....	B2s	.08	1.09	5	0.93	5	1.00	5	− .16	1.78
31617.....	B2s	− .10	0.35	3	0.46	3	0.41	3	.27†	1.19
32990.....	B3	− .08	0.58	3	0.57	3	0.49	4	− .02†	1.27
34251.....	B3n	− .04	0.60	2	0.41	2	0.49	2	− .39:†	1.27
35395.....	B2s	.02	0.94	4	0.57	4	0.70	4	− .53	1.48
35653.....	B1s	− .04	0.39	2	0.67	3	0.55	3	.53:	1.33
35921.....	O9	− .02	0.68	2	0.50	1	0.61	2	.....	1.39
41117.....	B2ss	− .02	0.88	3	0.67	3	0.78	4	− .27	1.56
42087.....	B2s	− .05	0.77	2	0.61	2	0.65	3	− .24:	1.43
43384.....	B2s	.01	1.27	6	1.11	6	1.20	7	− .13	1.98
45314.....	B2ne	− .06	0.49	3	0.23	3	0.44	3	− .59†	1.22
45910*....	B3emq	.00	1.20	2	0.54	2	0.90	3	− .73:	1.68
52382.....	B2	− .05	0.59	1	0.38	1	0.51	1	.....	1.29
53367.....	B1ne	.06	0.87	1	0.88	1	0.93	2	.....	1.71
190603....	Boss	.13	1.23	1	0.45	1	1.03	1	.....	1.81
193183....	B2s	.08	0.97	3	0.93	3	1.01	4	− .03	1.79
195592....	Bos	.30	1.76	3	1.60	2	1.64	3	− .10	2.42
198781....	B1n	− .07	0.35	1	0.44	1	0.42	2	.....	1.20
198846....	O9nn	− .13	0.22	3	0.11	3	0.23	3	.43†	1.01
202214....	O9s	− .08	0.53	2	0.47	2	0.54	3	− .11:	1.32
206165....	B2s	.02	0.75	5	0.71	4	0.82	6	− .05	1.60
216014....	Bo	.05	0.84	3	0.66	3	0.70	3	− .26	1.48
217297....	Bo	.01	0.81	2	0.79	2	0.79	2	− .02:	1.57
220562....	B5	− .01	0.69	2	0.76	2	0.90	5	.08:	1.68
223960....	(Bo)	.21	1.50	2	1.41	4	1.50	4	− .06:	2.28
224151....	Bo	−0.06	0.77	2	0.60	2	0.70	4	−0.24:	1.48

* 45910 is the variable AX Mon and has a composite spectrum.

NOTE.—The spectral types are Victoria classifications except for those in parentheses, which are from the *Henry Draper Catalogue*.

The stars with daggers (†) in column C have small values of $\Delta\varphi_{1-9}$, so that C is essentially indeterminate.

A colon indicates that the determination is uncertain.

and the Stebbins and Huffer color indices. The zero point of the present set of gradients, φ, was therefore adopted as the Greenwich gradient, 0.78, corresponding to photoelectric color -0.20 mag. (see Fig. 1).

Table 4 gives the gradients $\Delta\varphi$ of the reddened stars relative to a star of color index -0.20 mag. The final mean absolute gradient, φ_{1-9}, is obtained by adding 0.78 to $\Delta\varphi_{1-9}$. The quantity w is an estimate of the weighted number of spectra involved in the determination of the relative gradient. The mean error of a gradient from one plate is ± 0.12 over the range of points 1–9; over the half ranges

TABLE 5

THE GRADIENTS OF STARS OF LATER TYPES

HD	Type	Gradient (φ)	w	HD	Type	Gradient (φ)	w
9200	A0	1.16:	.....	192394	A0	1.04	1
10362	B8	1.70:	.....	192766	A0	0.84::	.....
14171	A0	0.97	2	193237	B1q†	1.60	2
23288	B5	1.01	1	193576	O5‡	2.32:	.....
41040	B8	1.02	3	198413	F0	1.38:	.....
43583	B9	0.76	1	198692	K0	2.87	1
43740	G5	2.83	2	199007	B9	0.97	2
44602	A3	1.01	1	218753	A3	1.63:	.....
48393	K0	3.17	1	224014	F8p	2.46	1
CI Cygni	M*	3.68::	.....	224364	Ma	4.11	1
188074	F0	1.76	2				

* CI Cygni is a peculiar variable of spectral type near M.
† 193237, P Cygni. ‡ 193576, Wolf-Rayet star.

the mean error is ± 0.18. The curvature, C (see Table 1), is the percentage change of slope along the spectrum and is defined as

$$C = \frac{\Delta\varphi_{4-9} - \Delta\varphi_{1-4}}{\Delta\varphi_{1-9}}. \qquad (7)$$

C is essentially indeterminate unless $\Delta\varphi_{1-9}$ is at least 0.7 and unless the determinations of $\Delta\varphi_{1-4}$ and $\Delta\varphi_{1-9}$ are both of good quality. If the reddening of the B stars arises solely from interstellar extinction, $\Delta\varphi_{1-9}$ is a measure of the total interstellar reddening and C is a constant depending on the law of variation of extinction coefficient with wave length, given in Table 1.

Table 5 gives the gradient for the later-type stars that were meas-

urable on plates taken for the B stars. The weights of these determinations are low, in view of the small dispersion and the presence of absorption lines and bands in late-type spectra.

Figure 2 gives the Harvard gradients for the reddened B stars as a function of Stebbins and Huffer's photoelectric color index, *I;* Figure 3 gives the gradients of the later-type stars as a function of the Henry Draper spectral type. The dotted line in Figure 2 is the

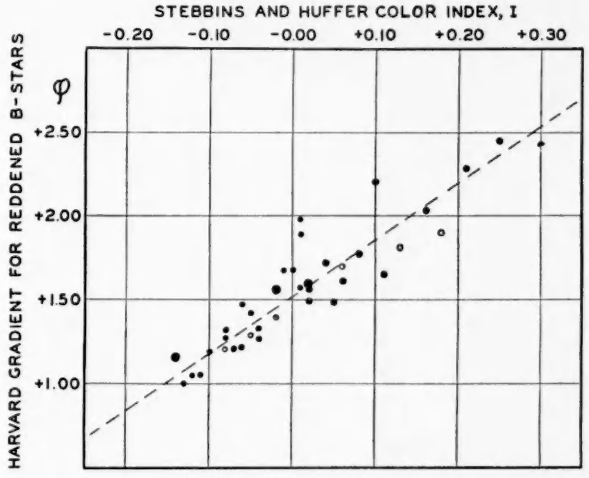

FIG. 2.—Relation between new Harvard gradients and photoelectric color index, for B stars.

adopted relationship between Harvard gradient and color index. The dotted line in Figure 3 is the relationship between Greenwich gradient and spectral type.

RELATIONSHIPS BETWEEN GRADIENT AND COLOR INDEX

The systematic errors in the relative gradients are probably small. The effect of faulty standardization, or of scale errors in the tube photometer, can be estimated from a comparison of the relative gradients as obtained from the stronger and from the weaker spectrum on a plate. The mean values of the differences are found to be

$$(\Delta\varphi_{\text{bright}} - \Delta\varphi_{\text{faint}})_{1-4} = +0.06 \pm 0.02\,,$$

$$(\Delta\varphi_{\text{bright}} - \Delta\varphi_{\text{faint}})_{4-9} = \quad .00 \pm \quad .02\,,$$

$$(\Delta\varphi_{\text{bright}} - \Delta\varphi_{\text{faint}})_{1-9} = \quad 0.00 \pm 0.01\,.$$

It is obvious that the photometric standardization is substantially free from error. The difference for the points in the red may be real and has an explanation in the halation and Eberhard effects near the dense sensitization humps such as are present on the Eastman 1F plates. The general scale of gradients, which depends on the homogeneity of the magnitude system for the various rows of photometer spots, is confirmed by the data in Figure 3, where the var-

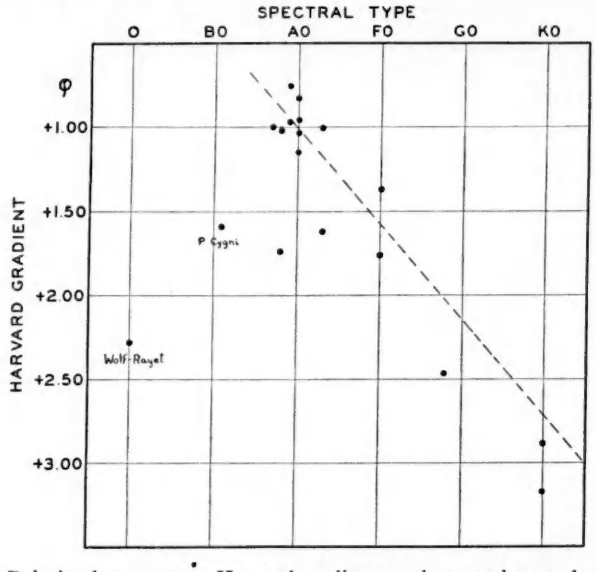

FIG. 3.—Relation between new Harvard gradients and spectral type, for later-type stars.

iation of the gradients of the present investigation with spectral type is seen to be roughly the same as that given by the Greenwich observers. Equation (6.2) for the relation of Greenwich gradient and photoelectric color index, I, is

$$\varphi_{Gw} = 1.40 + 3.08I . \qquad (6.2)$$

The present gradients are well expressed by the formula

$$\varphi_{1-9} = 1.51 + 3.36I . \qquad (8)$$

It should be remembered that the Harvard scale of gradients is independent of the Greenwich scale, except for zero point. The ap-

parent difference in zero point of the two relations, (6.2) and (8), arises from the small number of stars common to the Greenwich and the photoelectric lists.

The good correlation between the photoelectric color indices over a very short base line and the Greenwich and Harvard gradients over the visible spectrum indicates that the Stebbins and Huffer photoelectric color indices are significant measures of differences in the total spectral distribution of energy in the B stars. It is interesting to note that, if the stars radiated like black bodies, we could compute the theoretical relation between the gradient and the photoelectric color index. The gradient is given by

$$\varphi = 0.921 \frac{d(\Delta m_\lambda)}{d\frac{1}{\lambda}} + \text{Constant} . \tag{9.1}$$

The color index, I, between wave lengths λ_1 and λ_2 is

$$I = \Delta m_{\lambda_1} - \Delta m_{\lambda_2} = \frac{\Delta(\Delta m_\lambda)}{\Delta\frac{1}{\lambda}} \Delta\frac{1}{\lambda} + \text{Constant} . \tag{9.2}$$

Therefore, we find that

$$I = 1.086\varphi\Delta\frac{1}{\lambda} + \text{Constant} . \tag{9.3}$$

Since the effective wave lengths of the photoelectric cell plus filter are given as 0.426 μ and 0.477 μ, we can compute φ from

$$\varphi = \text{Constant} + 3.67I . \tag{9.4}$$

The theoretical coefficient of I, 3.67, is close to the observed ones (3.08 or 3.36) and indicates that the law of interstellar extinction is such as to make the apparent energy distribution of a reddened star very similar to that of a black body at a lower color temperature, a conclusion reached by several other investigators.[9,10,11,12,13]

[9] Trumpler, *Pub. A.S.P.*, **42**, 267, 1930.

[10] Struve, Keenan, and Hynek, *Ap. J.*, **79**, 1, 1934.

[11] J. Rudnick, *ibid.*, **83**, 394, 1936.

[12] Hall, *ibid.*, **85**, 145, 1937.

[13] Bennett, *ibid.*, p. 257.

A comparable series of measures of gradients of reddened B stars has been made by Gerasimovič,[14] who also used the 24-inch reflector and the 3° prism. The stars which he observed were brighter than the fifth magnitude, and the only standardization available was obtained from a set of off-axis apertures. When Gerasimovič's gradients, φ_{Ger}, are plotted against photoelectric color index for 62 stars common to both lists, the scatter is found to be rather large, and the relationship indicated is

$$\varphi_{\text{Ger}} = -0.68 - 5.32I . \qquad (10)$$

The coefficient of I, 5.32, is nearly 60 per cent larger than in equations (6.2) and (8). The scale of Gerasimovič's gradients is therefore

TABLE 6

COLOR TEMPERATURES OF NORMAL B STARS

Spectral Type	Normal Color (I)	Gradient ($\varphi_{1\text{-}9}$)	Color Temperature (Degrees)
O	$-0^{M}23$	0.72:	38,000:
B1	.21	0.78	30,000
B3	.19	0.85	24,500
B5	.17	0.92	21,000
B8	.13	1.05	16,500
A0	−0.10	1.15	14,500

too open; his reddened stars are too red. The very low color temperatures derived by him for the bright reddened B stars are therefore not confirmed. The coefficient 5.32 is not compatible with the black-body relationship in (9.4). It is probable that the plate calibration was insufficient.

The apparent low color temperatures of some fainter B stars are confirmed by the present set of gradients. The gradient of HD 17088, a B2 star, is 2.45; that of HD 195592, a B0s star, is 2.42. Such gradients normally correspond to stars of spectral type G5. For high-latitude unreddened B stars, very much smaller gradients are found. The relation between photoelectric color index and Greenwich and Harvard gradient makes it possible to determine color temperatures

[14] *Harvard Circ.*, No. 339, 1929.

for the normal blue B stars of the Stebbins and Huffer catalogue. Table 6 gives, as a function of spectral type, the mean normal color index adopted by Stebbins and Huffer, the corresponding gradient on the basis of this investigation, and the deduced color temperature. It should be remembered that the mean color of the unreddened O stars is uncertain because of their low galactic latitude, and that the conversion of color index to gradient for B8 and Ao stars is an extrapolation of the observational material of the present investigation. The temperatures are higher than the usual scale of ionization temperatures, partly because of the revision of the Greenwich zero point for Ao stars. There is also considerable uncertainty, of the order of ± 0.05, in the actual setting of the zero point of the Harvard gradients; in any case, the temperature of unreddened Bo stars is found to be at least 25,000°.

ABSOLUTE-MAGNITUDE EFFECTS

Stars of high intrinsic brightness are necessarily involved in most studies of interstellar selective absorption. In many highly luminous B stars, radial outflow of matter and turbulence, emission lines of variable intensity, and slight variability in radial velocity and magnitude are observed, suggesting real deviations from both gravitational and thermodynamic equilibrium. If such deviations are accompanied by lower color temperatures, a spurious correlation of color excess with luminosity, and therefore with galactic latitude and distance, would exist. A preliminary estimate of the effect of absolute magnitude can be obtained from the color indices of the high-latitude B stars in the Stebbins and Huffer catalogue. A measure of absolute magnitude is given for these B stars by line sharpness, in spite of uncertainties arising from rotation and incipient emission.

All stars of type Bo to B7 with galactic latitudes greater than $\pm 15°$, for which line grades are given, were tabulated. Their color excesses were corrected to the galactic pole by the use of a cosecant formula for interstellar selective absorption and with an optical thickness on the photoelectric scale of 0.08 mag., as determined by Stebbins and Whitford.[15] (The corrections are always smaller than

[15] *Ap. J.*, **84**, 132, 1936.

−0.15 mag. because of the choice of high-latitude objects.) After selective absorption is eliminated, it is found that there is no obvious variation of color with line-characteristic for these 91 stars, some of which attain an absolute magnitude of − 4. Table 7 gives the mean corrected color excess, together with the number of stars involved, and the spread in corrected color excess. The normal colors adopted by Stebbins and Huffer seem to be slightly too red. There are no traces of large absolute-magnitude effects for the wave lengths involved in the photoelectric measurements; whatever deviations exist may be farther toward the violet than 4260 A. Nevertheless, exceptionally luminous stars and those of peculiar spectra should be avoided in future studies of interstellar selective absorption.

TABLE 7

ABSOLUTE-MAGNITUDE EFFECTS

Line Grade	*e*	*nn*	*n*	*s*	*ss*
Mean color excess....	$-0^{M}04(15)$	$-0^{M}03(2)$	$-0^{M}08(38)$	$-0^{M}05(35)$	$-0^{M}01(1)$
Extreme color excesses	$\left\{\begin{matrix}-.10\\+0.02\end{matrix}\right\}$	.....	$\left\{\begin{matrix}-.11\\+0.05\end{matrix}\right\}$	$\left\{\begin{matrix}-.14\\+0.07\end{matrix}\right\}$	.....

The effect of hydrogen absorption should be briefly considered. Karpov[16] has measured the total absorption of the Balmer lines in some early B stars. The total light loss in magnitudes suffered by a star in the spectral region 3970 A to 3735 A from line absorption varies from +0.07 for a B0e star to +0.19 for a B7 star. The complete disappearance of the hydrogen lines can produce an ultraviolet excess (at 3850 A) of 0.2 mag. at most. The absorption beyond the Balmer limit is larger, and variations in the continuous absorption will probably reach 1 mag. An attempt to measure selective absorption beyond 3800 A would therefore be subject to a systematic error depending on absolute magnitude.

THE CURVATURE OF THE RELATIVE GRADIENTS

We have shown that the present measures yield a satisfactory scale of gradients and that absolute-magnitude effects in the colors

[16] *Lick Obs. Bull.*, **16**, 159, 1934.

of B stars are probably small. We are able, then, to assume that the difference in gradient between a reddened B star and a normal B star arises solely from selective absorption. The values for the curvature C in Table 4 enable us to determine the law of interstellar extinction. The quantity C, a ratio, has a mean error (for the normal number of plates—say three) of ± 0.25 if $\Delta\varphi_{1-9}$ is of the order of 0.5. If $\Delta\varphi_{1-9}$ is larger than 0.75, then C has a mean error less than ± 0.18. Neglecting small values of $\Delta\varphi_{1-9}$ as subject to extreme statistical fluctuations, we are left with nine values of $\Delta\varphi_{1-9}$ greater than 0.75. Of these, seven are negative, one is positive, and one is zero. The mean is -0.08 ± 0.04, which indicates a slight negative curvature of the gradients. For 21 stars with $\Delta\varphi_{1-9}$ greater than 0.50, the mean of C is -0.10 ± 0.04. The color temperature seems to rise slightly toward the violet for reddened stars, and in no case does there exist a positive curvature (decrease of temperature toward the violet) such as that expected for strongly selective absorption. The actual value of C, -0.08, corresponds to the law of selective absorption

$$k_\lambda = \frac{k}{\lambda^{0.8}}. \qquad (11)$$

Not much weight can be given to this direct determination, but it is obvious that no serious departure from linearity of relative gradients seems to exist even in the most reddened stars, which is in agreement with the results of previous investigations.[9, 10, 11, 12, 13]

A more significant measure of the nonlinearity of the gradients is obtained by using the relations between the photoelectric colors and the gradients over the shorter ranges of wave length, $\Delta\varphi_{1-4}$ and $\Delta\varphi_{4-9}$. These relations are more strongly determined than are the curvatures of the individual gradients, but they may be affected by photometric errors depending on wave length. The linear relations are found to be

$$\Delta\varphi_{1-4} = 0.77 + 3.65I, \qquad \text{red}, \quad (12.1)$$

$$\Delta\varphi_{4-9} = 0.64 + 3.14I, \qquad \text{violet}. \quad (12.2)$$

The red gradient has a coefficient of I close to that for a black body, which would yield 3.67. The gradients are essentially linear from

6500 A to the violet limit of the photoelectric color indices, 4260 A. The relation for the gradient in the violet is definitely such that the color temperature is higher in the violet. There is an excess of violet energy, the same effect as that found from the curvatures. Trumpler[9] found indications of negative curvature in several faint B stars; J. Rudnick[11] found a slight effect in ζ Persei but not in 55 Cygni. Hall[12] suggests that the exponent n in the law of selective absorption decreases in ζ Persei from 1.6 in the infrared to 1.2 in the violet.

The excess of violet energy cannot at present be directly interpreted in terms of the interstellar absorption coefficient. While there is no obvious correlation of the value of the curvature, C, with the absolute magnitude as indicated by the sharpness of the lines, there is a possibility that the weaker hydrogen lines and continuum in the more luminous stars may produce an apparent excess of violet energy. The existence of a systematic difference in absolute magnitude between the normal blue B stars and the reddened stars is very probable, since only high-luminosity stars are able to suffer severe absorption in dark nebulae and still be sufficiently bright to lie within a given limiting apparent magnitude. Normal stars down to the same magnitude limit will be intrinsically less luminous. At present we may conclude that the approximation to linearity of relative gradients of reddened stars is sufficient to permit us to assume that the selective absorption varies roughly as

$$k_\lambda = \frac{k}{\lambda}. \tag{13}$$

THE RELATION BETWEEN THE PHOTOGRAPHIC AND SELECTIVE ABSORPTION

If absolute magnitudes and trigonometric parallaxes were available for the reddened B stars, it would be a simple matter to evaluate the absorption coefficients in the galaxy. The measures of gradient can be converted into color excesses on the International Scale, and the absorption at the photographic wave length can be determined from the apparent and true moduli. Since spectroscopic parallaxes are affected by absorption and since the irregularity of the absorbing medium will be serious for the comparatively near-by stars which we have observed, no statistical treatment of the data is advisable.

The actual absorption at the photographic effective wave length varies from nearly zero to 4 mag. for stars one kiloparsec distant from the sun in the galactic plane.

The most direct way of measuring the interstellar absorption for such near-by stars is based on the determination of the total absorption in the obvious dark nebulae in front of the star. The stars of this investigation show a color excess with reference to normal stars; and, therefore, if they are found to lie in an obscured region, there is a good chance that they are actually behind the obscuring material. An inspection of the star fields around the reddened stars, on Harvard patrol plates taken with short-focus, high-speed cameras, showed that many of the stars were in dark regions. An attempt has been made to evaluate roughly, by means of star counts, the amount of the absorption in the dark nebulae in which the stars seem to be involved.

Each reddened star was identified on patrol plates of various series, with magnitude limits ranging from 13.5 to 16.0 mag. The Harvard results have been supplemented during a stay[17] at the Yerkes Observatory by the use of the original plates of the Ross *Atlas of the Milky Way*, with a magnitude limit near 17.0 mag. The known regions of heavy obscuration[18] were outlined and the various plates inspected in order to determine whether the star was in an obscured region. In the case of every one of the 38 stars there were obvious obscuring clouds immediately surrounding the stars. For three stars no suitable plates were available for detailed investigation, but in these cases cursory inspection revealed the existence of obscuring material. While a proper determination of the obscuration involves a complete set of star counts down to various magnitude limits, a first approximation can be made by comparing the star counts to the plate limit in a normal field at the same galactic latitude, that is unaffected by the dark nebula, with the star counts in the darkened region. Counts were therefore made in an area of 0.25 cm^2 centered on each of the 35 reddened stars. A comparison region of the same area was counted in a normal star field. Since the ob-

[17] The work at Yerkes has been made possible by a Fellowship granted by the National Research Council.

[18] Greenstein, *Harvard Ann.*, **105**, No. 17, 1937.

scuring clouds are highly irregular in form and are of great extent, it was sometimes necessary to choose the normal field at distances as far as 15° from the star. Care was taken to avoid errors arising from the distance correction of the plates. The logarithmic defect, log (N_m/N'_m), was thus obtained, where N'_m is the number of stars brighter than the plate limit in the obscured field, and N_m the number in the normal field. A rough value of the magnitude limit, m, required in the reduction, can be obtained from the tables of log N_m as a function of galactic latitude and longitude. The limiting magnitudes ranged from 13.5 mag. to 17.0 mag., the counted numbers from 32 to 1350 per unit area, and the counted areas from 0.1 to 2.8 square degrees.

We should, properly, obtain counts to extremely faint limiting magnitudes in order to be sure that we have obtained a measure of the full absorbing power of the cloud. If this has been done, a good estimate of the total absorption at the photographic effective wave length, δm, in the nebula, is given by the relation

$$\delta m = 2.46 \log_{10} \left(\frac{N_m}{N'_m} \right). \qquad (14)$$

If the star is not behind the absorbing cloud, we shall have overestimated the total absorption suffered by the stellar radiation. However, the fact that the star is reddened is in itself evidence that the star is in or behind a region of high absorbing power. δm is the total absorption in the cloud only if we have counted to a sufficiently faint limit. If the dark nebula is at a distance greater than a few hundred parsecs it is easy to see that the relation (14) is not sufficient to give a full measure of the absorption.

It is therefore necessary to use some results of the theory of stellar statistics to interpret the observed logarithmic defect in terms of the total absorption. The run of the counted number of stars at a given magnitude, A_m, as a function of magnitude, is fixed for a nebula of known distance and total absorption. Such predicted values, A'^*_m, are given in discussions of dark nebulae by Greenstein[18] and by F. D. Miller.[19] From such computations it is possible to predict the

[19] Bok, *The Distributions of the Stars in Space* ("Astrophysical Monograph"), p. 43, 1937.

counted number of stars, N'^*_m, in the field of a dark nebula of known distance and total absorption. The predicted logarithmic defect, $\log_{10}(N^*_m/N'^*_m)$, is then determined as a function of the distance of the nebula and of the limiting magnitude

$$N^*_m = \int_{-\infty}^{m-(1/2)} A^*_m dm\,, \qquad N'^*_m = \int_{-\infty}^{m-(1/2)} A'^*_m dm\,, \tag{15.1}$$

$$\delta m^* = F\left[\log_{10}\left(\frac{N^*_m}{N'^*_m}\right), \text{distance}\right]. \tag{15.2}$$

Values of δm^* have been computed by the author. Since the approximate distances of the dark nebulae are known,[18] as well as the limiting magnitudes, it is possible to use these predicted values to interpret the observed defect in star numbers in terms of the total absorption of the nebula. The results agree closely with those of equation (14) for nebulae closer than 300 parsecs; the deviations for larger distances are considerable. This is to be expected, since large numbers of foreground stars are projected against the surface of a distant nebula. To the absorption, δm, produced by dark nebulae, we must add the effect of the normal absorption, about 0.5 mag./kpc in photographic light, in the galactic plane. The total absorption at the photographic effective wave length suffered by the star is

$$A_{pg} = \delta m + 0^{M}5R'\,, \tag{16}$$

where R' is the true distance of the star in kiloparsecs. A measure of the distance was obtained from the mean absolute magnitudes adopted by Stebbins and Huffer for the spectral type and line characteristics of the star. The distance, uncorrected for absorption, R, was then used to compute R' and the general absorption from (16).

The determination of ϵ, the ratio of the selective absorption on the International Scale to the photographic absorption, then becomes possible. The color excess on the International Scale, E, can be computed from the relation

$$E = 1.086\Delta\varphi'_{I-g}\left(\frac{1}{0.44} - \frac{1}{0.55}\right), \tag{17.1}$$

$$E = 0.494\Delta\varphi'_{I-g}. \tag{17.2}$$

TABLE 8

COLOR EXCESSES AND PHOTOGRAPHIC ABSORPTION FOR REDDENED B STARS

HD	$\log_{10} \frac{N_m}{N_m'}$	$\Delta\varphi'_{1\text{-}9}$	δm	ϵ	R Distance Uncorrected for Absorption	Remarks
2083	0.24	0.36	0.8	0.15	1050	
9105	.60	1.12	1.9	.26	800	
14010	.70	1.19	2.0	.27:	660	
15690	.56	1.09:	1.5	.32:	630	
17088	.60	1.67	2.2:	.34:	720	Counts difficult. Comparison region obscured
19243	.24	0.82	0.7	.41	830	
21483	.77	0.84	1.8	.17	480	
21803	.....	0.43:	.....	.....	500	Slightly obscured. No suitable material
23800	.58	1.11	2.0	.26	500	
25090	.21	0.97	0.8	.44	1050	
27795	.66	0.76	1.5	.24	570	
30614	.....	0.49	.....	.....	980	High-latitude Cepheus flare. No suitable material
31327	.68:	1.00	1.9:	.25	480 330	
31617	.....	0.41	.....	.....	800	Slightly obscured. No suitable material
32990	.32	0.46	0.7	.25	230 250	
34251	.28	0.46:	0.7	.23:	570	
35395	.41	0.70	1.0	.27	630	
35653	.11:	0.58	0.3	.40:	1150	
35921	.15:	0.71:	0.5	.35:	1380	
41117	.43	0.78	1.6	.20	1100	
42087	.29	0.65	0.8	.32:	400	Obscured only if supergiant
43384	.43	1.20	1.2	.39	500 1000	
45314	.30	0.44	0.8	.20	1100	
45910	.26	0.87:	0.7	.48:	800	Composite spectrum. Rejected
52382	.37	0.51:	1.1	.17:	440	Obscured only if giant
53367	.56	0.96:	1.8	.20:	1450	Nebulous; involved in cloud
190603	.30	1.10:	0.8	.39:	1740	
193183	.42	1.01	1.4	.31	730	
195592	.55	1.74	1.9	.37	2300	
198781	.50	0.45:	2.2	.08:	550	Doubtful. Possibly in front of most of obscuring material
198846	.11	0.33	0.3	.18	1660	
202214	.54	0.64	1.9	.14	870 500	
206165	.48	0.82	1.7	.19	1200	
216014	.60	0.77	2.2	.16	1100	
217297	.65	0.86:	2.6	.15:	1320	
220562	.57	0.80	2.0	.18	320	Obscured if giant
223960	.59	1.57	1.8	.25	1100	
224151	0.33	0.77	0.9	0.29	990	

The value of ϵ is then

$$\epsilon = \frac{0.494\Delta\varphi'_{1-9}}{\delta m + 0^{M}5R'}. \qquad (18)$$

Table 8 contains a compilation of the available data on each of the reddened B stars for which $\Delta\varphi_{1-9}$ is available. The logarithmic defect is obtained from star counts. The corrected gradient, $\Delta\varphi'_{1-9}$, relative to the normal star of the given spectral type is obtained from $\Delta\varphi_{1-9}$, which was relative to a star of color index -0.20 mag. A_{pg} is obtained from (16), and ϵ from (18). The distance R, uncorrected for absorption, is given, and occasionally the distance corresponding to the parallax in Schlesinger's catalogue. The remarks, finally, give my judgment as to whether the star is behind a near-by, obvious, dark nebula.

The value of ϵ can be determined from the data of Table 8. The fluctuations are considerable because of the uncertainties in the estimates of the total photographic absorption. The following means of the value of ϵ are obtained:

Source	Number	ϵ
All determinations	34	0.26 ± 0.02
Good determinations	22	$.25 \pm .02$
Values of A_{pg} greater than 1.0 mag.	22	0.23 ± 0.02

The color excess on the International Photovisual Scale is definitely of the order of one-fourth the total photographic absorption.

CONCLUSION

Two essentially independent estimates of ϵ are now available, based on the observed gradients of the reddened B stars. The close approach to linearity of the relative gradients and the small value of the curvature, $C = -0.08$, resulted, by reference to Table 1, in my first estimate that ϵ was near 0.17. The determination of the total photographic absorption suffered by the stars for which gradients had been obtained gave a value of ϵ near 0.25. It is profitable to compare these estimates with that obtained from the optical thickness of the galactic absorbing layer. Stebbins and Whitford[15]

have determined the total selective absorption from pole to pole through the layer as 0.128 mag. on the International Scale of color index. The optical thickness in photographic light lies between 0.5 and 0.8 mag., as derived from the discussion of counts of extragalactic nebulae.[20,21,22] The value of ϵ derived from these data lies between 0.17 and 0.26, in good agreement with the possible range of values suggested by the spectrophotometry of reddened B stars. Schalén has made estimates of the color excess and of the absorption coefficient in various obscured regions of the Milky Way.[23] After transformation of his results to the International Scale of color excess, the value of ϵ is found to be 0.26. A similar investigation, by Sticker, of the Cepheus region[24] yields a value of ϵ equal to 0.28.

It is reasonable to conclude that measures of color excess over almost any convenient base line of wave length between the red and the near-violet regions of the spectrum seem justified by the close approximation to linearity found for relative gradients arising from selective interstellar extinction. The agreement between the values of ϵ obtained by the most diverse methods suggests that measures of color excess can be converted into measures of total absorption by means of a constant multiplying factor, for measures over large regions of the galaxy. The value of this factor is now fairly well known; it lies between 4 and 6.

The discussion in my paper on the theory of selective absorption[25] provides a possibility of interpreting the observational results outlined in the foregoing pages. The observed value of ϵ can arise from a process of scattering and absorption by small metallic particles of the type discussed by Schalén[23] and, after him, by Schoenberg and Jung.[26] In no case can Rayleigh scattering be a dominant factor. On the other hand, I have indicated, in the paper referred to, the probability of the existence in space of mixtures of particles of various sizes, in which the high selectivity of the extinction by small

[20] Van de Kamp, *A.J.*, **42**, 97, 1932.

[21] Hubble, *Ap. J.*, **79**, 8, 1934.

[22] Shapley, *Harvard Reprint*, No. 90, 1933.

[23] *Upsala Medd.*, No. 58, 1934; No. 64, 1936. [24] *Bonn Veröff.*, **30**, 1937.

[25] Greenstein, *Harvard Circ.*, No. 422, 1938 (in press).

[26] *A.N.*, **253**, 261, 1934; *Breslau Mitt.*, No. 4, 1937.

particles is reduced by the essentially nonselective extinction by larger particles. Absorption coefficients of the observed order of magnitude will arise from such mixtures of particles, with total space densities well below the Kapteyn-Oort limit. The theoretical selectivity, as measured by ϵ, is close to that determined in this observational investigation, when we assume that the frequency function of particles of various sizes are of the type given in Tables XIV–XIX of my paper.[25] It is particularly interesting that a frequency function near the one suggested for the distribution of hyperbolic meteors[27] seems to provide the best agreement of theory and observation. In this distribution the number of particles of radius a is given by $\psi(a)$:

$$\psi(a)da = a^{-3.6}da \,. \tag{19}$$

Values of ϵ derived from Table XVI of my paper,[25] based on this function, range from 0.09 to 0.44, depending on the optical properties of the substances present in space. Metallic substances yield values of ϵ near 0.25. The total space density of all sizes of particles required for a general photographic absorption coefficient of 0.5 mag./kpc in the galactic plane is between 1.3×10^{-26} and 2.8×10^{-26} gm/cm^3. We can conclude that the extinction of light by an interstellar medium consisting of a reasonable distribution of small dust particles, continuous with that of the hyperbolic meteors, is such as to satisfy the available observational data.

I am grateful to Dr. Harlow Shapley for his personal encouragement and for his liberal provision of observational facilities for this investigation. Dr. Bok has suggested the mode of attack on the general problem of selective absorption. I am indebted also to Dr. C. Payne-Gaposchkin and to Dr. Whipple for their advice on photometric problems and technique.

HARVARD OBSERVATORY
YERKES OBSERVATORY
October 1937

[27] Watson, *Harvard Ann.*, **105**, No. 32, 1937.

AN IMPROVED DESCRIPTION OF THE THORIUM SPECTRUM

MARK FRED

ABSTRACT

Part of the spectrum of thorium has been separated into about 750 *Th* I lines and 2000 *Th* II lines (of which only the most important are given here), primarily on the basis of relative intensities in different parts of the arc gap. This classification has been confirmed by Zeeman patterns where resolved, by furnace data, etc. Certain of the lines of each spectrum have been designated as low-temperature lines. Most of the wave lengths are given to seven significant figures. It is believed that these data are sufficient for the term analysis of *Th* I. For *Th* II better Zeeman patterns are probably necessary.

I

The spectrum of thorium appears to have received very little attention since the work quoted in 1912 by Kayser,[1] who listed 1300 lines from 2400 A to 7000 A in Rowland units. No further wave lengths have been published except in the vacuum region, where *Th* IV has been analyzed by Lang.[2] The *raies ultimes* have been determined by De Gramont,[3] Pollok and Leonard,[4] and others. Allin[5] reports certain ultraviolet lines reversed in the underwater spark. The Zeeman patterns of a number of lines were partly resolved and measured by Moore.[6]

For a term analysis the foregoing data are quite inadequate. Since there are no obvious regularities, a start on a term scheme must be made by a search for constant differences and application of the combination principle. But it will be recalled that one can expect, by chance, approximately $2\epsilon N^2/I$ pairs with any given wave-number difference,[7] where ϵ is the wave-number error of the N lines considered in the total spectrum range I cm^{-1}. Moreover, some differences will be repeated by chance by more than this number of

[1] *Handbuch der Spectroscopie*, **6**, 636, 1912. [2] *Can. Jour. Res.*, **14**, 43, 1936.

[3] See F. Twyman, *Wavelength Tables for Spectral Analysis* (London: Adam Hilger), p. 114, 1931.

[4] Quoted by Twyman, p. 95.

[5] *Trans. Roy. Soc. Can.*, **21**, 231, 1927. [6] *Ap. J.*, **30**, 144, 1909.

[7] S. Goudsmit, quoted by G. R. Harrison, *Rev. Sci. Inst.*, **4**, 584, 1933.

pairs, other differences by less; i.e., one expects a probability distribution (of the Poisson type) of the number of pairs, whose maximum is given by the foregoing expression. Since many thousand differences are examined to find those which are repeated, one desires the probability that any differences are repeated by chance several times to be less than one in some thousands. For this to be true the most probable number of pairs must be considerably less than one. From the expression $2\epsilon N^2/I$ one sees that this can be reduced by increasing the wave-length accuracy and by restricting N (preferably by subtracting only those lines expected to show the greatest number of constant differences, i.e., low-temperature lines). Of course, a term analysis is perfectly possible with a greater number of chance relationships, but experience suggests that considerable preliminary preparation is quite profitable.

Another obvious requirement is that the lines be classified as arc or spark. This difficulty is by no means trivial. Most of the lines show very little intensity change in the spark as compared with the arc as source, and some other criterion must be adopted. A convenient characteristic, which has been verified for similar elements, for example, hafnium,[8] is the enhancement of the spark lines at the cathode of the arc.

This paper presents material which to a certain extent satisfies the preceding objectives.

II

The wave lengths given below are taken from several sources. Most of them were measured by the writer on plates taken in this laboratory on the new thirty-foot grating, which has a dispersion of 0.9 and 0.4 A/mm in the first and second orders, respectively. The source was an arc between thorium electrodes in an atmosphere of nitrogen. The plates were measured on a Geneva comparator. Half of the iron comparison exposure was made before the thorium exposure, and the rest afterward. The 1928 wave lengths of the International Astronomical Union were used where available, supple-

[8] W. F. Meggers and B. F. Scribner, *Bur. Stand. Jour. Res.*, **13**, 625, 1934.

mented by Burns's vacuum-arc interferometer measurements[9] in the ultraviolet. Second-order iron lines were used in the red, with 0.015 A added to the first-order wave lengths calculated from them to correct for failure of the grating law.

Through the courtesy of Professor G. R. Harrison, of the Massachusetts Institute of Technology, preliminary values were obtained for about twelve hundred selected thorium lines from 4436 A to 2826 A, measured by means of an automatic measuring machine on plates taken with a thirty-five-foot grating. Harrison states that similar measurements on the cobalt spectrum show an average deviation of 0.002 A from interferometer measurements, and the final thorium values are expected to be as good, each wave length being the average of three to ten determinations. The second-order ultraviolet wave lengths described above agree with Harrison's values to within an unweighted average of 0.004 A, while the first-order visible lines spread, by about the same amount, about a systematic difference of 0.005 A. From this agreement the average wave-number error for lines measured by the writer may be expected to be about 0.02 or 0.03 cm^{-1}.

The remaining wave lengths, given to six figures, are taken from earlier work done by the writer[10] with M. Ference, Jr.,[11] and with R. B. Bowersox.[12] These measurements (on 6000 lines) were made on plates taken in the first order of a twenty-one-foot grating which had a dispersion of 2.4 A/mm. The source was a hollow cathode discharge in which $ThCl_4$ was vaporized and excited by helium. The values are good to about 0.01 or 0.02 A, except in the infrared, where the wave-length error is somewhat more.

The separation of the lines quoted below into two tables was made purely on the basis of relative intensities at different parts of the arc gap: lines which were definitely enhanced at the anode were called *Th* I; lines having equal intensity all the way across the arc and lines enhanced at the cathode were called *Th* II or *Th* III. This classification is in agreement with practically all the available Zeeman patterns and furnace data. The intensities quoted are visual estimates,

[9] K. Burns and F. M. Walters, Jr., *Pub. Allegheny Obs.*, **8**, No. 4, 39, 1931.

[10, 11, 12] Master's dissertations, University of Chicago, 1934.

TABLE 1

THORIUM I

λ	ν	− o +	Remarks
8967.65	11148.19	 2	
8758.22	414.71	 2	
8748.02	28.02	 3	
8573.10	661.19	.. o 3	
8478.36	791.50	.. o 5	
8446.51	835.96	.. o 4	
8445.46	37.43	 2	
8421.22	71.52	.. o 4	
8417.98	76.07	 3	
8416.70	77.88	.. o 6	
8330.48	12000.82	.. o 9	
8320.86	14.69	.. o 5	
8275.63	80.35	.. o 3	
8186.92	211.26	.. o 3	
8159.75	51.91	.. o 2	
8143.15	76.89	.. o 3	
8032.48	446.04	 2	
7978.97	529.50	 6	
7900.35	54.19	 2	
7865.99	709.47	 2	
7847.53	39.36	 6	
7817.78	87.85	 5	
7798.33	819.74	 2	
7788.95	35.17	oo .. 4	
7653.86	13061.71	 2	
7647.40	72.75	1 o 8	
7585.73	179.03	2 o 9	
7567.72	210.39	2 o 6	
7549.33	42.57	oo .. 3	
7483.62	358.84	.. oo 3	
7481.36	62.88	.. o 4	
7447.84	423.02	 2	
7444.75	28.58	 2	
7430.27	54.76	o o 6	
7428.96	57.13	2 1 8	
7418.57	75.98	 2	
7402.31	505.58	o oo 2	
7385.485	36.30	3 2 8	
7384.21	38.69	 3	
7383.74	39.54	o .. 3	
7376.95	52.00	o .. 4	
7341.20	618.01	o o 4	
7328.34	41.90	o o 5	
7324.86	48.39	o .. 2	
7288.98	715.57	.. o 3	

TABLE 1—*Continued*

λ	ν	− o +	Remarks
7287.05	13719.20	.. o 2	
7284.95	23.15	.. o 5	
7244.73?	99.33	 2	
7242.09	804.37	 2	
7230.88	25.78	 2	
7219.18	48.18	 2	
7218.11	50.23	3 1 6	?
7217.79	50.84	 4	?
7212.75	60.53	o .. 4	
7208.005	69.56	2 1 8	
7206.55	72.45	 2	
7200.08	84.91	 3	
7173.42	936.51	oo .. 3	
7168.888	45.34	2 2 10	
7164.88	53.13	 2	
7159.98	62.68	 3	
7159.10	64.39	o o 4	
7158.56	65.45	 2	
7156.98	68.53	o .. 2	
7155.55	71.32	o o 3	
7155.05	72.30	o o 3	
7153.61	76.11	oo .. 2	
7150.34	81.50	oo .. 3	
7148.59	84.94	oo oo 3	
7124.61	14032.00	1 o 5	
7084.177	112.08	 6	
7064.48	51.43	 2	
7060.71	58.99	 2	
7036.30	208.10	 2	
7018.574	43.99	 5	
7000.795	80.16	 6	
6989.657	302.92	1 .. 8	
6943.610	97.77	o .. 7	
6911.238	465.20	o .. 7	
6874.77	541.94	o .. 2	
6868.55	55.11	o .. 2	
6834.921	626.72	o .. 6	
6829.05	39.30	 5	
6824.73	48.56	 4	
6809.35	81.64	 2	
6791.27	720.73	 3	
6789.028?	25.59	o .. 2	
6787.917?	28.00	o .. 2	
6780.268	44.62	2 .. 7	
6780.147	44.88		

TABLE 1—*Continued*

λ	ν	−	o	+	Remarks
6778.451?	14748.57	..	..	3	
6772.283	62.00	..	..	2	
6713.971	890.21	..	..	2	
6678.711	968.82	o	..	2	
6674.701	77.82	o	..	2	
6662.274	15005.75	3	4	8	fl
6658.681	13.85	o	1	2	fl
6593.96	161.21	2	3	6	
6591.480	66.92	2	2	5	
6588.540	73.69	2	3	6	
6583.907	84.36	3	3	5	
6577.203	99.84	2	2	4	
6554.148	253.31	o	1	2	
6531.348	306.55	3	4	7	fl
6512.365	51.17	o	1	2	
6501.991	75.67	1	1	2	
6493.198	96.48	..	1	2	
6457.286	482.11	4	5	9	fl
6413.596	587.59	2	3	3	w fl?
6411.884	91.74	3	4	5	fl?
6390.129	644.82	o	o	1	w fl
6376.950	77.15	3	4	5	fl
6371.951	89.45	1	2	3	
6369.141	96.37	2	2	3	
6355.632	729.74	..	o	2	
6342.864	61.40	5	6	8	fl
6337.615	74.45	o	o	2	
6331.408	89.92	o	o	2	
6327.163?	800.51	2	3	5	fl
6326.356	02.53	o	1	2	
6266.167	954.31	6	7	8	fl
6234.851	16034.45	o	2	4	fl
6224.508	61.09	1	2	4	w fl
6207.744	104.47	2	3	5	w fl
6207.217	05.79	1	1	2	
6203.488	15.69	2	2	3	w fl
6198.219	29.21	1	2	3	w fl
6191.912	45.64	1	2	3	w fl
6184.729	64.39	4	4	5	
6182.629	69.88	3	4	6	fl
6170.71	201.12	..	o	1	w fl
6169.822	03.45	2	3	6	fl
6164.476	17.50	o	1	2	
6151.991	50.41	2	3	4	fl
6121.414	331.58	1	2	3	s fl

TABLE 1—*Continued*

λ	ν	−	o	+	Remarks
6102.596	16081.95	o	1	3	w fl
6088.037	421.12	o	1	2	
6053.380	515.14	o	1	2	
6049.058	26.93	..	o	3	w fl
6037.705	58.01	1	2	3	w fl
6021.038	603.84	2	2	3	w fl
6010.162	33.89	o	1	2	
6007.075	42.44	1	2	3	
6000.769	59.93	2	3	4	
5994.136	78.36	2	3	4	fl
5991.014	87.05	o	1	2	
5975.070	731.58	3	4	5	w fl
5973.671	35.50	2	3	5	fl
5938.835	833.67	4	5	6	fl
5885.704	985.62	..	..	2	
5804.12	17224.4	3	4	6	
5800.80	34.2	o	1	3	
5792.435	59.12	oo	o	2	
5767.781	332.89	oo	o	2	
5760.553	54.64	6	7	9	fl
5753.028	77.34	1	2	3	
5725.389	461.23	2	3	4	
5720.183	77.12	4	4	5	fl
5719.621	78.84	2	2	3	
5677.054	609.90	o	1	2	
5665.180	46.80	1	1	2	
5657.926	69.43	1	1	2	
5601.613	847.06	o	1	2	
5599.782	52.90	o	1	2	
5599.665	53.27				
5595.076	67.91	1	2	3	
5587.032	93.64	2	3	4	fl
5579.377	918.19	2	3	3	
5576.216	28.34	2	2	3	
5573.364	37.52	2	3	4	
5572.478	40.37	2	2	3	
5571.202	44.48	2	2	4	
5559.903	80.94	1	2	3	
5558.346	85.98	3	3	4	
5548.085	18019.25	3	3	5	
5542.907	36.08	2	2	3	
5539.270	47.92	3	3	4	
5519.001	114.20	1	1	2	
5514.876	27.75	1	1	2	
5509.999	43.79	2	2	3	

TABLE 1—*Continued*

λ	ν	−	o	+	Remarks
5504.313	18162.54	1	1	3	
5499.257	79.24	2	2	4	
5492.645	201.12	0	1	2	
5431.129	407.28	1	1	2	
5417.485	53.63	2	3	4	
5410.73	76.7	1	1	2	
5407.61	87.4	1	1	2	
5398.88	517.2	1	2	3	
5394.71	31.6	0	1	2	
5386.56	59.6	1	1	2	
5378.79	86.4	0	1	2	
5343.55	709.0	2	3	4	
5326.95	67.3	1	2	3	
5312.88	817.0	1	2	3	
5312.50	18.3				
5311.97	20.2	1	2	3	
5297.74	70.7	1	1	3	
5289.88	98.8	1	0	2	
5266.67	982.1	0	0	2	
5260.08	19005.8	00	00	2	
5258.34	12.1	2	3	5	
5238.80	83.0	00	0	2	
5231.14	111.0	2	3	5	
5219.10	55.1	1	2	3	
5213.35	76.2	0	0	2	
5211.23	84.0	1	2	4	
5203.85	211.1	1	1	2	
5199.113	28.71	1	2	3	
5195.769	41.09	2	2	3	
5176.94	311.1	2	1	3	I?
5161.537	68.69	0	1	2	
5158.615	79.66	2	2	3	
5154.246	96.09	1	2	2	
5143.919	435.03	1	1	2	
5132.239	79.26	1	1	2	
5100.615	600.03	1	1	2	
5096.476	15.95	0	1	2	
5067.983	726.23	2	2	3	w fl
5039.236	838.76	1	1	2	
5002.105	986.03	1	2	3	
4989.320	20037.24	0	0	2	
4985.385	53.05	1	1	2	
4945.465	214.92	1	1	2	
4937.827	46.19	1	1	2	
4894.948	423.54	2	2	3	w fl; fur

TABLE 1—*Continued*

λ	ν	−	o	+	Remarks
4878.739	20491.39	1	1	2	fur
4874.366	509.78	1	1	2	
4861.220	65.24	1	1	2	
4848.355	619.81	1	2	3	w fl; fur
4840.831	51.86	1	2	2	fur
4826.699	712.32	1	1	2	
4826.40	13.6	..	oo	oo	fur
4813.907	67.36	1	1	2	
4813.714	68.19				
4809.625	85.85	1	1	2	fur
4808.127	92.33	2	2	3	w fl; fur
4795.93	845.2	0	0	2	
4789.381	73.71	2	2	3	fur
4786.535	86.12	1	1	2	
4778.287	922.17	1	2	3	fur
4777.188	27.00	1	2	3	
4766.595	73.49	1	1	2	fur
4758.147	21010.73	1	1	2	fur
4729.114	139.72	1	0	2	
4703.992	252.61	1	1	3	fl
4691.638	308.57	oo	oo	2	u w sp?
4676.057	79.57	1	1	2	v w fl; u w sp
4669.986	407.37	1	1	2	v w fl
4668.177	15.66	1	1	2	w fl
4666.798	22.00	1	1	2	
4592.668	767.76	2	2	3	w fl
4570.990	870.99	2	2	3	w fl
4561.364	917.14	2	2	3	
4555.917	43.35	2	2	3	fl; u w sp
4555.825	43.79				
4552.172	61.40	1	1	2	w fl
4545.264	22043.27	1	1	2	
4530.338	67.24	1	1	2	
4515.135	141.54	1	1	2	fur
4482.170	304.38	1	1	2	fur
4458.009	425.27	2	2	3	w fl; fur; u w sp
4452.576	52.63	1	1	2	
4408.886	675.12	4	4	5	w fl; fur
4378.183	834.13	1	1	2	w fl; fur
4311.808	23185.63	1	0	2	
4307.183	210.52	1	1	2	
4299.849	50.11	1	1	2	v w fl
4288.677	310.68	1	1	2	
4253.552	503.17	1	1	2	
4235.470	603.51	1	1	2	fur

TABLE 1—*Continued*

λ	ν	−	o	+	Remarks
4227.661	23647.11	1	1	2	
4213.073	728.98	1	1	2	
4210.928	41.07	2	3	4	fl; fur
4210.768	41.97				
4193.00	842.6	1	1	2	w fl
3980.099	25117.92	1	1	2	
3973.228	61.36	1	2	2	
3972.160	68.13	1	2	2	
3941.731	362.41	1	2	2	v w fl
3941.364	64.77				
3935.642	401.65	2	2	3	
3932.951	19.03	2	2	3	
3919.003	509.50	1	2	3	
3911.914	55.72	1	1	2	
3875.647	794.86	2	2	3	
3873.825	806.99	3	3	4	w fl
3869.981	32.62	1	1	2	
3869.670	34.70				
3866.894	53.25	1	1	2	
3852.142	952.25	2	2	3	
3851.160	58.87	0	0	2	
3846.888	87.70	1	1	2	
3845.095	99.82	0	0	2	
3845.016	26000.35				
3842.912	14.58	2	2	3	
3835.413	65.44	0	0	2	
3835.345	65.91				
3830.061	101.86	0	0	2	
3828.389	13.76	3	4	5	fl
3822.862	51.02	1	1	2	
3818.671	79.72	0	1	2	
3817.375	88.61	1	1	2	
3817.290	89.19				
3811.065	231.97	1	2	3	
3808.612	48.86	0	1	2	
3803.983	80.80	2	2	3	
3803.079	87.05	3	4	4	fl; fur
3801.446	98.34	2	2	3	
3780.972	440.74	1	2	2	
3771.379	508.00	2	3	3	w fl; fur
3759.314	93.07	1	2	2	w fl
3757.699	604.50	1	2	2	w fl
3755.217	22.08	1	2	2	
3754.035	30.46	1	2	2	
3742.922	709.53	2	3	3	

TABLE 1—*Continued*

λ	ν	−	o	+	Remarks
3727.901	26817.15	1	2	2	w fl
3698.113	27033.15	1	2	2	w fl
3661.622	302.55	2	2	3	w fl
3658.808	23.55	0	1	2	w fl; fur
3649.733	91.49	1	2	2	w fl
3642.255	447.72	3	4	4	fl; fur
3635.942	95.38	1	2	2	w fl
3634.580	505.68	1	2	2	w fl
3612.868	671.21	1	2	2	w fl; fur
3612.429	74.34	2	2	3	w fl; fur
3598.123	784.37	2	3	3	fl; fur
3592.777	825.71	2	2	3	w fl
3591.454	35.96	1	2	2	w fl
3576.558	951.89	2	3	3	w fl
3526.629	28347.62	0	1	1	fur
3521.062	92.84	0	1	2	fur
3518.402	413.90	1	1	2	w fl; fur
3511.154	72.55	0	0	1	fur
3498.625	574.51	0	1	1	fur
3496.809	89.35	1	1	2	fur
3495.705	98.38	0	1	2	fur
3489.511	649.14	00	0	0	fur
3488.837	54.67	00	0	0	fur
3486.520	73.72	3	3	4	fl; fur
3469.337	815.73	1	2	2	w fl; fur
3466.646	38.10	1	2	3	fl; fur
3466.532	39.05				
3461.216	83.34	..	..	..	fur; 1?
3461.022	84.96	4	5	4	fur
3457.069	917.98	0	0	1	fur
3451.699	62.97	1	2	2	fur
3442.580	29039.69	0	0	1	fur
3437.303	84.27	2	3	3	w fl; fur
3436.680	89.54	1	2	2	w fl; fur
3428.990	154.78	1	1	2	fur
3423.991	97.34	2	3	3	w fl; fur
3421.174	221.38	2	3	3	w fl; fur
3417.494	52.85	0	0	1	fur
3398.548	415.92	0	1	1	fur
3397.518	24.84	0	1	1	fur
3380.883	569.60	0	1	1	fur
3374.979	621.33	0	1	1	w fl; fur
3373.500	34.32	0	0	1	fur
3372.794	40.52	0	0	1	fur
3372.696	41.39				

TABLE 1—*Continued*

λ	ν	−	o	+	Remarks
3365.336	29706.21	o	o	1	fur
3333.129	993.24	1	2	2	fur
3313.651	30169.54	oo	o	1	fur; u w sp
3309.361	208.65	o	1	1	fur
3301.654	79.17	o	1	1	v w fl; fur; u w sp
3285.750	425.72	o	o	1	fur
3272.025	553.34	o	1	1	fur
3253.872	723.79	o	1	2	fur
3244.450	813.00	o	1	1	fur
3232.307	928.76	o	1	2	fur
3232.123	30.52	o	1	2	fur
3116.281	32080.23	2	2	3	w fl; u w sp

on a scale oo:10, of lines photographed with a stigmatic spectrograph (Wadsworth mounting) which had a dispersion of 5 A/mm. Both arc and spark sources were used, and the plates were examined by projection with such magnification that wave lengths could be identified directly to 0.2 A, with a centimeter scale. Some close lines are bracketed together with the same intensity: this is due to the poor resolving-power of this type of grating mounting and means that the indicated intensity is the sum of both lines and that either or both are enhanced accordingly. The minus (−), zero (o), and plus (+) headings mean intensities at the cathode, the center, and the anode of the arc.

Observation of the stigmatic images showed that some lines persisted with appreciable intensity for a much greater length than the geometrical image of the arc gap. These flame lines have been called "low-temperature lines" and are designated by "fl" in the tables ("w fl" for weak flame). Flame lines were found for both *Th* I and *Th* II.

It has been possible to confirm the temperature classification assumed above through the kindness of Dr. A. S. King, of the Mount Wilson Observatory, who at the writer's request very graciously consented to photograph the furnace emission spectrum. The region from 5050 A to the ultraviolet limit of the furnace emission was covered and the lines were identified partly by Dr. King and

TABLE 2

THORIUM II

λ	ν	−	o	+	Remarks
7525.52	13284.46	10	6	8	R; w fl
7393.433	521.75	10	5	7	R; w fl
6619.877	15101.86	10	10	10	w fl
6605.432	34.88	9	9	9	fl
6279.175	921.26	7	7	6	w fl
6274.105	34.13	10	10	10	fl
6261.064	67.32	10	10	10	w fl
6248.091	16000.57	3	2	2	w fl
6112.840	354.49	10	10	10	fl
6104.581	76.62	6	6	5	w fl
6073.106	461.49	10	10	10	w fl
6044.439	539.56	9	9	8	w fl
5998.048	692.53	15	15	15	s fl
5925.895	870.42	5	5	5	w fl
5925.413	71.80	3	3	2	w fl
5914.400	903.21	15	15	12	s fl
5707.097	17517.19	9	8	7	fl; u w sp
5700.915	36.19	10	9	9	fl
5639.746	726.39	9	6	5	fl
5615.324	803.48	2	2	2	u w sp
5568.019	954.74	5	3	3	u w sp
5415.425	18460.65	6	4	4	u w sp
5143.272	19437.48	4	2	2	u w sp
5110.853	560.77	2	1	1	u w sp
5049.805	797.24	6	4	4	fl; fur; u w sp; $J' \neq J''$
5044.72	817.2	2	2	2	fur
5028.610	80.68	4	3	2	u w sp
5017.249	925.70	7	4	4	w fl; u w sp
4987.167	20045.89	5	3	2	u w sp
4954.665	177.38	4	2	2	R?; fur; u w sp
4954.569	77.77				
4919.812	320.32	8	5	5	fl; u w sp
4872.92	515.9	2	1	2	fur; u w sp; II?
4863.167	57.01	8	6	4	fl; u w sp
4858.336	77.45	3	2	1	u w sp
4850.434	610.97	4	2	2	w fl; u w sp
4849.042	16.89	2	1	1	u w sp
4840.468	53.41	2	2	1	u w sp
4832.798	86.51	4	2	2	w fl
4831.15	93.3	2	2	2	v w fl; fur
4818.657	746.89	3	2	1	u w sp
4800.175	826.77	3	1	0	u w sp
4761.108	997.66	4	2	2	u w sp
4752.401	21036.13	6	4	4	fl; u w sp; 7/2−7/2
4740.515	88.87	3	2	2	fl; u w sp; 7/2−7/2
4729.89	136.3	2	1	0	u w sp

TABLE 2—*Continued*

λ	ν	−	o	+	Remarks
4723.773	21163.61	4	2	2	fl; u w sp
4723.436	65.13	3	2	3	fl; u w sp; II?
4718.615	86.75	2	2	2	u w sp
4706.348?	241.97	1	1	1	u w sp
4694.091	97.44	2	1	1	fl
4689.169	319.79	2	1	2	w fl; u w sp; II?
4673.65	90.6	2	1	2	fl; II?
4651.562	492.16	2	1	1	fl; u w sp
4641.259	539.87	1	0	0	u w sp
4639.708	47.07	2	1	0	u w sp
4633.833	74.38	2	1	1	w fl
4633.753	74.76				
4631.761	84.03	3	2	2	fl; u w sp; $J' \neq J''$
4623.893	620.76	2	1	0	u w sp
4619.557	41.06	3	1	1	fl; u w sp
4619.472	41.45				
4609.363	88.92	2	1	0	u w sp
4603.15	718.2	2	2	2	w fl
4602.90	19.4				
4595.42	54.7	3	3	3	fl
4588.42	87.9	3	3	3	fl
4563.66	906.1	3	2	3	fl; fur; II?
4563.316	07.77	3	2	2	fl; fur; u w sp; 63.2: 1/2−3/2
4563.228	08.19				
4537.11	22034.3	3	2	2	fur
4534.130	48.79	3	1	1	fl
4510.548	164.06	6	5	5	fl; u w sp
4505.226	90.24	1	1	1	w fl
4499.96	216.2	2	1	2	fur; II?
4498.93	21.3	3	2	3	fl; II?
4493.31	49.1	5	5	5	fl; fur
4487.500	77.89	4	2	1	fl; fur
4480.822	311.09	3	3	3	w fl
4465.577	87.26	4	3	2	fl (prob. 65.3); 65.3: 5/2−7/2
4465.351	88.40				
4447.844	476.51	4	2	2	fl; 1/2−3/2
4440.876	511.78	4	2	2	fl; 3/2−5/2
4439.137	20.60	4	2	2	fl; $J' = J''$
4432.963	51.96	5	4	4	fl; u w sp
4412.744	655.29	6	5	4	fl; u w sp
4412.530	56.40				
4402.93	705.8	2	2	2	w fl
4391.106	66.93	8	6	6	R; fl; u w sp; P_1; 5/2−7/2?
4381.860	814.97	7	5	4	fl; u w sp; P_1; 1/2−1/2??
4374.788	51.85	3	2	2	w fl
4374.139	55.24	3	2	2	w fl; fur

TABLE 2—*Continued*

λ	ν	−	o	+	Remarks
4350.849	22977.58	2	2	1	fl
4344.99	23008.6	2	2	1	fl
4338.07	45.3	1	1	1	v w fl
4337.398	48.85	2	2	1	w fl
4337.282	49.46				
4313.003	179.21	3	2	2	fl; fur
4310.002	95.39	3	2	2	w fl; u w sp
4295.08	275.9	2	1	0	u w sp
4282.050	346.76	7	5	4	fl; u w sp; 7/2−9/2
4277.327	72.53	6	4	4	fl; u w sp; 3/2−3/2
4273.363	94.22	3	2	1	fl; u w sp
4260.33	465.7	2	1	2	w fl; II?
4257.501	81.37	2	2	2	w fl; fur
4256.229	88.39	3	2	2	w fl; low *J*
4250.337	520.95	3	2	2	fl; fur
4208.897	752.49	7	5	5	fl; u w sp; 1/2−1/2 or 3/2
4201.853	92.34	3	1	1	v w fl; u w sp
4195.957	825.77	1	0	0	u w sp
4195.836	26.46	0	0	0	
4179.969	916.90	4	3	2	fl; u w sp
4179.725	18.30				
4178.068	27.79	3	2	2	fl; u w sp; 5/2−5/2
4171.353	66.31	1	.	.	u w sp
4170.543	70.95	2	2	2	w fl; u w sp
4170.472	71.37				
4168.96	80.1	1	1	1	u w sp
4168.62	82.0	1	1	1	
4163.652	24010.63	1	0	0	u w sp
4162.691	16.18	1	1	1	u w sp
4159.669	33.62	1	0	0	u w sp
4156.520	51.83	3	2	2	fl; u w sp
4149.992	89.66	2	2	2	w fl; u w sp
4148.179	100.19	2	1	1	u w sp
4142.702	32.08	3	2	2	fl; u w sp
4142.474	33.38				
4132.752	90.15	1	0	0	u w sp
4116.719	284.36	2	2	2	fl; P_2; u w sp; 7/2−9/2
4115.767	89.98	2	2	2	fl
4112.762	307.72	2	2	2	w fl; fur
4110.876	18.88	2	2	2	u w sp
4110.638	20.29				
4108.429	33.36	4	3	2	fl; u w sp; 1/2−3/2 or 1/2
4105.928	48.18	1	1	1	u w sp
4100.838	78.40	2	1	0	u w sp
4097.751	96.77	1	1	1	R? fur
4097.686	97.16				

TABLE 2—*Continued*

λ	ν	−	o	+	Remarks
4094.740	24414.68	4	3	2	fl; u w sp; 3/2−3/2
4086.524	63.79	3	3	3	fl; u w sp; 3/2−5/2
4085.042	72.67	3	3	3	u w sp
4069.204	567.92	4	3	3	fl; u w sp; 3/2−5/2
4041.205	738.13	2	1	1	u w sp
4036.564	66.57	2	1	1	w fl
4036.056	69.69	2	1	2	w fl; fur; II?
4030.854	801.66	2	2	2	w fl; fur
4019.143	73.92	8	6	5	R; fl; P_2; fur; u w sp; 3/2−5/2
4012.501	915.10	2	2	2	w fl; fur
4003.310	72.29	4	2	2	u w sp
4003.103	73.60				
3996.063	25017.59	2	1	1	u w sp
3994.554	27.03	4	3	3	fl; u w sp
3988.016	68.06	2	1	1	u w sp
3981.111	111.54	2	1	1	u w sp
3976.418	41.18	3	2	2	v w fl
3967.412	98.24	3	2	2	fl; fur; u w sp
3956.682	266.58	4	2	1	u w sp
3951.521	99.58	3	2	1	u w sp
3950.392	306.81	2	1	2	fur; u w sp; II?
3948.970	15.92	2	2	2	u w sp
3945.515	38.09	3	2	1	u w sp
3944.260	46.15	2	1	1	u w sp
3929.670	440.25	5	4	3	fl; u w sp; 3/2−5/2
3927.178	56.39	2	1	1	u w sp
3925.095	69.90	2	2	2	w fl
3916.732	524.29	3	1	1	u w sp
3905.188	99.73	3	2	2	u w sp
3900.885	627.97	5	3	3	v w fl; u w sp
3895.424	63.90	4	3	3	v w fl; fur
3886.918	720.06	2	2	2	fur
3885.154?	31.74	3	2	2	u w sp
3884.829	33.89	1	..	..	
3872.729	814.30	4	3	3	u w sp
3863.414	76.53	3	3	3	w fl; u w sp
3859.84	900.5	5	4	4	fl; fur
3854.514	36.28	3	3	3	u w sp
3841.965	26020.90	4	3	3	w fl; u w sp
3839.686	36.45	5	4	4	fl; u w sp
3831.736	90.46	3	2	2	u w sp
3825.043	136.01	2	2	2	u w sp
3822.144	55.93	2	2	2	u w sp
3821.430	60.82	2	2	2	u w sp
3813.063	218.22	4	3	2	u w sp

TABLE 2—*Continued*

λ	ν	−	o	+	Remarks
3807.872	26253.97	4	3	2	u w sp
3805.824	68.09	2	2	2	u w sp
3789.115	383.92	3	3	2	fl
3785.605	408.38	3	3	2	w fl; u w sp
3783.295	24.51	5	3	2	w fl; u w sp
3765.25	551.1	2	2	2	v w fl
3762.883	67.85	3	2	2	fl; u w sp
3752.573	640.84	5	3	0	w fl; u w sp
3741.187	721.92	8	5	4	R; fl; P_2; u w sp
3721.833	860.87	5	4	4	fl; u w sp
3720.00	74.0	3	3	3	fl; u w sp
3719.83	75.3				
3719.434	78.20	3	3	3	fl; fur
3711.312	937.01	..	..	..	P_2; u w sp
3706.769	70.03	3	3	3	w fl; u w sp
3675.572	27198.94	3	3	3	w fl; u w sp
3669.94	240.7	3	3	3	v w fl
3659.632	317.40	3	3	3	w fl; fur; u w sp
3658.068	29.08	..	..	..	fur; u w sp; II?
3625.924	571.35	3	2	2	v w fl; u w sp
3625.625	73.62	4	3	2	w fl; u w sp
3617.126	638.40	4	3	2	u w sp
3617.023	39.19				
3615.131	53.65	4	3	3	w fl
3609.445	97.21	4	3	2	fl; u w sp
3603.207	745.17	4	3	2	v w fl; u w sp
3601.040	61.86	3	2	1	u w sp
3575.317	961.60	4	3	3	v w fl; u w sp
3567.265	28024.71	3	2	2	v w fl; fur
3559.960	82.22	..	..	..	u w sp; II?
3559.457	86.18	..	..	..	u w sp; II?
3553.110	136.35	..	..	..	u w sp; II?
3545.288	98.43	..	..	..	u w sp; II?
3539.588	243.84	5	4	4	fl; fur; u w sp
3539.324	45.94	3	2	1	fur
3538.846	49.75	..	..	..	P_2; II?
3528.948	328.99	4	3	2	u w sp
3528.823	29.99				
3521.919	85.53	..	..	..	u w sp; II?
3516.824	426.65	..	..	..	u w sp; II?
3507.522	502.03	..	..	..	u w sp; II?
3493.517	616.39	..	..	..	u w sp; II?
3471.219	800.10	1	1	1	fur
3469.928	10.82	4	3	3	v w fl; P_2; fur; u w sp
3468.221	25.00	3	2	2	v w fl; u w sp

TABLE 2—*Continued*

λ	ν	−	o	+	Remarks
3465.929	28844.06	4	3	2	v w fl; u w sp
3465.763	45.45				
3463.723	62.43	..	..	..	u w sp; II?
3462.854	69.68	..	..	..	u w sp; II?
3452.679	954.75	3	2	1	
3439.713	29063.89	..	..	..	u w sp; II?
3438.952	70.32	..	..	..	u w sp; II?
3435.970	95.56	3	3	2	w fl, fur; u w sp
3433.998	112.26	3	3	2	w fl; u w sp; 3/2−5/2
3422.657	208.72	1	1	0	fur
3413.015	91.23	1	1	1	v w fl; fur
3408.748	327.90	1	1	0	fur
3405.560	55.35	1	1	1	fur
3402.701	80.02	..	..	..	P_2; u w sp; II?
3396.733	431.64	1	1	1	fur?
3392.041	72.35	5	4	4	fl; R; fur; u w sp
3389.464	94.75	..	..	..	fur; II?
3380.49	573.1	1	0	0	v w fl
3378.579	89.78	..	..	..	u w sp; II?
3376.847	604.95	..	..	..	u w sp; II?
3371.799	49.27	..	..	..	u w sp; II?
3367.823	84.28	..	..	..	u w sp; II?
3366.526	95.71	..	..	..	u w sp; II?
3358.606	765.73	2	1	0	fur; u w sp
3354.614	801.15	..	..	..	P_4; II?
3354.185	04.97	..	..	..	P_4; u w sp; II?
3351.230	31.25	3	2	2	v w fl; P_4; fur
3348.777	53.23	2	2	2	v w fl; fur
3343.613	99.19	..	..	..	u w sp; II?
3337.869	950.65	..	..	..	u w sp; 3/2−5/2
3334.605	79.97	3	2	1	v w fl; P_4; u w sp
3330.475	30017.14	2	2	2	v w fl; fur
3327.196	46.72	1	0	0	fur
3325.125	65.44	4	3	2	v w fl; P_4; u w sp
3321.445	98.72	..	..	..	u w sp; II?
3310.248	200.55	..	..	..	u w sp; II?
3304.238	55.48	2	2	2	v w fl; fur
3301.351	81.94	..	..	..	u w sp; II?
3300.611	88.73	..	..	..	P_2; II?
3298.054	312.21	1	0	0	fur
3292.521	63.15	2	2	2	v w fl; u w sp
3291.744	70.31	3	2	2	v w fl; u w sp
3290.59	80.9	..	..	..	P_4; u w sp; II?
3275.070	524.93	..	..	..	u w sp; II?
3262.672	640.93	..	..	..	u w sp; 7/2−7/2

TABLE 2—*Continued*

λ	ν	−	o	+	Remarks
3257.35	30690.9	2	2	2	fur
3256.115	702.62	..	..	..	u w sp; II?
3251.917	42.26	1	1	1	fur
3245.764	800.53	..	..	..	u w sp; II?
3238.118	73.26	..	..	..	u w sp; II?
3235.842	94.97	..	..	..	u w sp; II?
3229.011?	960.33	..	..	..	u w sp; II?
3225.409	94.90	..	..	..	u w sp; II?
3221.288	31034.55	..	..	..	u w sp; II?
3216.632	79.47	..	..	..	u w sp; II?
3198.232	258.27	..	..	..	u w sp; II?
3188.234	356.29	4	3	2	v w fl; P_2; u w sp
3180.194	435.55	4	3	3	R; v w fl; u w sp
3175.730	79.74	..	..	..	u w sp; II?
3154.771	688.87	..	..	..	u w sp; II?
3151.651	720.24	..	..	..	u w sp; II?
3150.456	32.27	..	..	..	u w sp; II?
3148.06	56.3	..	..	..	u w sp; 1 − 2? II?
3146.036	76.85	..	..	..	u w sp; II?
3142.837	809.19	..	..	..	u w sp; II?
3141.848	19.20	..	..	..	P_4; II?
3139.306	44.98	..	..	..	P_4; II?
3125.463?	986.00	..	..	..	u w sp; II?
3124.388	97.02	..	..	..	u w sp; II?
3122.957	32011.67	..	..	..	u w sp; II?
3119.530	46.85	3	3	2	v w fl; u w sp
3108.295	162.68	..	..	..	P_2; u w sp; II?
3088.473	369.05	..	..	..	u w sp; II?
3080.223	455.77	..	..	..	u w sp; II?
3078.833	70.42	..	..	..	P_2; II?
3070.824	555.10	..	..	..	u w sp; II?
3067.733	87.90	..	..	..	u w sp; II?
3063.125	636.94	..	..	..	u w sp; II?
3063.026	38.00				
3049.100	787.06	..	..	..	u w sp; II?
3046.954	810.11	..	..	..	u w sp; II?
3034.058	949.56	..	..	..	P_2; II?
3008.491	33229.60	..	..	..	P_2; II?
2993.800	392.66	..	..	..	u w sp; II?
2988.232	454.87	..	..	..	u w sp; II?
2983.825	504.28	..	..	..	u w sp; II?
2981.42	31.3	..	..	..	u w sp; II?
2978.64	62.6	..	..	..	P_2; u w sp; II?
2968.692	675.07	..	..	..	u w sp; II?
2964.924	717.86	..	..	..	u w sp; II?

TABLE 2—*Continued*

λ	ν	− o +	Remarks
2961.49	33757.0	. . . . .	u w sp; II?
2957.922	97.67	. . . . .	u w sp; II?
2942.864	970.60	. . . . .	P_3; II?
2932.67	34088.7	. . . . .	u w sp; II?
2932.51	90.4	. . . . .	II?
2928.253	140.09	. . . . .	u w sp; II?
2925.06	177.3	. . . . .	P_3; u w sp; II?
2910.599	347.15	. . . . .	r; II?
2899.727	475.93	. . . . .	u w sp; II?
2898.97	84.8	. . . . .	P_2; u w sp; II?
2897.074	507.50	. . . . .	u w sp; II?
2895.133	30.64	. . . . .	P_3; II?
2892.174	65.96	. . . . .	u w sp; II?
2891.79	70.5	. . . . .	u w sp; II?
2887.821	618.06	. . . . .	u w sp; II?
2885.053	51.27	. . . . .	u w sp; II?
2884.295	60.38	. . . . .	u w sp; II?
2870.39	828.1	. . . . .	R; P_1; u w sp; II?
2861.37	938.0	. . . . .	r; P_2; u w sp; II?
2851.25	35062.1	. . . . .	u w sp; II?
2842.81	166.0	. . . . .	P_3; II?
2837.299	234.45	. . . . .	R; u w sp; II?
2834.481	69.48	. . . . .	r; II?
2832.317	96.42	. . . . .	R; P_2; u w sp; II?
2824.67	392.0	. . . . .	u w sp; II?
2771.54	36070.4	. . . . .	P_2; II?
2768.87	105.2	. . . . .	P_2; II?
2764.66	60.0	. . . . .	P_2; II?
2752.18	324.2	. . . . .	P_2; II?
2747.17	90.3	. . . . .	P_2; II?
2729.34	627.9	. . . . .	P_2; II?
2722.38	721.7	. . . . .	P_2; II?
2716.32	803.5	. . . . .	P_2; II?
2708.19	914.1	. . . . .	P_2; II?
2703.96	71.8	. . . . .	P_2; II?
2695.24	37091.3	. . . . .	P_3; II?
2693.98	108.6	. . . . .	u w sp; II?
2692.43	30.0	. . . . .	P_3; II?
2687.15	203.0	. . . . .	u w sp; II?
2686.19	16.4	. . . . .	P_3; II?
2684.31	42.3	. . . . .	r; P_3; II?
2625.75	38072.9	. . . . .	P_2; II?
2618.83	173.5	. . . . .	P_2; II?
2600.90	436.8	. . . . .	P_2; II?
2597.06	93.6	. . . . .	P_2; II?

TABLE 2—*Continued*

λ	ν	− o +	Remarks
2583.37	38697.4	. . . . .	r; P_2; II?
2571.61	874.4	. . . . .	P_2; II?
2564.38	984.0	. . . . .	P_3; II?
2555.23	39123.5	. . . . .	P_1; II?
2554.73	31.4	. . . . .	r; P_1; II?
2549.55	210.8	. . . . .	P_1; II?
2549.12	17.5	. . . . .	P_1; II?
2475.32	40386.5	. . . . .	r; II?
2463.68	577.4	. . . . .	r; II?
2441.29	949.5	. . . . .	r; II?

partly by the writer. The *Th* II lines appeared only at the higher temperatures. The lines are designated "fur" in the tables.

Further work done by the writer includes the observation of lines emitted in the underwater spark. No lines of thorium were observed in absorption in the spark; only emission lines appeared.[13] These emission lines are marked "u w sp" in the tables. It will be observed that most of these lines are also emitted in the furnace and consequently this group is probably a somewhat enlarged list of *Th* II low-temperature lines.

The *J*-values quoted in the tables under "Remarks" were obtained by Ference, Bowersox, and Fred from Zeeman patterns of the thorium arc in a field of 30,000 gauss, photographed on the twenty-one-foot grating up to the fourth order. Most of the patterns could not be completely resolved, and a thorough Zeeman analysis with the thirty-foot grating is being undertaken at the present time.

The results of Pollok and Leonard[14] on the persistent lines observed with solutions of thorium are quoted as follows:

P_1 , Line appears at 0.01 per cent *Th*
P_2 , Line appears at 0.1 per cent *Th*
P_3 , Line appears at 1.0 per cent *Th*
P_4 , Line appears in strong solution

Lines found by Allin[15] to be reversed in the underwater spark are designated "r." The interpretation of these lines is doubtful. Lines

[13] Cf. W. F. Meggers and O. Laporte, *Phys. Rev.*, **28**, 642, 1926.

[14] *Op. cit.* [15] *Op. cit.*

marked "R" were reversed on plates taken by Ference, Bowersox, and Fred with an arc current of thirty amperes in nitrogen at a pressure of seven atmospheres.

Because of space limitations, only the most important lines are given below. Practically all *Th* I lines with an intensity of 2 or more are included. The *Th* II table consists of only the low-temperature lines and the *raies ultimes*. The importance and classification of the *raies ultimes* for which stigmatic intensities are not given (because the enhancements are not well pronounced) are not so well founded but are included by analogy with similar lines in the zirconium spectrum,[16] which are mostly *Zr* II.[17] Likewise, the underwater spark lines in the ultraviolet are merely assumed to be low-temperature *Th* II by comparison with the rest of the spectrum.

It is believed that the value of the table lies not in the wave lengths but in the selection of the most important lines. Nevertheless, the accuracy should be great enough to permit a term analysis for *Th* I, and this work is now in progress. The analysis of *Th* II will probably require the more complete set of Zeeman patterns and Harrison's more complete wave-length tables. Some constant differences have been found for both spectra.

The writer would like to acknowledge his indebtedness to Professor George S. Monk and Professor Carl Eckart for constant encouragement and advice. He would also like to thank Dr. H. C. Rentschler, of the Westinghouse Lamp Company, for generous gifts of pure thorium; Professor G. R. Harrison, of the Massachusetts Institute of Technology, for the advance copy of his thorium wave lengths; and Dr. A. S. King, of the Mount Wilson Observatory, for the furnace plates.

RYERSON PHYSICAL LABORATORY
UNIVERSITY OF CHICAGO
October 1937

[16] Twyman, p. 96.

[17] C. C. Kiess and H. K. Kiess, *Bur. Stand. Jour. Res.*, **5**, 1205, 1930.

A NEW BAND IN THE ABSORPTION SPECTRUM OF THE EARTH'S ATMOSPHERE

ARTHUR ADEL AND C. O. LAMPLAND

ABSTRACT

A new band at 7.6 μ in the absorption spectrum of the earth's atmosphere has been correlated with the probable presence of minute quantities of nitrogen pentoxide (N_2O_5) in the ozonosphere.

The present paper is a by-product of an investigation, not yet completed, of the transparency and variations in transparency of the local atmosphere to stellar and planetary radiations. To this end it has been necessary to locate and map the great regions of absorption belonging to the atmosphere. (The great pioneer work in this field was, of course, initiated by S. P. Langley more than fifty years ago; and this work has since been ably furthered by C. G. Abbot, F. E. Fowle, and their co-workers. See *Annals of the Astrophysical Observatory of the Smithsonian Institution.*) This phase of the problem was accomplished with apparatus similar in principle to that used by one of us in previous experiments of a related nature.[1] In the course of this procedure several new identifications have been made, and a new absorption band of importance has been discovered. The location of the new band in the solar prismatic spectrum will be made clear by the discussion which follows.

Plate III presents the appearance of the red and infrared end of the glass prismatic solar spectrum. The identification of the principal absorption bands is given in Table 1.

For our purpose the most interesting region of the spectrum lies beyond the cutoff of glass, and a rock-salt prism was consequently employed to map the remainder of the spectrum as far as the "curtain" dropped by the atmosphere in the vicinity of 14 μ. The rock-salt prismatic solar spectrum is shown in Plate IV. Curve *a* was made with a single setting of the spectrometer, the adjustment being

[1] A. Adel, V. M. Slipher, and E. F. Barker, *Phys. Rev.*, **47**, 580, 1935; A. Adel, V. M. Slipher, and O. Fouts, *ibid.*, **49**, 288, 1936; A. Adel and V. M. Slipher, *Ap. J.*, **84**, 354, 1936.

PLATE III

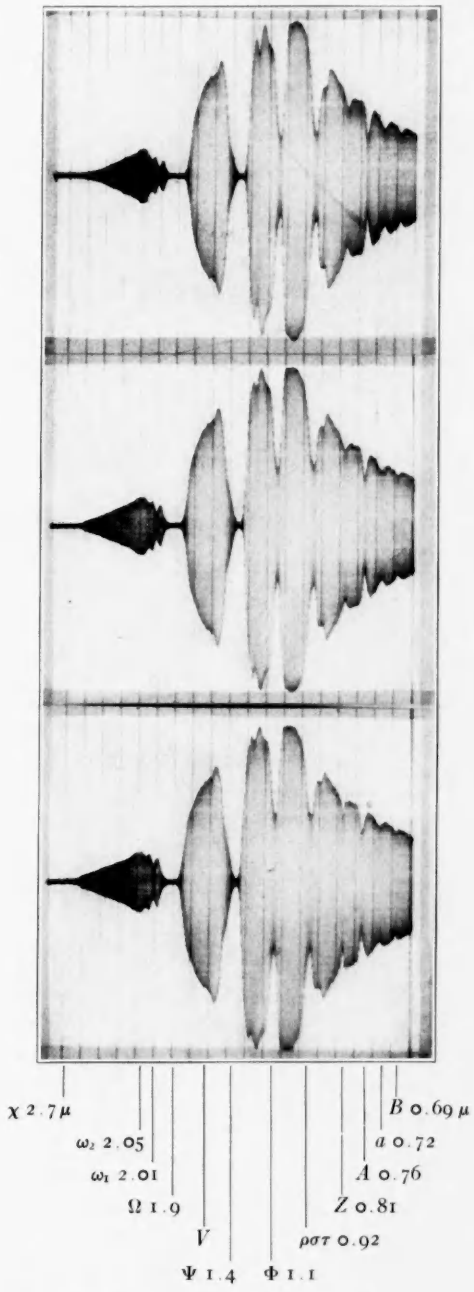

THE NEAR INFRARED SPECTRUM ON JULY 7, 1937
Order of decreasing air path: top to bottom and left to right

PLATE IV

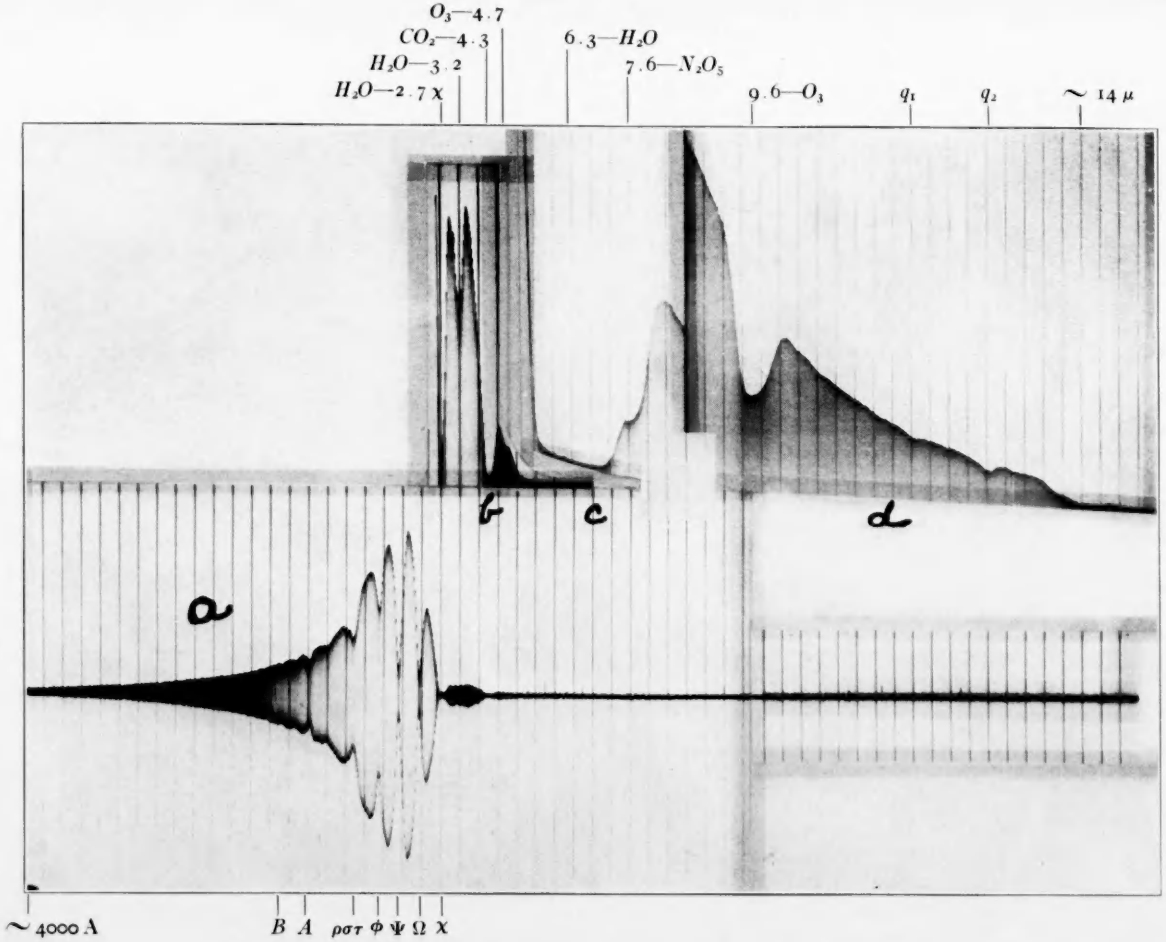

THE REMOTE INFRARED TELLURIC SPECTRUM

such as to provide convenient deflections in the near infrared region of the spectrum. Curves *b*, *c*, and *d* were made with vastly increased sensitivity, the scale being obviously different for the different sections. The curves *a* and *b-c-d* are arranged in Plate IV to correspond precisely in position. The major absorption bands are due to the

TABLE 1

INTERPRETATION OF THE NEAR INFRARED TELLURIC SPECTRUM*

Band (μ)		Absorbing Molecule	Band Designation
X	2.7	H_2O	ν_1 and ν_3†
ω_2	2.05	CO_2	The 4860 and 4982 cm^{-1} components of the resonance
ω_1	2.01	CO_2	group 4860, 4982, and 5110 cm^{-1}: $\left\{\begin{matrix}\nu_3+4\nu_2\\ \nu_3+2\nu_2+\nu_1\\ \nu_3+2\nu_1\end{matrix}\right\}$ The 5110 cm^{-1} component (1.96 μ) lies in the Ω band
Ω	1.9	H_2O	$\nu_2+\nu_3$
Ψ	1.4	H_2O	$\nu_1+\nu_3$
Φ	1.1	H_2O	$\nu_1+\nu_2+\nu_3$
$\rho\sigma\tau$	0.92	H_2O	$2\nu_1+\nu_3$ and $3\nu_3$
	0.81	H_2O	$2\nu_1+\nu_2+\nu_3$
A	0.76	O_2	$^1\Sigma \rightarrow {}^3\Sigma$; $v''=0 \rightarrow v'=0$
a	0.72	H_2O	$3\nu_1+\nu_3$
	0.698	H_2O	$\nu_1+3\nu_3$
	0.652	H_2O	$3\nu_1+\nu_2+\nu_3$
	0.632	H_2O	$3\nu_3+\nu_1+\nu_2$
Rain band	0.594	H_2O	$3\nu_1+2\nu_2+\nu_3$
	0.592	H_2O	$4\nu_1+\nu_3$
	0.573	H_2O	$2\nu_1+3\nu_3$

* For the sake of completeness the interpretation of the water-vapor bands appearing in the visible region of the solar spectrum is given. See Appendix for further information concerning the distribution of absorption in the solar spectrum.

† For the modes of vibration with which the frequencies listed in Tables 1 and 2 are associated, see the first paper referred to in footnote 1.

water vapor, carbon dioxide, and ozone constituents of the earth's atmosphere; and these are identified in Table 2. To the bands listed in Table 2 should be added the very intense fundamental ν_2 of CO_2 at 14.97 μ and the much weaker 14.1 μ band of O_3. These two bands are responsible for the beginning and for the first section of the rather abrupt cutoff of the atmosphere. Overlapping this region and extending toward longer wave lengths, lies the powerful pure rotation spectrum of the water-vapor molecule.[1] Mention

should also be made of the two small bands q_1 and q_2 near 12 μ and 13 μ, respectively, concerning which only tentative identifications have thus far been made.

The main purpose of this communication is to direct attention to the band at 7.6 μ, for the first time revealed in the spectrum of the atmosphere. The appearance of this band on several occasions is displayed in Plate V. It is a matter of considerable interest that the band cannot be traced to the spectra of water vapor, carbon dioxide, or ozone, since, for reasons presented elsewhere,[1] these are the only constituents of the earth's atmosphere expected to exercise banded absorption in the infrared region of the spectrum.[2] The spectrum of

TABLE 2

INTERPRETATION OF THE FAR INFRARED TELLURIC SPECTRUM

Band (μ)	Absorbing Molecule	Band Designation	Band (μ)	Absorbing Molecule	Band Designation
9.6	O_3	*	4.7	O_3	†
7.6	N_2O_5		4.3	CO_2	ν_3
6.3	H_2O	ν_2	3.2	H_2O	$2\nu_2$

* Concerning the analysis of the infrared spectrum of O_3, see the second paper referred to in footnote 1. The appearance of the 9.6 μ region is perhaps very slightly affected by the two weak CO_2 bands with centers at 9.4 μ and 10.4 μ: $\{\nu_3 - (\nu_1, 2\nu_2)\}$.

† The appearance of this region is perhaps influenced by the five weak CO_2 bands with centers at 5.17 μ, 4.82 μ: $\{3\nu_2, \nu_2 + \nu_3\}$, and 5.3 μ, 4.64 μ, and 4.78 μ: $\{(4\nu_2, 2\nu_2 + \nu_1, 2\nu_1) - \nu_2\}$.

pure ozone in quantities considerably in excess of the amount in the ozonosphere reveals no trace of this band.[3] (In the ozonosphere there is present approximately 3 mm-atmospheres in the zenith direction.) This is also the case for carbon dioxide. Moreover, the energy-level diagram of the CO_2 molecule is well known, and it does not yield a transition at 7.6 μ.[4] Although laboratory examination of the water-vapor spectrum does not display the band, the comparatively great

[2] N. R. Dhar and A. Ram (*Nature*, **132**, 819, 1933) have discovered minute traces of formaldehyde in the earth's atmosphere by chemical means. Formaldehyde possesses a weak band at 7.5 μ and an extremely intense one between 3.3 μ and 3.6 μ. The latter is absent from the solar prismatic spectrum, and there is therefore no reason to expect the appearance of the former. There is evidently insufficient formaldehyde in the atmosphere to reveal itself in the solar prismatic spectrum. (For the infrared spectrum of formaldehyde see H. H. Nielsen, *Phys. Rev.*, **46**, 117, 1934.)

[3] Hettner, Pohlman, and Schumacher, *Zs. f. Phys.*, **91**, 372, 1934.

[4] A. Adel and D. M. Dennison, *Phys. Rev.*, **43**, 716, 1933; **44**, 99, 1933.

PLATE V

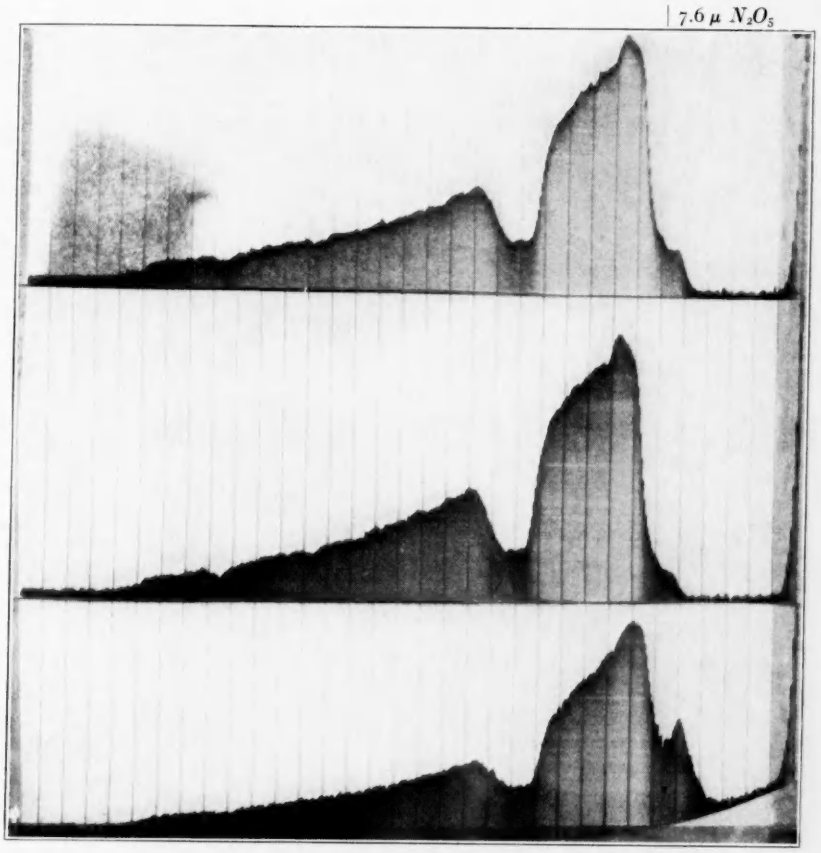

THE 7.6 μ BAND

amount of water vapor in the atmosphere makes other criteria imperative. Fortunately, the energy-level diagram of the H_2O molecule is also well known; and, like that of the CO_2 molecule, it does not provide a suitable transition.[5] (Lying at a wave length longer than that of the lowest water-vapor fundamental, the 7.6 μ band, if it were a member of the water-vapor spectrum, would have to be a band whose initial state was an excited one.)

The new band appears, therefore, to be due to a heretofore unrecognized constituent of the atmosphere. Attention is consequently directed to possible reaction products associated with the major constituents of the atmosphere. In this connection it is significant that the molecule N_2O_5 has been found to be a common impurity of ozone.[3] In fact, nearly all examinations of the infrared spectrum of ozone have yielded a strong band at 7.6 μ; and until recently, because of its great strength, this band was considered to be a member of the ozone spectrum. However, the splendid laboratory work of Hettner, Pohlman, and Schumacher has proved conclusively that this band is due to the nitrogen pentoxide molecule. Quoting these authors:

> 7.6 μ (1315 cm^{-1}). Diese Bande ist von Ladenburg und Lehmann, und von Gerhard bei 7.4 μ aufgefunden. Obwohl sie verhältnissmässig intensiv sein sollte, zeigte sich bei uns trotz mehrfacher Messungen nicht die geringste Andeutung von ihr. Das Fehlen einer einzelnen Bande deutet schon mit ziemlicher Sicherheit auf ihren Ursprung aus Verunreinungen hin wenn die übrigen Banden mit hinreichender Intensität vorhanden sind und ihrerseits die genügende Konzentration des absorbierenden Gases verbürgen. Um endlich die Art der Verunreinigung festzustellen, wurden zu 180 mm Ozon 1.7 mm NO_2 beigemischt. In der Tat trat nunmehr eine Absorption von 50% bei 7.6 μ ein! Hierdurch ist gezeigt, dass diese Bande, die in den meisten Arbeiten als Grundfrequentz des Ozons angesprochen wird, nicht dem Ozon, sondern dem N_2O_5 angehört.[3]

It remains to be seen whether the production of minute amounts of N_2O_5 in the ozonosphere may be reasonably expected. It is well known that the action of electrical discharges or ultraviolet radiation upon an N_2-O_2 mixture will produce some NO, and that, further, the presence of NO in O_2 will result in NO_2. It is also well known that in the presence of O_3, NO_2 yields N_2O_5. It appears reasonable, there-

[5] L. G. Bonner, *ibid.*, **46**, 458, 1934.

fore, to expect the presence of N_2O_5 in the ozonosphere and to attribute the 7.6 μ band to this molecule.

It is of interest to form a rough estimate of the quantity of N_2O_5

TABLE 3

	Spectral Region (μ)	Primary Transition	Band Center (μ)	Secondary Transitions	Band Center (μ)
	6.3	ν_2	6.27		
X_1X_2	3.2*	$2\nu_2$	3.17		
X	2.7†	ν_1	2.77		
		ν_3	2.66		
Ω	1.9	$\nu_2+\nu_3$	1.88	$\nu_2+\nu_1$	1.93
Ψ	1.4‡	$\nu_1+\nu_3$	1.38	$2\nu_1$	1.41
				$2\nu_3$	1.35
Φ	1.1	$\nu_1+\nu_2+\nu_3$	1.14	$\nu_2+2\nu_1$	1.16
				$\nu_2+2\nu_3$	1.11
$\rho\sigma\tau$	0.92	$2\nu_1+\nu_3$	0.942	$3\nu_1$	0.962
		$3\nu_3$	0.906	$2\nu_3+\nu_1$	0.924
	0.81	$2\nu_1+\nu_2+\nu_3$	0.823	$3\nu_1+\nu_2$	0.838
				$2\nu_3+\nu_1+\nu_2$	0.809
				$3\nu_3+\nu_2$	0.797
a	0.72	$3\nu_1+\nu_3$	0.723	$4\nu_1$	0.737
				$2\nu_1+2\nu_3$	0.710
	0.698	$\nu_1+3\nu_3$	0.698		
	0.652	$3\nu_1+\nu_2+\nu_3$	0.652		
	0.632	$\nu_1+3\nu_3+\nu_2$	0.632		
Rain band	0.594	$3\nu_1+2\nu_2+\nu_3$	0.594		
	0.592	$4\nu_1+\nu_3$	0.592		
	0.573	$2\nu_1+3\nu_3$	0.573		

* The appearance of this region is perhaps slightly affected by the two weak ozone bands with centers at 3.28 μ and 3.57 μ.

† This region contains also the two weak CO_2 resonance bands

$$\left\{\nu_3+\binom{\nu_1}{2\nu_2}\right\}$$

with centers at 2.77 μ and 2.69 μ.

‡ This region contains also the weak absorption band $3\nu_3$ of CO_2 with center at 1.43 μ.
It may be of interest to point out that the small region of absorption denoted in Plate III by the letter *V* is probably due to the CO_2 resonance group of four weak bands at 1.65, 1.60, 1.57, and 1.54 μ:

$$\left\{\nu_3+\binom{6\nu_2}{4\nu_2+\nu_1\ \ 2\nu_2+2\nu_1\ \ 3\nu_1}\right\}.$$

present in the ozonosphere, on the assumption that the foregoing identification is correct. This can be done by comparing the intensity of absorption at 7.6 μ in the solar prismatic spectrum with the intensity of absorption obtained by Hettner, Pohlman, and Schumacher, since it is known how much gas was employed by them. An

approximate calculation indicates the existence of one molecule of N_2O_5 for every one hundred molecules of O_3.

APPENDIX

In connection with the specification, in Tables 1 and 2, of the transitions responsible for the water-vapor bands, it should be remarked that certain of these regions consist of more than one band, but that in each case the most intense member was given. In Table 3 are listed the laboratory positions (band centers) of these most intense components, as well as the calculated band centers and corresponding transitions of the weaker components. This phenomenon of overlapping bands is due primarily to the accidental near equality in position of the two fundamental frequencies: ν_1 at 2.77 μ and ν_3 at 2.66 μ.

LOWELL OBSERVATORY
FLAGSTAFF, ARIZONA
November 1937

NOTE ADDED IN PROOF

This paper was presented before Section D of the A.A.A.S. at Indianapolis on December 29, 1937.

Apropos of the nature of atmospheric N_2O_5 as a photochemical product, we may strengthen our position by demonstrating that the new band at 7.6 μ is not due to any of the other probable photochemical products of the atmosphere. The principal photochemical resultant of CO_2 and H_2O is formaldehyde, CH_2O. The exclusion of this molecule from consideration has already been treated in the body of the paper. Besides the recent work of Dhar and Ram,[2] the existence of small quantities of CH_2O in the atmosphere has been affirmed from time to time since 1904. In this connection see *The Atmosphere*, by A. J. Berry (Cambridge University Press, 1913).

Small quantities of the oxides of nitrogen—NO, N_2O, NO_2, and N_2O_4—are to be expected in the upper layers of our atmosphere in consequence of the photochemistry of the nitrogen-oxygen mixture. NO need not be considered since its fundamental absorption band lies at 5.3 μ (C. P. Snow, A. M. Taylor, F. I. G. Rawlins, and E. K. Rideal, *Proc. R. Soc. London* [A], **124**, 442, 1929). The molecule N_2O possesses strong absorption bands at 7.8 and 8.6 μ, but no band at 7.6 μ (E. K. Plyler and E. F. Barker, *Phys. Rev.*, **38**, 1827, 1931). The molecule NO_2 has no absorption band in the neighborhood of 7.6 μ. N_2O_4 possesses a strong absorption band at 7.9 μ. At 7.9 μ the telluric spectrum reveals little or no absorption. For the infrared spectra of NO_2 and N_2O_4 see G. B. B. M. Sutherland, *Proc. R. Soc. London* (A), **141**, 342, 1933.

Although the two varieties of heavy water, D_2O and HDO, are not photochemical products, it is pertinent in the present connection to consider their spectra, for these two molecules may be expected to exist in the atmosphere in small amount. Neither of these molecules possesses a suitable transition (E. F. Barker and W. W. Sleator, *J. Chem. Phys.*, **3**, 660, 1935).

NOTES

ζ ORIONIS, A Be STAR

Spectrograms recently secured at the Perkins Observatory, with the Yerkes autocollimating spectrograph attached to the 69-inch reflector, definitely confirm my earlier suspicion of $H\alpha$ emission in the spectrum of ζ_b Orionis. The star is not listed in Merrill's catalogue of Be and Ae stars,[1] and no subsequent paper that has come to my attention mentions the presence of emission in its spectrum.

A spectrogram on I F emulsion, obtained on October 19, 1936, first indicated a weak region of uniform emission bordering the shallow $H\alpha$ absorption line on the long wave-length edge. The $H\alpha$ absorption line was of about the same width as $H\beta$ but was much more shallow, and it appeared to be split in two by a narrow bright line of slightly greater wave length than that of the center of the absorption line. The intensity of this bright line was somewhat less than that of the adjacent continuous background. The widths of the $H\alpha$ absorption and emission components were 7.7 and 9.3 A, respectively.

On the next plate (November 16, 1936; also I F) the region of $H\alpha$ presented a "washed-out" appearance. The absorption component was of about the width previously noted but was very poorly defined. The narrow bright line was not seen, and the contrast between the emission component and the adjacent continuous background was so weak that the presence of any actual emission was doubted. A third plate (I F), taken January 28, 1937, resembled the second spectrogram very closely.

The star was next observed on November 10, 1937. On this date a good spectrum was obtained on a III F emulsion. Although the plate was far superior to the first three spectrograms, the existence of the $H\alpha$ emission was still open to question. The presence of the narrow bright line near the center of the weak, broad $H\alpha$ absorption line was barely perceptible. The broad emission bordering the ab-

[1] *Ap. J.*, **78**, 87, 1933; Mt. W. Contr., No. 471.

sorption line on the long wave-length side again showed very little contrast to the adjacent continuous background. Furthermore, its profile differed considerably from that noted on the earlier spectrograms, showing a distinct maximum near the center of the region. Another III F plate was secured on November 29, 1937. On it the *Hα* absorption line was narrower. Although still weak, the line showed wing structure in contrast to the October, 1936, spectrogram, on which the absorption line appeared to have a nearly rectangular profile. Again the absorption line was split in two by the narrow bright line. The emission component on the long wave-length edge was so clearly revealed that its actual existence could no longer be doubted.

The structure of *Hα* in the spectrum of ζ_b Orionis resembles that noted in the case of ϵ Orionis,[2] except that none of our spectrograms of the former has given any indication of absorption on the long wave-length edge of the emission component. In addition to the Balmer lines, the spectrum of ζ_b Orionis contains in absorption sharp sodium D lines; *He* I 5048, 5876, and 6678; *He* II 5412; *Fe* II 4924 and 5018; a line at λ 5740 attributed to *Si* III; and one at λ 5592 attributed to *O* III.

As the foregoing summary indicates, the profile of *Hα* in ζ_b Orionis appears to be variable. Although some light from ζ_f Orionis probably entered the spectrograph, it is unlikely that the fainter star contributed appreciably to the spectrum, since the two are of practically the same type and since they differ in brightness by a ratio of more than 7 to 1. Furthermore, the difference in the adopted radial velocities of the two[3] would give rise to a relative shift of only 0.12 A at *Hα*, and thus could not account for the observed profile of that line. In this connection one may recall the work of Mellor,[4] whose observations led him to conclude that ζ_b Orionis is a spectroscopic binary with a range of about 20 km/sec and a period of about 19 days. However, Moore's fourth catalogue of spectroscopic binary stars[5] carries the note that thirty-nine spectrograms of ζ_b Orionis

[2] E. Cherrington, Jr., *Ap. J.*, **85**, 139, 1937.

[3] J. H. Moore, *Pub. Lick Obs.*, **18**, 1932.

[4] *Pub. Mich. Obs.*, **3**, 66, 1917.

[5] *Lick Obs. Bull.*, **18**, 30, 1936.

from the Yerkes, Lick, and Michigan Observatories indicate a constant radial velocity. Observations will be continued in order that a more thorough study of the behavior of $H\alpha$ may be made.

ERNEST CHERRINGTON, JR.

PERKINS OBSERVATORY
DELAWARE, OHIO
December 2, 1937

A STAR MODEL WITH SELECTIVE THERMO-NUCLEAR SOURCE

ABSTRACT

In this note thermo-nuclear reactions as a source of stellar energy are analyzed, and it is suggested that the energy-liberating processes are probably of a nature that occurs at some definite temperature ($\sim 10^7$ degrees). It then appears that the shell-source model should provide a satisfactory working basis for the studies in stellar structure.

It is at present generally accepted that the production of energy in stellar interiors is due to thermo-nuclear reactions consisting essentially in radiative captures of protons by light nuclei. The free neutrons which could be produced in some of these reactions will be ultimately captured by heavier nuclei, thus building up the elements of the periodic table. Inasmuch as the rate of the ordinary thermo-nuclear reaction increases exponentially with temperature, a good approximation is provided by the so-called point-source model. Simple conditions show, however, that the point-source model, with the energy production varying exponentially with the central temperature, leads to serious difficulties in its comparison with observational evidence. First of all, it can be shown that a star model of a given mass, supplied with such an energy source, will, during its life, steadily increase its luminosity and effective temperature (a total range of ~ 5 stellar magnitudes in luminosity and a factor of ~ 4 in effective temperature). This seems to be in direct contradiction to the empirical mass-luminosity relation, unless one makes a very special hypothesis about the distribution of stars of different ages in the Hertzsprung-Russell diagram.

In the comparison of individual stars one confronts also serious difficulties. For example, the central temperature and density of

Capella, as estimated from the point-source model, are considerably lower than those of the sun. Thus, one should expect that the total energy production in Capella must be very much smaller than in the sun, whereas, in reality, it is a hundred times larger.

Finally, the exponential dependence of the energy source on temperature makes the stability of the star somewhat uncertain.

In view of these difficulties, it seems reasonable to look for some other type of temperature dependence of nuclear reactions which is consistent with our present knowledge about nuclei and which would therefore represent better the actual behavior of a star. It seems that the only possibility of getting rid of the exponential temperature dependence of nuclear reactions in the interior of a star would be to introduce some type of selective effect which will give a maximum rate of reaction for a definite temperature. The simplest possibility would be to accept one of the possible reactions in the interior of a star which possesses a resonance level for the energy of the thermal protons (i.e., $\sim$ 10 kv). As far as the present development of nuclear physics has gone, it has shown the existence of resonance phenomena for various elements for radiative capture in the interval between one-half million volts (protons in carbon) and just a few volts (neutrons in certain elements). There is, therefore, nothing artificial in the hypothesis that there is a case of resonance around 10 kv. It is also known that in the presence of resonance capture the contribution of particles with nonresonance energy could be neglected, compared with the resonance region (for example, in the case of ${}_{6}^{12}C + {}_{1}^{1}H \rightarrow {}_{7}^{13}N + h\nu$ the nonresonance effect has never even been observed, and in the case of slow neutrons it is estimated to be several thousand times smaller). Thus, in a first approximation only the resonance energy production need be taken into account. It should be noticed, however, that, because of the Maxwellian distribution of the protons, even a very sharp resonance will give a rather broad maximum in the temperature dependence. The way to get a really sharp temperature maximum would be to suppose that the selective effect playing a role in the stars is not due to ordinary nuclear resonance but to a special kind of phenomenon. If, for instance, we suppose that the process, which is mainly responsible for the production of stellar energy, is the capture of protons by the ${}_{4}Be^{8}$ nucleus, we can get such a sharp temperature dependence,

owing to the fact that for low temperatures the protons will not be fast enough to penetrate through the potential barrier of this nucleus; whereas for high temperatures, all $_4Be^8$ nuclei will be dissociated into helium. Which particular selective effect should be accepted to take place in stellar interiors is, of course, the problem for further investigations.

Let us suppose that such an effect exists, and let us consider the consequences a little more closely. First of all, the energy production in this case will, in general, not be concentrated in the center of the star but in a spherical shell at such a distance from the center at which the temperature reaches the selective value. Inside of this shell the temperature will be constant (slightly more than the selective value), and the energy production will be negligible. With the progressive change in the chemical constitution of the star (owing to the burning-up of hydrogen) the radius of the energy-producing shell will change very slowly, resulting in a slow change of energy production. Thus, one can hope to obtain only small changes of luminosity with the age of the star, as required by the mass-luminosity relation.

The shell-source model also easily removes the foregoing paradox for the energy production in Capella and the sun. From this new point of view the temperatures inside of a star obtained by calculations with the point-source model have a physical meaning only as long as one is outside of the energy-producing shell, whereas inside of the shell the temperature remains constant. It is clear now that for Capella, which has a radius about ten times larger than that of the sun, the selective temperature will be reached at a much larger distance from the center than it will be for the sun. Consequently, the total energy production, which can be shown to be roughly proportional to the square of the radius of the shells of Capella, will be considerably larger than that for the sun. It should also be mentioned that the new model will not show the phenomena of overstability because the contraction or expansion of the star will cause only slight variations in the radius of the shell and will not, as in the case of the point-source model, give rise to rapid changes in the rate of energy production. A more detailed report on these problems will soon be published in the *Physical Review*.

G. GAMOW

GEORGE WASHINGTON UNIVERSITY

A SPECTROPHOTOMETRIC STUDY OF ϵ AURIGAE

The recent interpretation of ϵ Aurigae by Kuiper, Struve, and Strömgren[1] suggests that at long wave lengths the composite color of this binary system should be redder than that of a normal F supergiant. In other words, the infrared energy of the dark companion should, with increasing wave length, become larger with respect to the visually bright F star.

Becker[2] finds from photoelectric observations in the blue and violet that the color of ϵ Aurigae is normal for its spectral class (F2). On the other hand, infrared observations of its color which I made at the Yale Observatory[3] in 1932 indicate a positive color excess of 0.20 mag. All these color observations were made outside of eclipse.

The results of more recent observations[4] are given in Table 1.

As a comparison star, α Persei was chosen, because its spectrum is similar to that of ϵ Aurigae; ϵ Leonis was also used, despite its somewhat unfavorable position in the sky, since its apparent magnitude and color are similar to those of ϵ Aurigae. Although all observations were made near the meridian, small differential extinction corrections were always applied. The slit widths correspond to a spectral range of 480 A. In the case of the comparison of α Persei with β Tauri (mentioned below) small differential corrections were applied to reduce these observations to the same effective wave lengths. The largest of these corrections was 0.02 mag.

The mean difference in magnitude between ϵ Aurigae and α Persei is plotted in Figure 1 against the reciprocal of the wave length. In the case of ϵ Leonis the individual values are shown.

If stars radiate as black bodies, the observed difference in magnitude between any two stars is very nearly a linear function of the frequency over the spectral range with which we are concerned. Jensen[5] has found, from a discussion of his own results and from

[1] *Ap. J.*, **86**, 570, 1937.

[2] *Veröff. Sternwarte Berlin-Babelsberg*, **10**, No. 3, 1933. [3] *Ap. J.*, **79**, 145, 1934.

[4] For method of making these observations see *ibid.*, **84**, 372, 1936, and **85**, 145, 1937.

[5] *A.N.*, **248**, 223, 1933.

TABLE 1

Observed Magnitude—Differences

ϵ Aurigae *minus* α Persei

Date	Effective Wave Length												
	0.454μ	0.501μ	0.549μ	0.597μ	0.645μ	0.693μ	0.741μ	0.789μ	0.838μ	0.886μ	0.935μ	0.980μ	1.025μ
1938													
Jan. 18....	(1m26)	1m25	1m19	1m19	1m15	1m13	1m12	1m11	1m02	0m96	0m97	0m95	(0m96)
Jan. 23....	(1.23)	1.23	1.22	1.22	1.06	1.20	1.13	1.10	0.96	0.98	0.95	0.99	(0.88)
Jan. 26....	(1.36)	1.28	1.23	1.18	1.18	1.13	1.11	1.08	1.02	1.00	0.97	0.85	(0.96)

ϵ Aurigae *minus* ϵ Leonis

Date	Effective Wave Length												
	0.454μ	0.501μ	0.549μ	0.597μ	0.645μ	0.693μ	0.741μ	0.789μ	0.838μ	0.886μ	0.935μ	0.980μ	1.025μ
1938													
Jan. 26....	(−0m16)	−0m04	−0m02	+0m04	−0m02	+0m06	+0m04	+0m06	+0m02	−0m06	−0m02	−0m02	(−0m01)

Date	Effective Wave Length												
	0.478μ	0.525μ	0.573μ	0.621μ	0.669μ	0.717μ	0.765μ	0.813μ	0.862μ	0.910μ	0.958μ	1.000μ	
1938													
Feb. 7....	−0m20	−0m07	−0m03	+0m02	+0m07	0m00	+0m10	+0m10	−0m06	−0m06	−0m08	−0m09	

those of others, that the empirical data are best represented by two straight lines which intersect at 4800 A. It appears, therefore, that

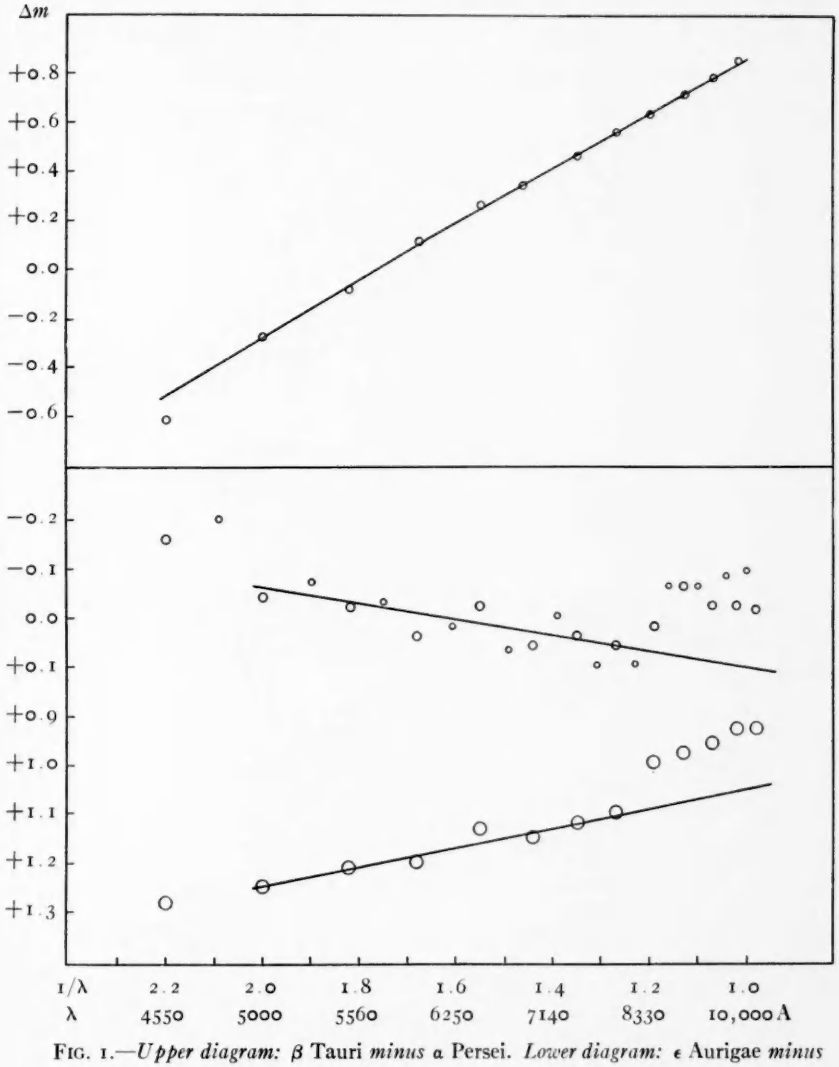

FIG. 1.—*Upper diagram:* β Tauri *minus* α Persei. *Lower diagram:* ε Aurigae *minus* ε Leonis and *minus* α Persei, respectively.

observations at less than 5000 A should not be used in deriving relative color temperatures in the red regions of the spectrum.

Since ε Aurigae is known to be a supergiant, it is, of course, desir-

able to know whether the excess infrared energy suggested by the color indices and by Figure 1 is not characteristic of stars of high luminosity. Becker and Hartwig[6] conclude, after a thorough discussion of Yale infrared colors and Babelsberg blue-violet colors, that in these spectral regions there is practically no such absolute-magnitude effect for stars whose spectral types range from Fo to F6. α Persei is also a supergiant. The observed difference in magnitude between α Persei and β Tauri (B8) is plotted against the reciprocal of the wave length in Figure 1. These data are the mean of determinations made on five different nights. The curved line has been computed on the assumption that the temperatures of these two stars are 6500° and 15,100°. This comparison indicates that α Persei is a normal star, and shows that the excess infrared energy of ε Aurigae would be indicated in the same degree had it been compared directly with β Tauri.

A comparison of ε Leonis with ε Geminorum was also made on February 7. Since a linear magnitude-frequency relationship was found to exist between these stars, it is probable that ε Leonis is also a normal star.

The data in Table 1 give no definite indication that the intensity of ε Aurigae has changed during the three-week interval represented by the observations.

Although ε Aurigae is in the galactic plane, it is difficult to explain the observed results on the basis of space reddening. In the first place, Becker's results show a normal color in the shorter wave lengths. Furthermore, Sproul observations[7] have shown that the observed difference in magnitude between a colored and normal B star is linear with the frequency. A comparison of infrared and blue-violet color indices by Bennett[8] gave a similar indication. More recently, Whitford[9] confirmed these results. These three discussions include a total of only 15 colored B stars; yet it seems significant that no obvious exception to this conclusion has been found.

If we assign half-weight to the comparison with ε Leonis, the excess energy of ε Aurigae is 0.13 mag. at 9600 A. If we assume that

[6] *Zs. f. Ap.*, **14**, 269, 1937.

[7] *Ap. J.*, **85**, 145, 1937.

[8] *Ibid.*, p. 275.

[9] Amer. Astr. Soc., December, 1937.

this represents the contribution of the dark companion, it means that this companion is 2.24 mag. fainter than the bright component at this wave length.

JOHN S. HALL

SPROUL OBSERVATORY
SWARTHMORE COLLEGE
SWARTHMORE, PENNSYLVANIA

NOTE ON HALL'S MEASURES OF ϵ AURIGAE

The foregoing results by Dr. Hall may be used as a first quantitative test of the assumption that the infrared component of ϵ Aurigae lies on the average mass-luminosity relation. This assumption was made[1] in order to estimate the effective temperature of the infrared component. The determination of the luminosity for this star is of particular importance. The radius and the mass are already fairly well known, considerably better than for the F component; this is due to the fact that small errors in the orbital inclination i, in ω, and in the assumption that the F component lies on the average mass-luminosity relation have a much smaller effect on the radius and mass of the I component than on the F component. This circumstance is partly apparent from Table 1[2] and follows partly from the fact that the known mass function depends much more on the mass of the I star than on the mass of the F star. With the luminosity also known, the star may be used in a discussion of stellar models,[3] which for this extreme case is of particular interest.

The luminosity of the I component will have to be referred to that of the F component as long as an independent parallax determination of ϵ Aurigae is lacking. Such a determination could only be of sufficient accuracy if made by measuring the apparent orbit of the F star.[4]

For the present, then, the luminosity must depend on the assumption that the F star lies on the average mass-luminosity relation. If this assumption is correct, the uncertainty in the mass of the F star

[1] *Ap. J.*, **86**, 575–576, 1937. [2] *Ibid.*

[3] S. Chandrasekhar, *Introduction to the Study of Stellar Structure*, "Astrophysical Monographs" (in press).

[4] *Ap. J.*, **86**, 612, 1937.

is relatively unimportant, since for massive stars the luminosity does not increase very rapidly with increasing mass. If the F star deviates from the average mass-luminosity relation, the full amount of the deviation will go into the luminosity of the I star. Fortunately, the evidence is that the deviations are generally small.

Since the ratio of the radii of the two components is known, the ratio of the intensities at a certain wave length will give the ratio of the effective temperatures, provided the stars radiate like black bodies. Hence, Hall's result that at 9600 A the I star contributes 0.13 mag. toward the total radiation, in connection with the adopted temperature, 6300° K, of the F star, will give the temperature of the I star.

A slight error in the adopted temperature of the F component is unimportant in this case, because the infrared intensity of the F star increases slowly with increasing temperature, whereas the opposite is true for the I star, which has its maximum intensity near 18,000 A. The ratio of the radii, obtained from the light-curve, refers to the radius of the ionized shell and not to the radius of the photosphere, which determines the surface temperature and energy distribution. From the constancy of the minimum we derive 0.85 R_I as the upper limit of the photospheric radius, if R_I, as before, is the radius of the shell. It is not probable that the photospheric radius is much smaller, because the shape of the minimum indicates that the ionized shell has a fairly sharp boundary, so that the density gradient could not be very small. Taking 0.85 R_I and 0.75 R_I as limiting values, we have, with $R_F/R_I = 0.025/0.357$, and $T_e(\mathrm{I}) = 1350°$[4]:

$$T_e \text{ (computed)} = 1350°/\sqrt{0.85} = 1460°, \text{ or } 1350°/\sqrt{0.75} = 1560°; \text{ and}$$
$$T \text{ (observed)} = 1600°, \text{ or } 1650°.$$

It is perhaps more significant to express the deviations, O−C, in terms of deviations from the average empirical mass-luminosity relation on which the computed temperatures are based. The residuals for the two assumed radii are 0.40 mag. for 0.85 R_I, and 0.24 mag. for 0.75 R_I, in the sense that the star lies above the mass-luminosity relation.

Adopting 0.8 R_I as the photospheric radius of the I star, we have the following provisional constants: log $\mathbf{m}_I = 1.39$; log R_I (photospheric) = 3.33; $M_{bol} = -6.5$; log $L = 4.47$; $T(I) = 1620°$ K = 1350° C.

Definitive values will only be obtained after the parallax of the system has been measured, as indicated above, and after radiometric observations have established the spectral energy-curve in the vicinity of the maximum. But Dr. Hall's measures show that, even for this star of extremely low temperature and large radius, the average mass-luminosity relation holds good, at least approximately.

G. P. KUIPER

YERKES OBSERVATORY

REVIEWS

Grundlagen und Methoden der Periodenforschung. By DR. KARL STUMPFF. Berlin: Julius Springer, 1937. Pp. vii+332. Figs. 41. Rm. 39; bound, Rm. 42.

This book is the second of three by the same author. The first, *Analyse periodischer Vorgänge,* was published about ten years ago. The third will consist, for the main part, of practical applications of periodogram theory to data, and of related problems. Investigators of cyclical data have been handicapped severely because there has been no satisfactory résumé of the great amount of research work that has been done during the last forty years. In a quite satisfactory manner Professor Stumpff has brought together and weighed the methods used in this type of investigation. Almost all these have developed since Schuster invented his periodogram less than fifty years ago. Most of them have been developed during the last fifteen years.

Stumpff divides the subject into six chapters. The first two of these are devoted to the fundamentals of the theory and practice of harmonic analysis. In the third chapter he considers the statistical fundamentals of periodogram calculation, dealing in much detail with the Schuster periodogram. The space devoted to this method is warranted by its historical importance, despite the fact that more modern methods are much shorter and more powerful. In this chapter he considers various schemes for shortening the work and discusses quite nicely the use of the Hollerith card system. The fourth chapter considers various statistical methods of handling the data of a periodicity problem. In the fifth chapter he especially considers newer methods of period determination which are related more or less closely to the Schuster method. In the last chapter he describes various mechanical devices for the aid of the computer, especially Douglass' cyclograph, which is excellently illustrated and explained. He then describes his own mechanical apparatus called the *Polarisations-periodometer,* and gives a schematic diagram explaining it. This has an advantage over the Douglass scheme in that it does give some measures of amplitude.

One of the very useful things in the book is the unusually fine Bibliography, with 319 references to articles on periodogram analysis. Most of these refer to theory, for the number of routine applications is too large to make it worth while to include more than samples of them.

DINSMORE ALTER

Griffith Observatory
Los Angeles, Calif.

Inaugural Lecture on Astronomy and Papers on the Foundations of Mathematics. By CARL FRIEDRICH GAUSS. Translated and edited by G. WALDO DUNNINGTON. Baton Rouge: Louisiana State University Press, 1937. $1.00.

The collected works of Gauss were published by the Gesellschaft der Wissenschaften zu Göttingen under the able editorship of Professor Martin Brendel. Since great care had been taken to include in these twelve volumes all known scientific contributions by Gauss, it was improbable that any really important papers had been omitted. Dr. Dunnington has recently uncovered several little-known Gaussian fragments and has presented them in their English translation, together with a description of the early life of Gauss. He expresses the hope that the appearance of these papers "will stimulate a further interest among English speaking people in the thought-world of a scientist whose achievements mark a turning point in the development and history of three sciences: mathematics, physics and astronomy."

The author is, of course, right when he states: "It is unnecessary to justify the publication of anything from the pen of a man who ranks with Archimedes and Sir Isaac Newton as one of the three greatest mathematicians of all times." But the "Inaugural Lecture on Astronomy," which had since 1927 remained unnoticed among the papers of Carl August Gauss (a grandson of Carl Friedrich Gauss), will be somewhat of a disappointment to a reader who is not already thoroughly acquainted with the work of Gauss. It contains relatively little of interest—even from the historical point of view—and it is quite evident that Gauss himself did not regard it as of sufficient value for publication. A translation or even a condensed account of the *Theoria motus corporum coelestium* would have been infinitely more effective in carrying out the author's desire to stimulate interest in Gauss. Nevertheless astronomy is indebted

to Dr. Dunnington for the work he has done, and the reviewer hopes that he will carry out his intention and complete the biography of Gauss. It is tantalizing to read an account which breaks off in the twenty-sixth year of the life of a man who died when he was seventy-eight.

O. S.

Eclipses of the Sun and Moon. By SIR FRANK DYSON and R. v. d. R. WOOLLEY. ("International Series of Monographs on Physics.") Oxford: Clarendon Press, 1937. Pp. 160. $5.00.

The new book on solar and lunar eclipses, by Sir Frank Dyson and R. v. d. R. Woolley, is a brilliant presentation of eclipse problems, both old and new. A short Introduction is followed by chapters on the cause of eclipses, the prediction of eclipses, and the saros. Chapter v treats eclipses of the moon, and chapter vi the secular acceleration. In chapter vii there is an unbiased summary of observational evidence for the existence of the Einstein deflection.

The remaining ten chapters are devoted mainly to astrophysical problems of the chromosphere, the prominences, and the corona. The section on eclipse instruments might have been expanded somewhat. In connection with expeditions, the authors remark, "Experience shows that it is well to leave ample time to erect the instruments before the day of the eclipse." This advice is a startling example of understatement.

The discussion of the flash spectrum is given from the historical viewpoint and clearly pictures the growth of knowledge up to the present. The text is interspersed with many comments that are extremely important, such as:

> Exception may be taken to the identification of every line with a line or group of lines in Rowland's solar spectrum, in view of the difference of dispersion and the dissimilarity of the spectra. In the view of the authors it is better to compare directly with the spectra of the elements in their normal and ionized states, gradually working down in intensity until lines are no longer seen.

Of course, the procedure recommended by the authors has been followed by some investigators, but the Rowland identifications for the fainter lines have undoubtedly been given too much weight.

Critical summaries are given, respectively, of Milne's, Chandrasekhar's, and McCrea's theories of chromospheric support. Several important criticisms that might have been urged against the validity of the

first two of these are omitted, such as the disagreement between calculated and observed values of line intensities. The authors favor the McCrea theory of a chromosphere supported by turbulence, but readily admit that no fully satisfactory theory of chromospheric mechanics has yet been proposed.

In reading the discussion of the various anomalies presented by the flash spectrum, one is surprised not to find mention of the most outstanding chromospheric problems, e.g., that of explaining the occurrence of lines of helium and especially of ionized helium. The authors apparently follow Mitchell in assuming that the lower chromospheric pressure, with ionization increased according to the Saha theory, will account for the discrepancy. The paragraph where ionized helium is mentioned is concluded with the statement: "Pressure being taken into account, it seems only natural to expect a high degree of ionization in the outermost layers of the solar atmosphere, and it now requires an effort of historical imagination to appreciate the difficulties felt only twenty years ago." Would that the difficulties were a matter of history! Although ionization at low pressure may be the explanation for the occurrence of enhanced metallic lines of low excitation potential, it cannot account for the high intensity of He^+ 4686, which line requires, after atomic ionization, further excitation of some fifty volts. The author's failure to mention Gurney's theory of helium excitation is probably justified, since there are many objections to the idea.

The last five chapters deal with the corona and associated problems. There is a very fine summary of the measurements both of the integrated intensity and of the intensity gradient. The high light of the book, in the reviewer's opinion, is reached in chapter xvi, which deals with the spectrum of the corona. The authors present some hitherto unpublished observations, by Lyot, of new coronal lines detected outside of eclipse. Infrared lines have been recorded at λλ 7060, 7892, 8024, 10747, and 10798. The first of these lines was discovered independently on spectra secured in 1936 by the Harvard–M.I.T. expedition to Russia. The two new lines last mentioned are among the most intense of all coronal lines. In view of Lyot's remarkable work, we might expect the authors to conclude the volume with a hopeful, rather than a sour, note: "The nature of the corona seems accordingly destined to remain one of the outstanding puzzles of astrophysics during the next decade."

The book is well illustrated and contains many useful tables and

bibliographic references. There are very few misprints. The coronal line λ 6702 is called λ 6707, and λ 3388 is noted as λ 3888. The sins, if any, are of omission. One has the feeling that so excellent a summary would be even more useful if the subject matter were not so condensed. Students unfamiliar with the original papers will have difficulty with the sections containing astrophysical theory. The authors might have given a table of eclipse dates. That a detailed subject index was not provided is indeed regrettable.

D. H. MENZEL

Atomic Spectra and Atomic Structure. By GERHARD HERZBERG. New York: Prentice-Hall, 1937. Pp. xiv+257. Figs. 80. $4.25.

This little volume by Dr. Herzberg has been translated from the German by Dr. J. W. T. Spinks. It is designed as an elementary introduction to the theory of atomic spectra as interpreted by quantum mechanics. There is no attempt at completeness, the aim throughout being to discuss only the fundamentally important aspects of atomic spectra. The theoretical discussion of the various topics of atomic spectra is always prefaced by the results of experimental investigations. Although mathematical developments are carefully avoided, the author discusses many of the important results of quantum mechanics from the standpoint of their physical significance, while leaving the details of derivations to more advanced treatises.

Among the topics treated in this fashion are the wave mechanics of the hydrogen and helium atoms, transition probabilities and selection rules, the interpretation of the alkali spectra, multiplet structure and electron spin, the physical interpretation of quantum numbers, Zeeman and Stark effects, the Pauli principle and its application to the periodic system, the various types of electron coupling, and hyperfine structure.

The translation by Dr. Spinks reads easily and logically, and astronomers who require a knowledge of the basic principles of atomic spectra will find the book admirably suited to their needs.

LEO GOLDBERG

Astrophysik: Handbuch der Experimentalphysik, Vol. **26.** Edited by B. STRÖMGREN. Leipzig: Akademische Verlagsgesellschaft M.B.H., 1937. Pp. xv+997. Bound, Rm. 76.–; unbound, Rm. 73.60.

The *Handbuch der Experimentalphysik* is devoted principally to the exposition of methods of research rather than to the results obtained with

these methods. In keeping with this general plan, the new volume on astrophysics deals almost exclusively with practical problems, and it should therefore appeal principally to the observational astronomer. In this respect it furnishes a welcome addition to the seven monumental volumes of the *Handbuch der Astrophysik*, in which the results of research were given preference over the methods with which they were secured.

The editor has planned the book for physicists as well as for astronomers. He says:

> The general principles of astronomical spectroscopy and photometry are by their nature identical with those used in the laboratory. But for the solution of the astrophysical problems many independent procedures and methods have been developed which should be of interest to the physicist.

The book is divided into seven chapters, written by five authors. J. Stobbe has contributed an article on the fundamental ideas of astronomy. This chapter is intended primarily for those readers who are not thoroughly acquainted with the more elementary aspects of astronomy. W. Schaub writes on qualitative spectral analysis. Next comes a long chapter by B. Strömgren on the problems of astronomical photometry. J. Hellerich writes on visual photometry; H. Kienle, on photographic photometry; B. Strömgren, on objective methods of photometry, including the use of the pyrheliometer, the bolometer, the radiometer, the thermocell, the photoelectric cell and selenium cell. The volume is concluded by a chapter on the measurement of color, written by J. Hellerich.

All chapters are interesting and well worth reading. But while some of them contain relatively little that is not already available in the *Handbuch der Astrophysik* or elsewhere, others are really much more than simple compilations. For example, Strömgren's chapter on "Tasks and Problems of Astronomical Photometry," comprising 241 pages, is probably the only complete modern account of practical photometry. After an introduction on the theoretical foundations of photometry, the author discusses, in turn, the measurement of brightness and of color index, the methods of spectrophotometry, the influence of extinction, and the principal problems, as well as some of the results obtained. The practical astronomer will be especially interested in those sections which deal with the comparison and reduction of photometric systems and catalogues, with the determination of relative and absolute intensities, fundamental and differential color-index measurements, etc. The section on spectrophotometry is admirable and may well be recommended as an intro-

ductory textbook to students who wish to familiarize themselves with the methods now in use for the determination of line contours or stellar energy distributions.

The chapters by Kienle and Hellerich are also very complete, and they constitute an admirable account of photographic and visual methods in photometry.

The amount of space devoted to spectroscopy is relatively small, but in part this is due to the inclusion of spectrophotometric methods in Strömgren's chapter on astronomical photometry. Nevertheless, the reviewer would have expected a somewhat more advanced treatment of radial-velocity determinations, of stellar rotation, of Stark broadening in stellar absorption lines, and of various other branches of astronomical spectroscopy. For example, an astronomer would probably fail to derive much use from the section on stellar rotation, containing as it does a diffuse description of some of the least important and not too convincing arguments in favor of large rotational velocities in certain stars. Since the book was to be primarily of a methodological character, it would have been appropriate to discuss the integral equation of stellar rotation and to outline Carroll's method of deriving both the rotational velocity and the true contour of the undisturbed line.

The optical and mechanical requirements of stellar spectroscopy are discussed in greater detail. But it is difficult to contribute new information in a field that has already been exhaustively treated elsewhere. The most important consideration in the construction of an astronomical spectrograph is its efficiency. This is relatively less important in the laboratory, and we would have expected to find an exhaustive treatment of this subject. Instead, the author gives only some scattered information on short-focus camera objectives as well as on the most favorable prism angle, and he deals at length with the relatively unimportant gain in efficiency produced by spilling some light over the refracting edge of the prism. The relative merits of aperture and focal length of the telescope and of the collimator are not discussed. A translation or résumé of Keeler's excellent account in *Sidereal Messenger*, **10**, 433, 1881, would be well worth the trouble; it is appropriate to repeat here a remark made by him forty-seven years ago:

> It may seem as if they [the principles of efficiency of astronomical spectroscopes] are too obvious, from well-known laws of optics, to require explanation, but examination of printed descriptions of spectroscopic observations will show that they have not been entirely understood, or, at least, not always borne in mind by many practical observers.

The problem of testing the lenses of a spectrograph is discussed in considerable detail. But one wonders about the exact meaning of the sentence: "The collimator lens must make all rays of different wave lengths, which emanate from the slit, exactly parallel." This oft-repeated statement[1] is likely to confuse the inexperienced observer. The question is: How accurately does the collimator have to be focused? Will it affect the results if the collimator is left without refocusing for long periods of time, involving marked changes in temperature? And will the definition be materially impaired by lack of proper focusing for those wave lengths for which the lens is not corrected? These important questions have not been adequately dealt with in any of the recent treatises of practical astronomical spectroscopy. And yet the answer is available in simple form in a paper by Wadsworth.[1]

The author's sweeping statement; "Die Lichtstärke des Objektivprismas kann durch keinen Spaltspektrographen erreicht werden," is not correct. The relative slowness of the slit spectrograph as compared with the objective prism is due to two causes: the greater purity of the former and the increased light losses by reflection and absorption in the lenses and prisms. Both factors can be reduced in the slit spectrograph by proper design and are not inherent in the use of a slit. On the other hand, the objective prism works at a great disadvantage when very faint stars or nebulae are observed: the light from the sky is not spread out into a spectrum when the objective prism is used and the limiting brightness of an object which can be photographed with a powerful instrument is greatly impaired. In a slit spectrograph, on the other hand, the light from the night sky is broken up into a spectrum of fairly strong emission lines and a faint continuous spectrum. Consequently, the contrast between object and sky background is increased. It is obvious that the slit spectrograph can reach fainter objects than the objective prism. The principal advantage of the objective prism is that it permits "mass production" in stellar spectroscopy.

The methods of measurement and reduction of stellar spectra are fully described. A section of fifteen pages is devoted to the investigation of the measuring machine—a topic which the practical worker will doubtless appreciate. But we wonder why after an elaborate account of the Hartmann method of reducing the measurements there is no instruction as to the sources of wave lengths which we are to employ. So many of the lines in stars of spectral type later than F are blends that an uncritical

[1] See Wadsworth, *Misc. Sc. Pap., Allegheny Obs.*, No. 10; *Ap. J.*, **17**, 1903.

selection of wave lengths is bound to result in large systematic errors. Similarly, the best wave lengths for radial velocity work on early-type stars have been gradually compiled by experienced observers. Some of these have been published in the *Transactions of the I.A.U.*, but others are scattered throughout the literature. A beginner will lose much time if he is not properly instructed in this respect.

It is not possible, for lack of space, to discuss in detail the remaining chapters. As a whole, the volume is a very important addition to the growing library of German *Handbuchs* and the editor is to be congratulated upon having produced a remarkably useful treatise.

OTTO STRUVE